Ciliary length control

Joost R. Broekhuis

Cover: IMCD-3 cell expressing IFT20-GFP

Cover design: Joost R. Broekhuis & Karima Bol

Layout: Joost R. Broekhuis

© Joost R. Broekhuis, 2012

This thesis was printed by Wöhrmann Print Service, Zutphen

The research presented in this thesis was performed at the Department of Cell Biology of the Erasmus MC in Rotterdam, the Netherlands.

The studies described in this thesis were supported by grants from the Dutch Kidney Foundation and the Netherlands Organisation for Scientific Research.

Ciliary length control

Regulatie van cilia lengte

Proefschrift

ter verkrijging van de graad van doctor aan de
Erasmus Universiteit Rotterdam
op het gezag van de
rector magnificus

Prof.dr. H.G. Schmidt

en volgens besluit van het College voor Promoties.

De openbare verdediging zal plaatsvinden op
woensdag 5 december 2012 om 09.30 uur

door

Joost René Broekhuis

Geboren te Rotterdam

Promotiecommissie

Promotor:	Prof.dr. F.G. Grosveld
Overige leden:	Dr.ir. N.J. Galjart
	Prof.dr. J.N.J. Philipsen
	Prof.dr. J.H. Gribnau
Co-promotor:	Dr. G. Jansen

Ook al zegt men dat

de wetenschap voor niets staat,

blijft het een feit

dat de zon voor niets opgaat

J.A. Deelder

Contents

Abbreviations **9**

Scope and aim of this thesis **11**

Chapter 1: Introduction **13**

1.1. Historical perspective 14

1.2. Structure of the cilium 14

1.3. The primary cilium as sensory organelle 17

1.4. Intraflagellar Transport 18

1.5. Membrane trafficking to the cilium 23

1.6. Regulation of ciliogenesis 25

1.7. Ciliopathies 29

Chapter 2: MRK and MOK regulate cilia length and intraflagellar transport in renal epithelial cells **41**

Chapter 3: Identification of MRK and MOK interacting proteins **59**

Chapter 4: SQL-1, homologue of the Golgi protein GMAP210, modulates Intraflagellar Transport in *C. elegans* **79**

Chapter 5: Discussion and prospects **109**

Chapter 6: Addendum **119**

Summary 120

Samenvatting 122

Curriculum Vitae 124

PhD portfolio 125

Dankwoord 126

Abbreviations

a.a.	: Amino acids
acTub	: Acetylated tubulin
ALPS	: ArfGAP-1 lipid-packing sensor
ANOVA	: Analysis of variance
ATP	: Adenosine-5'-triphosphate
BBS	: Bardet-Biedl syndrome
BLAST	: Basic local alignment search tool
cAMP	: Cyclic adenosine monophosphate
CCRK	: Cell cycle-related kinase
CDKs	: Cyclin-dependent kinases
cDNA	: Complementary DNA
CFP	: Cyan fluorescent protein
CTS	: Ciliary targeting sequences
DIC	: Differential interference contrast microscopy
DNA	: Deoxyribonucleic acid
FACS	: Fluorescence-activated cell sorting
FCS	: Fetal calf serum
FRAP	: Fluorescence recovery after photobleaching
GDP	: Guanosine diphosphate
GFP	: Green fluorescent protein
GPCR	: G protein coupled receptor
GPI	: Glycophosphatidylinositol
GRAB	: GRIP-related Arf-binding
GTP	: Guanosine-5'-triphosphate
HRP	: Horseradish peroxidase
IF	: Immunofluorescence
IFT	: Intraflagellar transport

Kbp : Kilo base pairs
KO : Knockout
MAK : Male germ cell-associated kinase
MDCK : Madin Darby canine kidney
MEF : Mouse embryonic fibroblast
MOK : MAPK/MAK/MRK overlapping kinase
MRK : MAK-related kinase
MS : Mass spectrometry
mTOR : Mammalian target of rapamycin
ND : Not determined
NEKs : (Never in mitosis gene a)-related kinases
ORF : Open reading frame
PBS : Phosphate buffered saline
PFA : Paraformaldehyde
PTMs : Posttranslational modifications
RCKs : *ros* cross-hybridizing kinases
PCR : Polymerase chain reaction
PP5 : Phosphoprotein phosphatase 5
RNA : Ribonucleic acid
RT-PCR : Reverse transcription polymerase chain reaction
SD : Standard deviation
SDS-PAGE : Sodium dodecyl sulfate polyacrylamide gel electrophoresis
shRNA : Short hairpin RNA
TIRF : Total internal reflection fluorescence
WB : Western blot
YFP : Yellow fluorescent protein

Scope and aim of this thesis

Primary cilia are microtubule-based organelles that can be found on the surface of most eukaryotic cells. Primary cilia detect external cues and play an important role in subsequent signal transduction pathways. In the kidneys primary cilia act as a flow sensor. However, both abnormally short and excessively long cilia fail to correctly act as a flow sensor, which results in the formation of cysts inside the kidney and eventually kidney failure. Primary cilia are assembled and maintained by a process known as intraflagellar transport. This process involves the bidirectional transport of multimeric protein complexes along the microtubule axis by motor proteins. It is likely that lengthening and shrinkage of cilia is modulated by the intraflagellar transport machinery. This thesis contains studies aimed to gain more insight in how intraflagellar transport and cilia length are regulated. To study intraflagellar transport we use cultured mammalian cells as well as the nematode *Caenorhabditis elegans*.

Chapter 1 gives an introduction to the different aspects of cilia biology. First, both the structure and function of the primary cilium are described. Next, intraflagellar transport inside the cilium and membrane trafficking to the cilium are discussed.

Chapter 2 describes the characterization of MRK and MOK. These two ciliary kinases negatively regulate cilia length, and MRK can modulate intraflagellar transport in cultured mammalian cells. Both MRK and MOK act through the mTOR pathway.

Chapter 3 describes the identification of MRK and MOK binding partners using a biotinylation-proteomics approach.

Chapter 4 describes the identification and characterization of SQL-1. SQL-1 is a Golgi protein that can modulate cilia length and intraflagellar transport in *C. elegans*.

Chapter 5 discusses the results of the previous chapters and their relations to our current understanding of the topic.

Chapter 1
Introduction

1.1. Historical perspective

The cilium is an organelle found in organisms spanning the eukaryotic lineage. They are antenna-like structures that project from the cell body. They are also known as flagella, but to prevent confusion with the bacterial flagella, which are structurally different from eukaryotic flagella, the term cilium is preferred over flagella. Cilia were probably first observed by Antonie van Leeuwenhoek at the end of the 17th century. When he looked through his homemade microscope he observed living protozoa moving around in rainwater using their motile cilia. Motile cilia make things move, which could be either the cells themselves, or fluids surrounding the cells. For a long time it was assumed that making things move was the sole function of cilia. Curiously, cells lacking a motile function were found to have a solitary cilium, which were named primary cilia (Sorokin, 1968). At that time the primary cilium was considered an evolutionary leftover and received little attention. However, at the beginning of the 21st century it was discovered that several signaling factors localize to the primary cilium (Corbit et al., 2005; Haycraft et al., 2005; Nauli et al., 2003; Pazour et al., 2002; Schneider et al., 2005; Yoder et al., 2002), showing that they function in signal transduction. In addition, ciliary dysfunction was linked to a variety of human diseases, collectively called ciliopathies. These two findings led to a renewed interest in this organelle.

1.2. Structure of the cilium

The cilium consists of a microtubule-based axoneme covered by a specialized membrane. The cilium's axoneme emerges from the basal body, which is derived from the mother centriole, and extends into the extracellular space. The inside of the cilium is separated from the cytosol by the transition zone. A schematic representation of the basic structure of the cilium is presented in figure 1.

1.2.1. The ciliary axoneme

The axoneme of the primary cilium typically consists of a ring of nine microtubules doublets, called a 9+0 axoneme. In motile cilia the nine microtubule doublets enclose a central pair of microtubule singlets, resulting in a 9+2 structure. In most cilia the segment of A-B-tubules is followed by a single A tubule extension. These distal singlets can be found in unicellular organisms, such as *Chlamydomonas* (Mesland et al., 1980), and invertebrates, such as the nematode *C. elegans* (Ward et al., 1975), but also in several tissues of the mammalian system, including pancreas, kidney, respiratory tissue, and in photoreceptors (Hidaka et al., 1995; Kubo et al., 2008; Steinberg and Wood, 1975; Webber and Lee, 1975).

Tubulin that is destined for the cilia is derived from the tubulin pool in the cell body. Experiments with tubulin tagged with a fluorescent protein have shown that tubulin is incorporated at the distal tip of the axoneme (Song and Dentler, 2001). Eventually, the fluorescence spread along the entire axoneme, showing that the microtubule axoneme turns over (Song and Dentler, 2001). However, the subunit exchange is slow, less than 5% per hour (Nelsen, 1975; Rosenbaum and Child, 1967; Rosenbaum et al., 1969; Thazhath et al., 2004). Incorporation of new tubulin continues under conditions in which the cilium is shrinking or elongating (Song and Dentler, 2001).

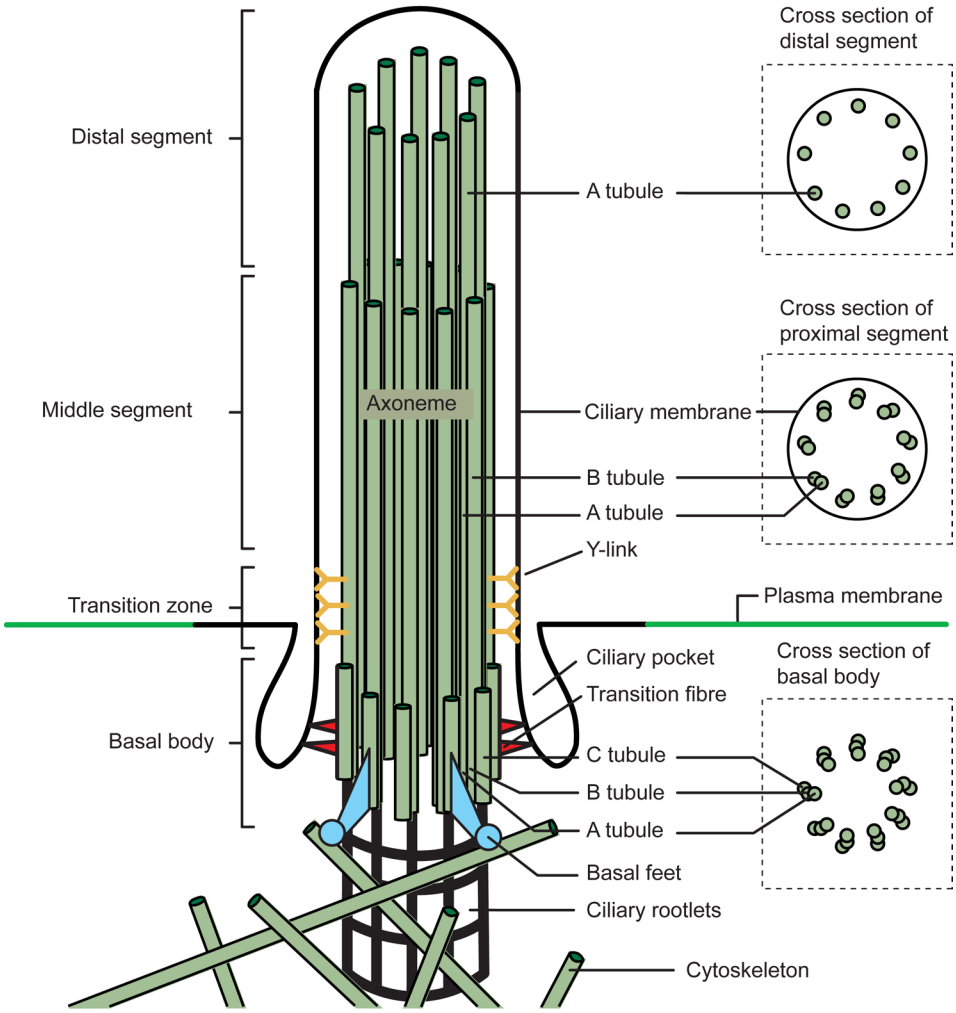

Figure 1. Architecture of a primary (9+0) cilium. The microtubule-based axoneme of the primary cilium originates from the basal body. Cross sections show the microtubule triplets of the basal body, microtubule doublets of the middle segment, and the microtubule singlets of the distal segment. The basal body is anchored to the cytosolic microtubules through the basal feet, and to the membrane through the transition fibers. The ciliary rootlets extend from the basal body into the cytoplasma. The inside of the cilium is separated from the cytosol by the transition zone, which is characterized by the presence of Y-links, which can be found at the beginning of the axoneme. The cilium is covered by the ciliary membrane, and at the ciliary base a plasma membrane invagination, called the ciliary pocket, is present.

Tubulin can undergo a large number of post-translational modifications (Verhey and Gaertig, 2007; Westermann and Weber, 2003), and these PTMs are especially abundant in axonemal tubulin. Axonemal tubulin has been shown to be acetylated (L'Hernault and Rosenbaum, 1985), detyrosinated (Sherwin et al., 1987), polyglutamylated (Fouquet et al., 1994), and polyglycylated (Rudiger et al., 1995). Loss-of-function studies with microtubule modifying enzymes suggest

that PTM's are important for the function, stability, and assembly of the cilium. For example, the deacetylation of axonemal tubulin by HDAC6 promotes disassembly of primary cilia (Pugacheva et al., 2007), and depletion of the acetyltransferase αTAT1 delays assembly of primary cilia (Shida et al., 2010). In addition, polyglutamylation of axonemal tubulin is necessary for the motile function of tracheal cilia (Ikegami et al., 2010). Studies of PTMs on non-axonemal tubulin have shown that PTMs are important for docking of motor proteins and plus end tracking proteins. Most likely these PTMs are also important for the binding of certain proteins that associate with microtubules, which could explain the importance of PTMs for the function of the cilium. Recently, the tubulin deglutamylase CCPP-1 was shown to control the velocity and localization of the ciliary kinesins, OSM-3 and KLP-6 (O'Hagan et al., 2011), which supports this idea.

1.2.2. The basal body

The basal body is a centriole-derived structure. A quiescent cell has two centrioles, of which the mother centriole can act as basal body. Centrioles are organized in cylinders of nine microtubule triplets. When the centriole acts as basal body the A and B microtubules of the triplet extend to form the axoneme, the third microtubule is terminated at the transition zone (Ringo, 1967). During the conversion of centriole to basal body, three accessory structures are formed: transition fibers, basal feet, and ciliary rootlets. Transition fibers anchor the basal body to the ciliary membrane at the curved base of the ciliary pocket (Anderson, 1972), an invagination of the plasma membrane directly next to the ciliary base. The ciliary rootlets extend from the basal body into the cytoplasm (Tachi et al., 1974), providing additional support for the primary cilium. Basal feet project laterally from the side of the basal body, where they anchor cytosolic microtubules (Anderson, 1974). The basal body comprises of a large number of proteins (Kobayashi and Dynlacht, 2011). Centrosomal proteins can positively and negatively affect cilia formation. Several of these centrosomal proteins, like for example ODF2 (Ishikawa et al., 2005) and Cep164 (Graser et al., 2007), have been shown to be necessary for the formation of a functional cilium. Two other centrosomal proteins, Cep97 and CP110, actively suppress ciliogenesis (Spektor et al., 2007).

1.2.3. The ciliary membrane

The ciliary membrane is continuous with the surrounding plasma membrane, however the composition of the ciliary membrane differs from the plasma membrane. Compared to the plasma membrane, the ciliary membrane is enriched in sterols (Souto-Padron and de Souza, 1983), glycolipids (Bloodgood et al., 1995), and sphingolipids (Kaneshiro et al., 1984; Kaya et al., 1984). In addition, since inositol-5-phospatase INPP5E localizes to the cilium (Bielas et al., 2009; Jacoby et al., 2009), it might also be enriched in the products of INPP5, PI(4)P and PI(3,4)P2.

To prevent diffusion of lipids and transmembrane proteins there must be a membrane diffusion barrier. Expression of a GPI-anchored fluorescent protein in Malin-Darby Canine Kidney (MDCK) cells showed fluorescence along the complete apical membrane, with the exception of a black hole surrounding the site where the cilium protruded from the membrane (Vieira et al., 2006), showing that such a diffusion barrier exists. Intriguingly, the diameter of the 'black hole' is 1.2-1.8 μm, greater than the 0.3 μm diameter of the cilium, showing that the ciliary

membrane is larger than only the membrane covering the axoneme. This additional stretch of membrane could be an ideal spot for docking and fusion of vesicles. This theory is supported by immunocytochemical studies in frog retina, which showed rows of vesicles with rhodopsin fusing around the base of the cilium (Papermaster et al., 1985). The diameter of the site of vesicle fusion is similar to the 'black hole' observed with the GPI-anchored fluorescent protein in MDCK cells. In addition, there is an invagination of the plasma membrane directly next to the ciliary base, which is called the ciliary pocket (Anderson, 1972).

1.2.4. The transition zone

The region where the centriolar triplet microtubular structure converts into the axonemal doublet microtubular structure is annotated as the transition zone. Transmission electron microscopy showed that the transition zone contains Y-links, that connect the axonemal microtubules to the ciliary membrane (Muresan and Besharse, 1994). Several proteins that have been linked to the ciliopathies nephronophthisis and Meckel syndrome localize to the transition zone, and are components of the Y-links. The loss of one these proteins, NPHP6/CEP290, in *Chlamydomonas* alters the protein composition of the flagellum (Craige et al., 2010). Absence of NPHP-1 and NPHP-4 in *C. elegans*, results in mislocalization of certain proteins involved in intraflagellar transport, the transport system within the cilium (Jauregui et al., 2008). Also in a mammalian system ciliary proteins fail to localize to the cilium in the absence of a number of transition zone proteins (Garcia-Gonzalo et al., 2011). Thus, the transition zone proteins appear to be required for entry of ciliary proteins in the cilium.

1.3. The primary cilium as sensory organelle

Primary cilia act as cellular antennae for a variety of signaling pathways (Berbari et al., 2009; Singla and Reiter, 2006). There are two apparent advantages to signal transduction in the cilium. First, regulating ciliary localization of signal transducers allows modulation of signaling pathways. Secondly, it provides the option to concentrate signal transducers, since there is a diffusion barrier between the cilium and the cell body.

Primary cilia can detect both physical and biochemical extracellular signals. In the collecting duct of kidneys primary cilia act as mechanosensors. By an unknown mechanism polycystin-1, polycystin-2, and fibrocystin convert mechanical stimuli into a calcium influx in the cell body (Nauli et al., 2003). Examples of biochemical signals are the ligands PDGF-AA and PDGF-BB, who bind the ciliary receptor PDGFRαα (Schneider et al., 2005). Primary cilia also play a critical role in the function of two important developmental signaling pathways: Hedgehog (Hh) and Wnt signaling. Mutations disrupting ciliogenesis have diverse effects on the Hh and Wnt pathway (Caspary et al., 2007; Corbit et al., 2008; Gerdes et al., 2007; Huangfu and Anderson, 2005; Huangfu et al., 2003; Tran et al., 2008; Zhang et al., 2012), and several key components of the mammalian Hh and Wnt pathway, Ptch1, Smoothened, Gli2, Gli3, Su(fu), and Inv all localize to primary cilia (Corbit et al., 2005; Haycraft et al., 2005; Rohatgi et al., 2007; Watanabe et al., 2003). Examples in both vertebrates and nematodes show that primary cilia are essential for sensing the external environment. Photoreceptors are specialized primary cilia, and olfactory sensory neurons have multiple sensory cilia capable of detecting odorants (Berbari et al., 2009). A *C. elegans* hermaphrodite has 302 neurons, of which 60 neurons posses primary cilia (Inglis et al., 2007). Mutations in genes that affect ciliogenesis or cilia function

result in defects in chemotaxis and osmotic avoidance (Inglis et al., 2007), indicating that *C. elegans* also uses primary cilia to sense its external environment.

1.4. Intraflagellar Transport

Since cilia lack the machinery necessary for protein synthesis all proteins that function in cilia need to be transported there. Transport within the cilium is mediated by a specialized transport system, which is called intraflagellar transport (IFT). During IFT large protein complexes are transported from the base of the cilium, along the axonemal axis, towards the distal tip by kinesin motors (anterograde transport), and from the distal tip back to the cell body by dynein motors (retrograde transport). IFT was first visualized by DIC in *Chlamydomonas* (Kozminski et al., 1993). Later the process was also visualized in other model systems, including *C. elegans* (Orozco et al., 1999) and cultured kidney epithelial cells (Follit et al., 2006; Tran et al., 2008), using GFP-tagged components of the IFT complex, indicating that IFT is conserved among ciliated organisms. Using the different model organisms, most of the proteins that make up the IFT particle have been identified and characterized (components of the IFT machinery are summarized in Table 1). Comparative genomics has shown that these genes are conserved in ciliated organism, but not present in non-ciliated organisms like plants and fungi (Avidor-Reiss et al., 2004; Li et al., 2004). The IFT particle is made up of three different subcomplexes: the ciliary motor proteins, complex A and complex B (Cole and Snell, 2009). Proteins that are part of the BBSome, a large protein complex that has been proposed to be involved in the trafficking of membrane proteins to the cilium, have been shown to move inside cilia with the same velocities as IFT particles (Blacque et al., 2004; Lechtreck et al., 2009a; Nachury et al., 2007; Ou et al., 2007). This suggests that the BBSome associates with at least a subset of IFT particles. A schematic representation of the IFT machinery in the cilium is presented in figure 2.

1.4.1. Ciliary motor proteins

The main ciliary kinesin is kinesin-II, a heterotrimeric complex which belongs to the kinesin-2 family (Miki et al., 2005). Kinesin-II consists of two motor subunits, KIF3A and KIF3B, and a nonmotor subunit called KAP3 (Cole et al., 1992; Cole et al., 1993; Wedaman et al., 1996). The importance of kinesin-II for a functional cilium was first shown using a *Chlamydomonas* mutant, *fla10*^{ts}, containing a temperature-sensitive mutation in *Chlamydomonas'* orthologue of KIF3A (Kozminski et al., 1995). Inactivation of FLA10 in deflagellated *Chlamydononas* cells blocked the assembly of new flagella. When FLA10 was inactivated in flagellated *Chlamydononas* cells IFT was no longer observed and the flagella shortened. This showed that kinesin-II is required for both the assembly and maintenance of the flagellum in *Chlamydononas*. Studies in mouse, *Tetrahymena*, and *Drosophila* showed that kinesin-II is also required for cilia assembly in these organisms (Brown et al., 1999; Marszalek et al., 1999; Nonaka et al., 1998; Sarpal et al., 2003).

Interestingly, inactivation of kinesin-II in *C. elegans* does not block cilia assembly and IFT. This is explained by the presence of an additional ciliary kinesin in *C. elegans*, OSM-3. Only when both kinesins are absent the sensory neurons of *C. elegans* fail to assemble cilia (Snow et al., 2004). In vivo motility measurements, as well as in vitro microtubule gliding assays, showed that kinesin-II and OSM-3 cooperate to transport *C. elegans'* IFT particles (Pan et al., 2006; Snow et al., 2004). However, kinesin-II and OSM-3 do not cooperate along the whole microtubule axis of the sensory cilia, but only travel in the middle segments of the axoneme,

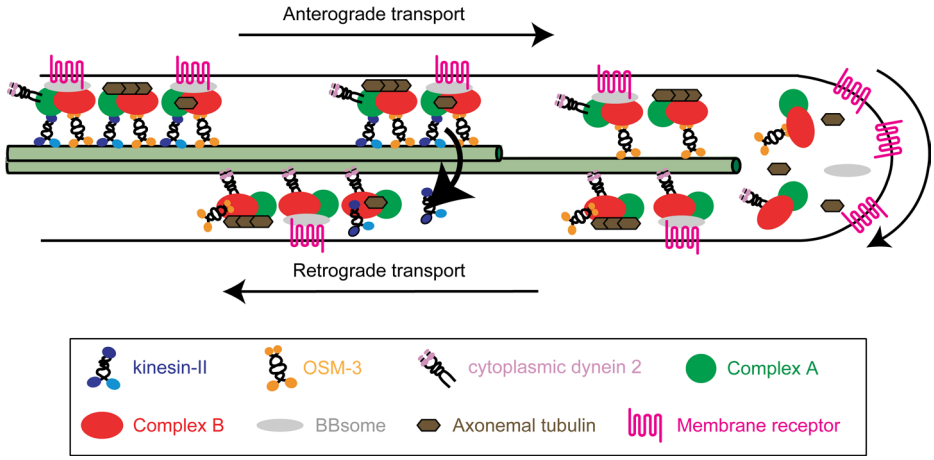

Figure 2. Intraflagellar transport machinery. Kinesin-II and OSM-3/KIF17 move IFT particles (composed of complex A, complex B, the BBsome, ciliary precursor proteins, signaling proteins, and cytoplasmic dynein 2) along the proximal segment of the cilium. In the sensory cilia of *C. elegans* and vertebrate photoreceptors (and likely more types of primary cilia), kinesin-II is removed at the end of the proximal segment, and OSM-3/KIF17 moves the IFT particles along the distal segment to the distal tip of the cilium. Cytosolic dynein 2 transports the IFT particles (now containing the kinesins and turnover products as cargo) back to the cell body.

which has microtubule doublets, whereas OSM-3 alone is responsible for anterograde IFT in the distal segment (Snow et al., 2004). This segmentation of the sensory cilia of *C. elegans* is similar to the structure of photoreceptor cilia invertebrates, which have a segment characterized by microtubule doublets, called the connecting cilium, and a segment characterized by microtubule singlets, called the outer segment (Ramamurthy and Cayouette, 2009; Reese, 1965). In several model organisms, kinesin-II has been shown to be restricted to the connecting cilium (Beech et al., 1996; Insinna et al., 2009; Muresan et al., 1999). However, the OSM-3 orthologue KIF17 localizes to both connecting cilium and outer segment, and is required for the formation of only the outer segment of the photoreceptor (Insinna et al., 2008). Together, this shows a resemblance between the IFT machinery in the sensory cilia of *C. elegans* and the photoreceptor cilia of vertebrates.

Additional kinesins have been found in genomic and proteomic screens for ciliary proteins (Avidor-Reiss et al., 2004; Blacque et al., 2005; Liu et al., 2007; Ostrowski et al., 2002; Pazour et al., 2005), some of which are still uncharacterized, while others, such as KLP-6, have been described to have clear ciliary functions. KLP-6 is expressed in the sensory neurons of *C. elegans* males, and is required for ciliary localization of polycystin-2 (Peden and Barr, 2005). In *C. elegans* polycystin-2 controls male mating behaviour (Peden and Barr, 2005) and in humans it functions in sensing fluid flow in the kidney (Nauli et al., 2003). In addition, dysfunction of this protein causes the ciliopathy polycystic kidney disease in humans (Hildebrandt et al., 2011). In the male-specifc CEM cilia of *klp-6* mutants the velocities of kinesin-II and OSM-3 are reduced (Morsci and Barr, 2011), but how this is achieved is unclear. A mammalian orthologue of KLP-6 exists, but has not yet been characterized. In vertebrates, KIF3A can form a heteromeric kinesin with both KIF3B and KIF3C (Muresan et al., 1998). In zebrafish, loss of *kif3c* alone

Table 1: Components of the IFT machinery; adapted from (Cole and Snell, 2009; Ishikawa and Marshall, 2011; Pedersen and Rosenbaum, 2008)

Subcomplex	Protein in H. sapiens	Protein in *C. elegans*	Protein in *Chlamydomonas*
Ciliary motors	KIF3A	KLP-20	FLA10
	KIF3B	KLP-11	FLA8
	KIFAP3	KAP-1	FLA3
	KIF17	OSM-3	-
	DYNC2H1	CHE-3	DHC1b
	DYNC2LI1	XBX-1	D1bLIC
	WDR34	DYCI-1	FAP133
	DYNLL1	DLC-4	FLA14
IFT Complex A	WDR19	DYF-2	FAP66
	IFT140	CHE-11	IFT140
	THM1	ZK328.7	FAP60
	IFT122	DAF-10	IFT122
	WDR35	IFTA-1	IFT121
	IFT43	-	IFT43
IFT Complex B	IFT172	OSM-1	IFT172
	IFT88	OSM-5	IFT88
	IFT81	IFT-81	IFT81
	IFT80	CHE-2	IFT80
	IFT74	IFT-74	IFT74/72
	TTC30A/B	DYF-1	IFT70
	IFT57	CHE-13	IFT57
	IFT54	DYF-11	IFT54
	IFT52	OSM-6	IFT52
	IFT46	DYF-6	IFT46
	IFT27	-	IFT27
	HSPB11	-	IFT25
	RABL5	IFTA-2	IFT22
	IFT20	IFT-20	IFT20
IFT complex A accessory	TULP3	TUB-1	TLP1
IFT complex B accessory	CLUAP1	DYF-3	FAP22
BBSome	BBS1	BBS-1	BBS1
	BBS2	BBS-2	-
	BBS4	F58A4.14	BBS4

	BBS5	BBS-5	BBS5
	BBS7	BBS-7	BBS7
	BBS8	BBS-8	BBS8
	BBS9	BBS-9	BBS9
	BBIP10	-	-

does not result in any obvious cilia defects, but loss of both *kif3c* and *kif3b* results in a more severe cilia defect than the loss of *kif3b* alone (Zhao et al., 2012). Moreover, overexpression of *kif3c* rescues cilia defects in *kif3b* mutant (Zhao et al., 2012). These data indicate that *kif3c* can act redundantly with *kif3b*. KIF3A and KIF3B knock out (KO) mouse die at midgestation (Marszalek et al., 1999; Nonaka et al., 1998), but KIF3C KO mice do not display any obvious phenotype (Yang et al., 2001). KIF7, a member of the kinesin-4 family, acts as a regulator of Hedgehog signaling (Cheung et al., 2009; Endoh-Yamagami et al., 2009; Hsu et al., 2011; Liem et al., 2009). KIF7 associates with Gli transcription factors, and is required for ciliary localization of GLI3 (Cheung et al., 2009; Endoh-Yamagami et al., 2009). Interestingly, KIF7 has been demonstrated to localize to both the basal body and the distal tip of mouse fibroblast cilia (Endoh-Yamagami et al., 2009; Liem et al., 2009). Whether KIF7 moves together with the IFT complex or moves alone is still unclear. In addition to KIF7, the closely related kinesin KIF27 also plays a role ciliary hedgehog signaling (Liem et al., 2009; Wilson et al., 2009). However, whether KIF27 also localizes to the primary cilium has not yet been determined.

Besides kinesins that function in cargo transport, the cilium also contains kinesins with other functions. In *Chlamydomonas*, KLP-1, a member of the kinesin-9 family, localizes to the central pair of microtubules and regulates the rate of flagellar beating (Yokoyama et al., 2004). In *Leishmania* and *Giardia* the microtubule depolymerising kinesin Kinesin-13 is involved in cilia length control (Blaineau et al., 2007; Dawson et al., 2007). Interestingly, Kinesin-13 requires the IFT machinery to be delivered to the distal tip (Piao et al., 2009).

The motor protein complex that is responsible for retrograde IFT is cytoplasmic dynein 2 (previously kown as cytoplasmic dynein 1b). Cytoplasmic dynein 2 is composed of a homodimeric heavy chain, DYNC2-H1 (Pazour et al., 1999), a light intermediate chain, DYNC2LI1 (Hou et al., 2004), an intermediate chain, WDR34 (Rompolas et al., 2007), and a light chain, DYNLL1 (Pazour et al., 1998). Biochemical studies demonstrated that these four proteins are part of the same complex (Perrone et al., 2003; Rompolas et al., 2007). Mutants for the different components of cytoplasmic dynein 2, in *Chlamydomonas, C. elegans,* and mouse, have stunted cilia which contain accumulations of IFT particles (Huangfu and Anderson, 2005; May et al., 2005; Orozco et al., 1999; Pazour et al., 1999; Pazour et al., 1998; Porter et al., 1999; Rana et al., 2004; Schafer et al., 2003; Wicks et al., 2000). When compared to anterograde IFT, retrograde IFT has received little attention, leaving much to explore on the composition, function, and regulation of retrograde IFT.

1.4.2. IFT complexes A and B

IFT particles where first isolated from the flagella of *Chlamydomonas* using sucrose density gradient centrifugation (Piperno and Mead, 1997). They were found to consist of two sub-

complexes (IFT-A and IFT-B) that dissociate at increased ionic strength (Cole et al., 1998). Sub-complex A is composed of four proteins (IFT144, IFT140, IFT139 and IFT122), and sub-complex B of eleven proteins (IFT172, IFT88, IFT81, IFT80, IFT 74/72, IFT57/55, IFT52, IFT46, IFT27, and IFT20). Later two more complex A proteins (IFT121 and IFT43), and four more complex B proteins (IFT70, IFT54, IFT25 and IFT22) have been identified (Bacaj et al., 2008; Blacque et al., 2006; Follit et al., 2009; Kunitomo and Iino, 2008; Lechtreck et al., 2009b; Li et al., 2008; Omori et al., 2008; Ou et al., 2005; Piperno et al., 1998; Schafer et al., 2006; Wang et al., 2009). The distinction of subcomplex A and B is not just biochemical, but also functional. Mutations in IFT-A proteins result in short and stumpy cilia with bulges filled with IFT proteins (Arts et al., 2011; Iomini et al., 2009; Piperno et al., 1998), which is similar to depletion of cytoplasmic dynein 2 subunits. Mutations in IFT-B proteins lead to absent or very short cilia (Cole, 2003). This difference in phenotype led to the idea that IFT-A and IFT-B complexes function specifically in retrograde and anterograde transport, respectively.

The most probable function of subcomplex A and B is to link cargo proteins to the motor proteins, to get the cargo transported from the base of the cilium to the distal tip and back. For this, IFT proteins need to interact among themselves, with cargo and with the ciliary kinesin and dynein complexes. After depletion of THM1/IFT139 and WDR35/IFT121, a complex of WDR19/IFT144, IFT140, and IFT122 remained (Mukhopadhyay et al., 2010), which suggests that these three proteins form the "core" of IFT-A, and that THM1/IFT139, WDR35/IFT121 and IFT43 act as "peripheral" proteins. Recently, biochemical analysis confirmed that WDR19/IFT144, IFT140, and IFT122 indeed form a heterotrimeric stable core complex (Behal et al., 2012). In addition, it was shown that WDR35/IFT121 directly interacts with THM1/IFT139, and with IFT43 (Behal et al., 2012). Sub-complex A associates with IFT complex A accessory protein TULP3, and both TULP3 and the IFT-A "core" proteins are necessary for ciliary localization of the GPCRs Sstr3 and Mchr1, but are not required for ciliary localization of the Hh-associated GPCR Smoothened (Mukhopadhyay et al., 2010). Further studies are needed to determine how sub-complex A interacts with the motor proteins, sub-complex B, and possibly the BBSome.

Sub-complex B was initially found to dissociate from sub-complex A at increased ionic strength (> 50 mM NaCl) (Cole et al., 1998). Purification of the IFT complex at even higher ionic strength (300 mM NaCl) led to the dissociation of four more "weakly" bound subunits, leaving behind the IFT-B "core" complex, which consist of IFT88/81/74/72/52/46/27 (Lucker et al., 2005). Yeast two-hybrid studies showed that IFT81 interacts with itself and with IFT74/72 (Lucker et al., 2005), and that IFT27 and IFT25 interact with each other (Follit et al., 2009; Rual et al., 2005; Wang et al., 2009). Recombinantly co-expressed IFT81/ IFT74/72/IFT27/IFT25 can form a stable complex (Taschner et al., 2011). This complex associates with IFT52, which in turn directly interacts with IFT88, IFT70, and IFT46 (Taschner et al., 2011). IFT88/IFT70/IFT46/IFT52 can also form a stable complex in vitro (Taschner et al., 2011). All complex B proteins are conserved among ciliated organisms, with the exception of IFT27 and IFT25, which are present in mammals and *Chlamydomonas*, but not in *C. elegans* and *Drosophila*. IFT27 and IFT25 have been shown to interact with each other in *Chlamydomonas*, mouse, and human (Follit et al., 2009; Rual et al., 2005; Wang et al., 2009), and are not required for cilia assembly (Keady et al., 2012). IFT27 is a Rab-like small G protein, and lacks the protein-protein interaction domains found in other IFT proteins (Qin et al., 2007). IFT25 has been proposed to couple Hh component to the IFT complex

(Keady et al., 2012). Of the remaining five "peripheral" complex B proteins (IFT172, IFT80, IFT57, IFT54, and IFT20), IFT172 appears to be required for the transition of anterograde to retrograde transport at the distal tip (Pedersen et al., 2005; Tsao and Gorovsky, 2008). IFT54 could be the link between the IFT complex and the membrane-associated complexes. It directly interacts with Rabaptin-5, which in turn interacts with the small GTPase Rab8 (Omori et al., 2008). Rab8 is important for transport of vesicles to the ciliary base and their subsequent fusion (Nachury et al., 2007). IFT54 interacts with another complex B protein, IFT20 (Omori et al., 2008). IFT20 localizes to both the cilium and the Golgi apparatus (Follit et al., 2006); this localization pattern is unique among the IFT proteins.

1.4.3. The BBSome

Bardet-Biedl syndrome (BBS) is a ciliopathy characterized by obesity, mental retardation, retinal degeneration, and cystic kidneys (Zaghloul and Katsanis, 2009). Thus far mutations in 14 genes have been linked to this ciliopathy, and seven of these BBS proteins (BBS1, BBS2, BBS4, BBS5, BBS7, BBS8, and BBS9) together form a complex that is known as the BBSome (Nachury et al., 2007). In *Chlamydomonas*, *C. elegans*, as well as in cultured in mammalian cells, BBS proteins have been shown to move along the axoneme, with similar rates as motor proteins and IFT complex A and B proteins (Blacque et al., 2004; Lechtreck et al., 2009a; Nachury et al., 2007; Ou et al., 2005; Ou et al., 2007). In mouse BBS knockout models, many cells do still assemble cilia, although sometimes with minor structural defects (Davis et al., 2007; Mykytyn et al., 2004; Nishimura et al., 2004; Ross et al., 2005; Zhang et al., 2011). In *C. elegans*, loss-of-function mutation of *bbs-1*, *bbs-7*, or *bbs-8* results in dissociation of complex A and B, where complex A is transported by kinesin-II and complex B by OSM-3 (Ou et al., 2005; Ou et al., 2007). In the neurons of *Bbs2*-/- and *Bbs4*-/- mice the GPCRs SSTR3 and MCHR1 no longer localize to the cilium (Berbari et al., 2008). In *C. elegans* a TRPV channel, OSM-9, mislocalizes and accumulates near the transition zone in *bbs-7* and *bbs-8* mutant animals (Tan et al., 2007). Thus, BBS proteins are not required for cilia assembly, but appear to be required for transport of specific cargo, and to maintain integrity of the IFT complex.

1.5. Membrane trafficking to the cilium

For its function the cilium depends on the delivery of specific proteins and lipids. This could be achieved in two ways, specific proteins/lipids that reside in the plasma membrane could cross the diffusion barrier that separate the plasma membrane from ciliary membrane, or by direct delivery of vesicles, from the Golgi apparatus at the ciliary base. Although there are some examples of the former (Hunnicutt et al., 1990; Milenkovic et al., 2009), the latter model is currently more accepted. Targeting of vesicles with membrane proteins to the cilium appears to be mediated by specific ciliary targeting sequences (CTS), of which several have been identified in a number of ciliary proteins (reviewed in (Pazour and Bloodgood, 2008)). The mechanisms behind sorting and transporting membrane proteins destined for the cilium are far from understood, but recent studies have identified several key proteins involved. The CTSs of rhodopsin, polycystin-1 and polycystin-2 are recognized by the small GTPase Arf4 (Deretic et al., 2005; Ward et al., 2011), which then forms a ciliary targeting complex together with ASAP1, Rab11 and FIP3 (Mazelova et al., 2009). The CTS of fibrocystin, which has no similarity with the CTS of rhodopsin and the two polycystins, is recognized by a different small GTPase, Rab8 (Follit et al., 2010). Rab8

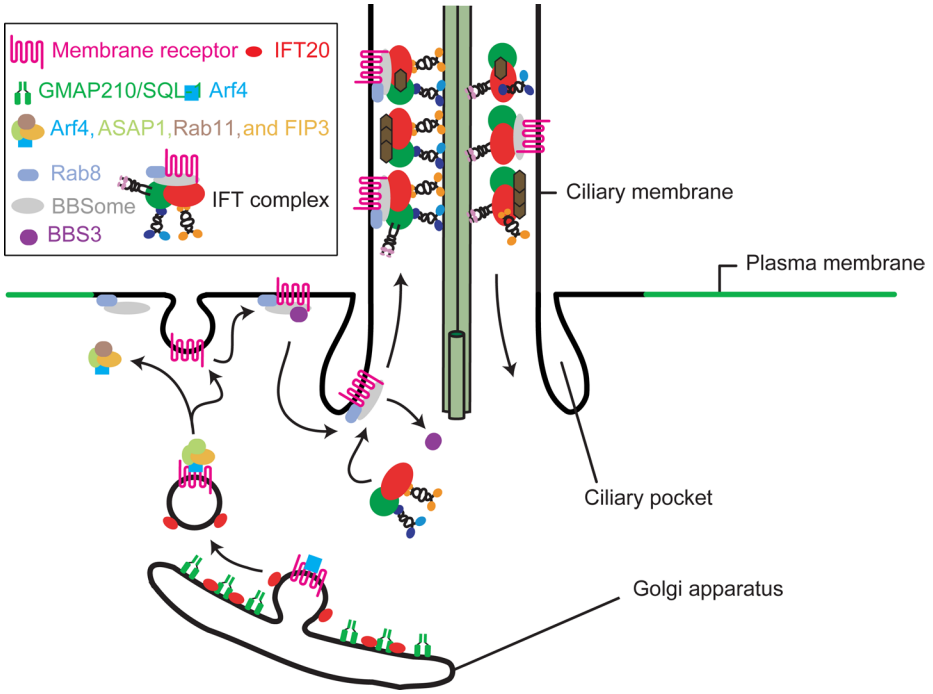

Figure 3. Membrane trafficking to the cilium. Vesicles containing specific cargo destined for the cilium are derived from the Golgi apparatus. Membrane receptors are thought to be recognized by Arf4, and targeted to the ciliary base by a complex composed of ASAP1, Rab11 and FIP3. In addition to membrane receptors, these post-Golgi vesicles also contain the adaptor/complex B protein IFT20. GMAP210/SQL-1, which anchors IFT20 to the Golgi membrane, is not present on these vesicles. Once the vesicles with membrane receptors arrive at the ciliary base they fuse with the ciliary membrane. This process is thought to be facilitated by Rab8 and possibly the BBSome. At the ciliary base the membrane receptors are recognized by IFT particles, and transported to the distal tip.

localizes to the cilium, and has been implicated in the docking and fusion of post-Golgi vesicles at the base of the cilium (Moritz et al., 2001; Mukhopadhyay et al., 2008; Nachury et al., 2007). The CTS of SSTR3 is recognized by the BBSome, and upon binding of SSTR3's CTS the BBSome is recruited to the cilium by BBS3/Arl6 (Jin et al., 2010). Interestingly, the BBSome associates with Rabin8, a guanine exchange factor for Rab8 and Rab11 (Knodler et al., 2010; Nachury et al., 2007).

In addition to the small GTPases discussed above, IFT complex proteins also function in membrane trafficking to the cilium. Complex B protein IFT20 is unique among the IFT complex proteins, because it localizes to the Golgi apparatus, in addition to the cilium and basal body (Follit et al., 2006). A complete knockdown of IFT20 blocks cilia assembly, but interestingly a moderate knockdown of IFT20 prevents the ciliary localization of the membrane protein polycystin-2, likely because of reduced transport from the Golgi apparatus (Follit et al., 2006). IFT20 is anchored to the Golgi apparatus by the Golgin protein GMAP210 (Follit et al., 2008). GMAP210 mutant cells also have less polycystin-2 localized to the cilium (Follit et al., 2008). IFT20 directly interacts with another complex B protein, IFT54 (Follit et al., 2009; Li et al.,

2008; Omori et al., 2008), which associates with Rab8 through Rabaptin-5 (Omori et al., 2008). A schematic representation of membrane trafficking to the cilium (based on current literature) is shown in figure 3.

1.6. Regulation of ciliogenesis

The timing of assembly and disassembly of the cilium is coupled to cell cycle progression. Cilia are assembled during G1 or G0, and disassembled prior to mitosis. Conditions that influence whether a non-dividing cell will assemble a cilium are cell confluence, fluid flow, and cell spreading (Besschetnova et al., 2010; Iomini et al., 2004; Pitaval et al., 2010). Different cell types possess cilia of different lengths, as well as morphology, suggesting that cilia length is subject to cell type specific regulation (Satir and Christensen, 2007). Furthermore, there are increasing numbers of examples showing that external cues can modulate cilia length (Miyoshi et al., 2011).

1.6.1. Assembly of the cilium

The formation of a primary cilium starts with the migration and docking of the mother centriole at the plasma membrane, which is followed by the transition of the mother centriole into a basal body (Santos and Reiter, 2008). This transition comprises the formation of ciliary rootlets, and the modification of the distal appendages and subdistal appendages into transition fibers and basal feet, respectively (Hoyer-Fender, 2010; Kobayashi and Dynlacht, 2011). The nine microtubule doublets subsequently extend from nine microtubule triplets of the basal body, which is mediated by IFT. The molecular pathways that control the decision of the cell to start cilia assembly are unknown, but there is some knowledge on how premature formation of cilia is prevented. Two centrosomal proteins, Cep97 and CP110, actively suppress cilia formation; Cep97 by recruiting CP110, and CP110 by capping the distal end of the distal centriolar microtubules (Spektor et al., 2007). CP110 was found to interact with Cep290, and this interaction is required for CP110 to prevent cilia assembly (Tsang et al., 2008). CP110 also interacts with a depolymerising kinesin, KIF24, which is predicted to counteract microtubule polymerization by remodelling microtubules at the distal end of centrioles that could otherwise lead to premature formation of cilia (Kobayashi et al., 2011).

1.6.2. Regulation of cilium length (by IFT)

Cilium length is not fixed, but can be modified, both by structural proteins and signaling proteins. An overview of cilia length altering proteins is shown in table 2. Structural proteins that can modify cilia length include basal body and transition zone proteins. In MEFs, loss of Tctn1, Tctn2, Tmem67 and Cc2d2, four transition zone proteins that form a multimeric protein complex, has been demonstrated to result in shorter cilia (Garcia-Gonzalo et al., 2011). Depletion of another transition zone protein, NPHP-8, in ciliated hTERT-RPE1 cells results in elongation of primary cilia (Patzke et al., 2010). Conversely, basal body protein Nde1 negatively regulates cilia length in hTERT-RPE1 cells, as well as in zebrafish embryos (Kim et al., 2011). Cilia length modulation by basal body and transition zone proteins could be explained by their proposed function in the recruitment of ciliary proteins from the cell body to the cilium. Cilia length can also be regulated by modification of axoneme stability. For example, two microtubule-associated proteins (MAPs), RP1 and DCDC2, positively regulate cilia length (Massinen et al.,

2011; Omori et al., 2010).

The majority of proteins that regulate cilia length are signaling proteins. Especially kinases have been found to regulate cilia length (Asleson and Lefebvre, 1998; Bengs et al., 2005; Berman et al., 2003; Bradley and Quarmby, 2005; Burghoorn et al., 2007; Ko et al., 2010; Miyoshi et al., 2009; Omori et al., 2010; Smith et al., 2006; Sohara et al., 2008; Tam et al., 2007; Thiel et al., 2011; Wang et al., 2006; Wloga et al., 2006), but also phosphatases (Clement et al., 2011; Kim et al., 2010) and G proteins (Burghoorn et al., 2010). Currently, it is largely unknown how signaling proteins mechanistically alter cilia length. They could act through structural proteins, like for example MAK (male germ cell-associated protein kinase), which acts through RP1 (Omori et al., 2010). However, in order for the cilium to increase in length, the IFT machinery has to deliver additional axonemal subunits at the distal tip, more than what is necessary to compensate for the continuous turnover of axonemal subunits when the cilium remains the same length. An influx of axonemal precursor proteins at the distal tip could be achieved by several changes in the IFT machinery, such as IFT particle size, IFT velocity, frequency of IFT events, and cargo selection. Therefore, it is likely that IFT plays an important role in the regulation of cilia length.

Because of the presence of two ciliary segments, two different ciliary kinesins, and the relative ease with which IFT can be visualized, the sensory cilia of *C. elegans'* amphid neurons provide an excellent model to study the regulation of IFT. The sensory cilia of *C. elegans'* amphid neurons can be divided in a middle segment, which has nine microtubule doublets, and a distal segment, which has nine microtubule singlets (Perkins et al., 1986; Ward et al., 1975). In the middle segment IFT is mediated by two members of the kinesin-2 family, kinesin-II and OSM-3, at a velocity of 0.7 μm/s (Figure 4A) (Snow et al., 2004). At the end of the middle segment kinesin-II dissociates from the complex, and OSM-3 moves alone at 1.2 μm/s in the distal segment (Figure 4A) (Snow et al., 2004). The intrinsic velocity of kinesin-II, for example in an *osm-3* mutant, is 0,5 μm/s (Snow et al., 2004). Thus, the velocity of IFT in the middle segment, where kinesin-II and OSM-3 cooperate to transport IFT particles, of 0.7 μm/s, is the intermediate velocity of the 'slow' kinesin-II and the 'fast' OSM-3.

Members of the family of *ros* cross-hybridizing kinases (RCKs) have been shown to negatively regulate cilia length in several organisms (Bengs et al., 2005; Berman et al., 2003; Burghoorn et al., 2007; Omori et al., 2010). Live imaging in *C. elegans* showed that the RCK *dyf-5* can modulate IFT. In *dyf-5* mutant animals kinesin-II is no longer restricted to the middle segment, and OSM-3 moves at a reduced speed and separately from kinesin-II and the IFT complex (Figure 4B) (Burghoorn et al., 2007). This indicates that *dyf-5* acts as a negative cilia length regulator by regulating the docking and undocking of ciliary motors from IFT particles.

In response to harsh environmental condition or overcrowding *C. elegans* enters an alternative developmental stage, called dauer (Cassada and Russell, 1975). During dauer formation the position and structure of several cilia are altered (Albert and Riddle, 1983). Interestingly, in animals exposed to dauer pheromone (a pheromone that induces entry into the dauer stage) the coordination of kinesin-II and OSM-3 appears to be affected (Burghoorn et al., 2010). Live imaging of IFT in the amphid channel cilia of these animals showed that kinesin-II moved at ~0.6 μm/s, OSM-3 at ~0.9 μm/s, and complex A and B proteins at ~0.7 μm/s (Burghoorn et al., 2010). Taken together, these velocities suggest that in pheromone-treated animals some

Table 2: Proteins that alter cilia length in vertebrates; adapted from (Avasthi and Marshall, 2011)

Name protein	Type/Class	Affects cilia length positively (↑) or negatively (↓)	Reference
RP1	MT associated protein	↑	(Liu et al., 2003)
DCDC2	MT associated protein	↑	(Massinen et al., 2011)
NPHP-8	Transition zone protein	↓	(Patzke et al., 2010)
Tctn1	Transition zone protein	↑	(Garcia-Gonzalo et al., 2011)
Tctn2	Transition zone protein	↑	(Garcia-Gonzalo et al., 2011)
Tmem67	Transition zone protein	↑	(Garcia-Gonzalo et al., 2011)
CC2D2A	Transition zone protein	↑	(Garcia-Gonzalo et al., 2011)
Nde1	Centrosomal protein	↓	(Kim et al., 2011)
Bromi	GTPase activating protein	↑	(Ko et al., 2010)
Tsc1	GTPase activating protein	↓	(DiBella et al., 2009)
Tsc2	GTPase activating protein	↓	(Bonnet et al., 2009)
Rab8	Small GTPase	↑	(Nachury et al., 2007)
PLA2G3	Phospholipase	↓	(Kim et al., 2010)
HDAC6	Histone deacetylase	↑	(Pugacheva et al., 2007)
HEF1	Scaffolding protein	↑	(Pugacheva et al., 2007)
Foxj1	Transcription factor	↓	(Cruz et al., 2010)
ACTR3	Actin-related protein	↓	(Kim et al., 2010)
Notch	Transmembrane protein	↑	(Lopes et al., 2010)
Fleer	TC repeat protein	↑	(Pathak et al., 2007)
KIF17	Kinesin	↑	(Insinna et al., 2008)
Nek8	Kinase	↓	(Smith et al., 2006)
Nek1	Kinase	↑	(Thiel et al., 2011)
Nek4	Kinase	↑	(Coene et al., 2011)
MAK	Kinase	↓	(Omori et al., 2010)
Aurora A	Kinase	↑	(Pugacheva et al., 2007)
S6k1	Kinase	↑	(Yuan et al., 2012)
Gsk3β	Kinase	↓	(Miyoshi et al., 2009)
AC III	Adenylate cyclase	↓	(Ou et al., 2009)
Cdc14B	Phosphatase	↑	(Clement et al., 2011)
PTPN23	Phosphatase	↓	(Kim et al., 2010)
Fgfr1	Receptor	↑	(Neugebauer et al., 2009)

IFT particles are transported only by kinesin-II, while others are transported only by OSM-3, in addition to the 'normal' IFT complex transported by both ciliary kinesins (Figure 4B). Animals with a mutation of the sensory Gα subunit *gpa-3* do not enter dauer stage (Zwaal et al., 1997). Interestingly, mutation of *gpa-3* affects the coordination of the IFT kinesins very similar to exposure to dauer pheromone, and these effects are not cumulative, suggesting that *gpa-3* functions in the same pathway as dauer pheromone to regulate the coordination of IFT kinesins. These data suggest that external cues can alter cilia length, and that this is achieved by modulation of IFT.

In addition to studies in *C. elegans*, there are also examples described of modulation of cilia length by regulation of IFT in *Chlamydomonas* and cultured mammalian cells. In *Chlamydomonas*, it has been shown that directly after flagellar regeneration IFT particle size increases, while IFT velocity decreases (Engel et al., 2009). However, in fully elongated flagella particle size decreases again, and IFT velocity increases (Engel et al., 2009). The quantity of IFT proteins is the same in long and short flagella (Engel et al., 2009; Marshall et al., 2005). These data suggest that in short, elongating flagella IFT particles form long and slow moving trains, while in long, fully elongated flagella IFT particles form short and fast moving particles. Intriguingly, similar experiments in cultured kidney epithelium cells gave conflicting results. The length of primary cilia of cultured kidney epithelium cells can be increased by either a decrease of intracellular calcium or by an increase of intracellular cAMP (Besschetnova et al., 2010). Interestingly, when elongation of primary cilia was induced in this way, the velocity of IFT particles moving in the anterograde direction was increased, but the velocity of IFT particles moving in the retrograde direction was not affected (Besschetnova et al., 2010). These data suggest a model where an increase of anterograde IFT velocity, with no changes in retrograde IFT velocity, results in increased delivery of axonemal precursors, and leads to elongation of cilia length.

1.6.4. Disassembly of the cilium

Removal of the primary cilium, for example to allow cell division to proceed, can occur via two different mechanisms, either by deciliation, or by resorption. The fastest mechanism by which a cell can remove its cilium is by shedding its cilium (a process known as deciliation). This process has been observed in both *Chlamydomonas* and cultured mammalian cells, and it occurs as a result of environmental stress, or in order to facilitate rapid re-entry into the cell cycle (Overgaard et al., 2009; Quarmby, 2004). In *Chlamydomonas*, a microtubule-severing protein, Katanin, has been described to cleave the axoneme between the basal body and the transition zone prior to deflagellation (Rasi et al., 2009). Resorption of *Chlamydomonas'* flagella is accompanied by an increased number of empty IFT particles moving in the anterograde direction, while IFT particles moving in the retrograde direction continue to return ciliary proteins to the cell body (Pan and Snell, 2005). A decrease or complete stop of delivery of axoneme subunits to the distal tip, while disassembly products continue to be transported back to the cell body, would eventually lead to the resorption of the flagellum. In cultured mammalian cells IFT proteins are required for the disassembly of primary cilia (Pugacheva et al., 2007), suggesting that IFT-mediated resorption of cilia is conserved.

Several proteins promote the disassembly of primary cilia. One of these proteins, Pitchfork (Pifo) accumulates at the basal body during cilia disassembly, where it activates Aurora A kinase (Kinzel et al., 2010). Aurora A kinase, in turn, activates a microtubule deacetylase HDAC6,

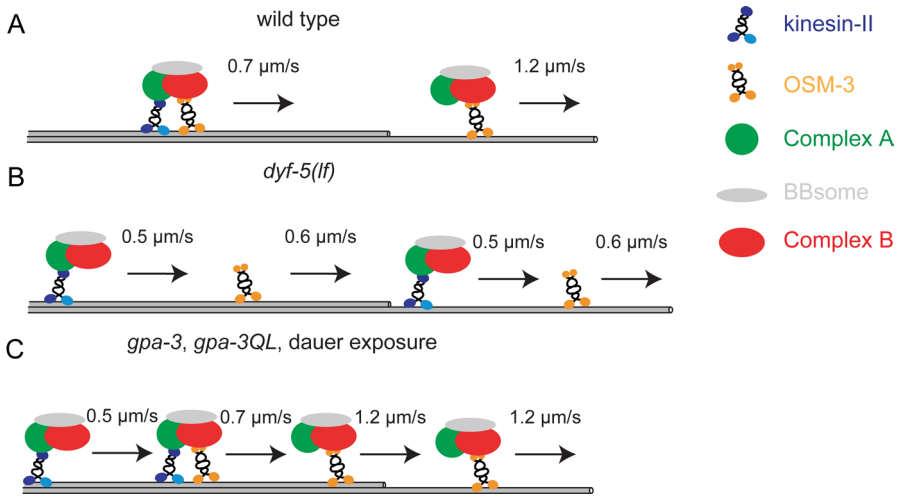

Figure 4. Examples of regulation of IFT in *C. elegans*. (A) In wild type animals IFT particles in the middle segment of the amphid channel cilia are transported by both OSM-3 and kinesin-II, after the middle segment kinesin-II is removed, and the IFT complex is transported by OSM-3 (Snow et al., 2004). (B) In *dyf-5* animals kinesin-II and OSM-3 no longer travel together, the IFT complex associates only with kinesin-II, kinesin-II can move into the distal segment and the velocity of OSM-3 alone is lower than the normal 1.2 µm/s (Burghoorn et al., 2007). (C) In *gpa-3(lf)* and *gpa-3QL* animals, and in animals exposed to dauer pheromone the IFT particles are partially uncoupled, generating additional IFT particles transported only by kinesin-II and only by OSM-3 (Burghoorn et al., 2010).

which deacetylates, and destabilizes axonemal microtubules (Pugacheva et al., 2007). A light chain subunit of cytoplasmic dynein Tctex-1 is recruited to the transition zone before S phase, where it controls cilia disassembly (Li et al., 2011). Flagellar proteins have been found to be labelled with ubiquitin during flagellar resorption (Huang et al., 2009), suggesting that the ubiquitination system also plays a role in cilia/flagella resorption.

1.7. Ciliopathies

Because of the important sensory and motile function of cilia it is no surprise that ciliary dysfunction has been linked to several genetic diseases, which are collectively ciliopathies. As a result of the role of primary cilia in developmental signaling pathways, such as Wnt and Hh, mutations that block ciliogenesis result in lethality early in embryogenesis. Therefore, mutations that cause ciliopathies often result in only minor defects, such as small changes in cilia morphology and/or mislocalization of ciliary signaling proteins. Currently, more than a dozen diseases are considered ciliopathies, which include Joubert syndrome, nephronophthisis, Senior-Loken syndrome, oral–facial–digital syndrome, Jeune syndrome, autosomal dominant and recessive polycystic kidney disease, Leber congenital amaurosis, Meckel-Gruber syndrome, Bardet-Biedl syndrome, Usher syndrome, and retinitis pigmentosa (Novarino et al., 2011). Common conditions observed in ciliopathy patients include polydactyly, cystic kidneys, retinal degradation, situs inversus, and mental retardation (Baker and Beales, 2009). A better understanding of cilia biology would provide increased insights into the molecular mechanisms involved in these disorders.

References

Albert, P.S., and D.L. Riddle. 1983. Developmental alterations in sensory neuroanatomy of the Caenorhabditis elegans dauer larva. *J Comp Neurol*. 219:461-81.

Anderson, R.G. 1972. The three-dimensional structure of the basal body from the rhesus monkey oviduct. *J Cell Biol*. 54:246-65.

Anderson, R.G. 1974. Isolation of ciliated or unciliated basal bodies from the rabbit oviduct. *J Cell Biol*. 60:393-404.

Arts, H.H., E.M. Bongers, D.A. Mans, S.E. van Beersum, M.M. Oud, E. Bolat, L. Spruijt, E.A. Cornelissen, J.H. Schuurs-Hoeijmakers, N. de Leeuw, V. Cormier-Daire, H.G. Brunner, N.V. Knoers, and R. Roepman. 2011. C14ORF179 encoding IFT43 is mutated in Sensenbrenner syndrome. *J Med Genet*.

Asleson, C.M., and P.A. Lefebvre. 1998. Genetic analysis of flagellar length control in Chlamydomonas reinhardtii: a new long-flagella locus and extragenic suppressor mutations. *Genetics*. 148:693-702.

Avidor-Reiss, T., A.M. Maer, E. Koundakjian, A. Polyanovsky, T. Keil, S. Subramaniam, and C.S. Zuker. 2004. Decoding cilia function: defining specialized genes required for compartmentalized cilia biogenesis. *Cell*. 117:527-39.

Bacaj, T., Y. Lu, and S. Shaham. 2008. The conserved proteins CHE-12 and DYF-11 are required for sensory cilium function in Caenorhabditis elegans. *Genetics*. 178:989-1002.

Baker, K., and P.L. Beales. 2009. Making sense of cilia in disease: the human ciliopathies. *Am J Med Genet C Semin Med Genet*. 151C:281-95.

Beech, P.L., K. Pagh-Roehl, Y. Noda, N. Hirokawa, B. Burnside, and J.L. Rosenbaum. 1996. Localization of kinesin superfamily proteins to the connecting cilium of fish photoreceptors. *J Cell Sci*. 109 (Pt 4):889-97.

Behal, R.H., M.S. Miller, H. Qin, B.F. Lucker, A. Jones, and D.G. Cole. 2012. Subunit Interactions and Organization of the Chlamydomonas reinhardtii Intraflagellar Transport Complex A Proteins. *J Biol Chem*. 287:11689-703.

Bengs, F., A. Scholz, D. Kuhn, and M. Wiese. 2005. LmxMPK9, a mitogen-activated protein kinase homologue affects flagellar length in Leishmania mexicana. *Mol Microbiol*. 55:1606-15.

Berbari, N.F., J.S. Lewis, G.A. Bishop, C.C. Askwith, and K. Mykytyn. 2008. Bardet-Biedl syndrome proteins are required for the localization of G protein-coupled receptors to primary cilia. *Proc Natl Acad Sci U S A*. 105:4242-6.

Berbari, N.F., A.K. O'Connor, C.J. Haycraft, and B.K. Yoder. 2009. The primary cilium as a complex signaling center. *Curr Biol*. 19:R526-35.

Berman, S.A., N.F. Wilson, N.A. Haas, and P.A. Lefebvre. 2003. A novel MAP kinase regulates flagellar length in Chlamydomonas. *Curr Biol*. 13:1145-9.

Besschetnova, T.Y., E. Kolpakova-Hart, Y. Guan, J. Zhou, B.R. Olsen, and J.V. Shah. 2010. Identification of signaling pathways regulating primary cilium length and flow-mediated adaptation. *Curr Biol*. 20:182-7.

Bielas, S.L., J.L. Silhavy, F. Brancati, M.V. Kisseleva, L. Al-Gazali, L. Sztriha, R.A. Bayoumi, M.S. Zaki, A. Abdel-Aleem, R.O. Rosti, H. Kayserili, D. Swistun, L.C. Scott, E. Bertini, E. Boltshauser, E. Fazzi, L. Travaglini, S.J. Field, S. Gayral, M. Jacoby, S. Schurmans, B. Dallapiccola, P.W. Majerus, E.M. Valente, and J.G. Gleeson. 2009. Mutations in INPP5E, encoding inositol polyphosphate-5-phosphatase E, link phosphatidyl inositol signaling to the ciliopathies. *Nat Genet*. 41:1032-6.

Blacque, O.E., C. Li, P.N. Inglis, M.A. Esmail, G. Ou, A.K. Mah, D.L. Baillie, J.M. Scholey, and M.R. Leroux. 2006. The WD repeat-containing protein IFTA-1 is required for retrograde intraflagellar transport. *Mol Biol Cell*. 17:5053-62.

Blacque, O.E., E.A. Perens, K.A. Boroevich, P.N. Inglis, C. Li, A. Warner, J. Khattra, R.A. Holt, G. Ou, A.K. Mah, S.J. McKay, P. Huang, P. Swoboda, S.J. Jones, M.A. Marra, D.L. Baillie, D.G. Moerman, S. Shaham, and M.R. Leroux. 2005. Functional genomics of the cilium, a sensory organelle. *Curr Biol*. 15:935-41.

Blacque, O.E., M.J. Reardon, C. Li, J. McCarthy, M.R. Mahjoub, S.J. Ansley, J.L. Badano, A.K. Mah, P.L. Beales, W.S. Davidson, R.C. Johnsen, M. Audeh, R.H. Plasterk, D.L. Baillie, N. Katsanis, L.M. Quarmby, S.R. Wicks, and M.R. Leroux. 2004. Loss of C. elegans BBS-7 and BBS-8 protein function results in cilia defects and compromised intraflagellar transport. *Genes Dev*. 18:1630-42.

Blaineau, C., M. Tessier, P. Dubessay, L. Tasse, L. Crobu, M. Pages, and P. Bastien. 2007. A novel microtubule-depolymerizing kinesin involved in length control of a eukaryotic flagellum. *Curr Biol*. 17:778-82.

Bloodgood, R.A., M.P. Woodward, and W.W. Young. 1995. Unusual distribution of a glycolipid antigen in the flagella of Chlamydomonas. *Protoplasma*. 185:123-130.

Bradley, B.A., and L.M. Quarmby. 2005. A NIMA-related kinase, Cnk2p, regulates both flagellar length and cell size in Chlamydomonas. *J Cell Sci*. 118:3317-26.

Brown, J.M., C. Marsala, R. Kosoy, and J. Gaertig. 1999. Kinesin-II is preferentially targeted to assembling cilia and is required for ciliogenesis and normal cytokinesis in Tetrahymena. *Mol Biol Cell*. 10:3081-96.

Burghoorn, J., M.P. Dekkers, S. Rademakers, T. de Jong, R. Willemsen, and G. Jansen. 2007. Mutation of the MAP

kinase DYF-5 affects docking and undocking of kinesin-2 motors and reduces their speed in the cilia of Caenorhabditis elegans. *Proc Natl Acad Sci U S A*. 104:7157-62.

Burghoorn, J., M.P. Dekkers, S. Rademakers, T. de Jong, R. Willemsen, P. Swoboda, and G. Jansen. 2010. Dauer pheromone and G-protein signaling modulate the coordination of intraflagellar transport kinesin motor proteins in C. elegans. *J Cell Sci*. 123:2077-84.

Caspary, T., C.E. Larkins, and K.V. Anderson. 2007. The graded response to Sonic Hedgehog depends on cilia architecture. *Dev Cell*. 12:767-78.

Cassada, R.C., and R.L. Russell. 1975. The dauerlarva, a post-embryonic developmental variant of the nematode Caenorhabditis elegans. *Dev Biol*. 46:326-42.

Cheung, H.O., X. Zhang, A. Ribeiro, R. Mo, S. Makino, V. Puviindran, K.K. Law, J. Briscoe, and C.C. Hui. 2009. The kinesin protein Kif7 is a critical regulator of Gli transcription factors in mammalian hedgehog signaling. *Sci Signal*. 2:ra29.

Clement, A., L. Solnica-Krezel, and K.L. Gould. 2011. The Cdc14B phosphatase contributes to ciliogenesis in zebrafish. *Development*. 138:291-302.

Cole, D.G. 2003. The intraflagellar transport machinery of Chlamydomonas reinhardtii. *Traffic*. 4:435-42.

Cole, D.G., W.Z. Cande, R.J. Baskin, D.A. Skoufias, C.J. Hogan, and J.M. Scholey. 1992. Isolation of a sea urchin egg kinesin-related protein using peptide antibodies. *J Cell Sci*. 101 (Pt 2):291-301.

Cole, D.G., S.W. Chinn, K.P. Wedaman, K. Hall, T. Vuong, and J.M. Scholey. 1993. Novel heterotrimeric kinesin-related protein purified from sea urchin eggs. *Nature*. 366:268-70.

Cole, D.G., D.R. Diener, A.L. Himelblau, P.L. Beech, J.C. Fuster, and J.L. Rosenbaum. 1998. Chlamydomonas kinesin-II-dependent intraflagellar transport (IFT): IFT particles contain proteins required for ciliary assembly in Caenorhabditis elegans sensory neurons. *J Cell Biol*. 141:993-1008.

Cole, D.G., and W.J. Snell. 2009. SnapShot: Intraflagellar transport. *Cell*. 137:784-784 e1.

Corbit, K.C., P. Aanstad, V. Singla, A.R. Norman, D.Y. Stainier, and J.F. Reiter. 2005. Vertebrate Smoothened functions at the primary cilium. *Nature*. 437:1018-21.

Corbit, K.C., A.E. Shyer, W.E. Dowdle, J. Gaulden, V. Singla, M.H. Chen, P.T. Chuang, and J.F. Reiter. 2008. Kif3a constrains beta-catenin-dependent Wnt signalling through dual ciliary and non-ciliary mechanisms. *Nat Cell Biol*. 10:70-6.

Craige, B., C.C. Tsao, D.R. Diener, Y. Hou, K.F. Lechtreck, J.L. Rosenbaum, and G.B. Witman. 2010. CEP290 tethers flagellar transition zone microtubules to the membrane and regulates flagellar protein content. *J Cell Biol*. 190:927-40.

Davis, R.E., R.E. Swiderski, K. Rahmouni, D.Y. Nishimura, R.F. Mullins, K. Agassandian, A.R. Philp, C.C. Searby, M.P. Andrews, S. Thompson, C.J. Berry, D.R. Thedens, B. Yang, R.M. Weiss, M.D. Cassell, E.M. Stone, and V.C. Sheffield. 2007. A knockin mouse model of the Bardet-Biedl syndrome 1 M390R mutation has cilia defects, ventriculomegaly, retinopathy, and obesity. *Proc Natl Acad Sci U S A*. 104:19422-7.

Dawson, S.C., M.S. Sagolla, J.J. Mancuso, D.J. Woessner, S.A. House, L. Fritz-Laylin, and W.Z. Cande. 2007. Kinesin-13 regulates flagellar, interphase, and mitotic microtubule dynamics in Giardia intestinalis. *Eukaryot Cell*. 6:2354-64.

Deretic, D., A.H. Williams, N. Ransom, V. Morel, P.A. Hargrave, and A. Arendt. 2005. Rhodopsin C terminus, the site of mutations causing retinal disease, regulates trafficking by binding to ADP-ribosylation factor 4 (ARF4). *Proc Natl Acad Sci U S A*. 102:3301-6.

Endoh-Yamagami, S., M. Evangelista, D. Wilson, X. Wen, J.W. Theunissen, K. Phamluong, M. Davis, S.J. Scales, M.J. Solloway, F.J. de Sauvage, and A.S. Peterson. 2009. The mammalian Cos2 homolog Kif7 plays an essential role in modulating Hh signal transduction during development. *Curr Biol*. 19:1320-6.

Engel, B.D., W.B. Ludington, and W.F. Marshall. 2009. Intraflagellar transport particle size scales inversely with flagellar length: revisiting the balance-point length control model. *J Cell Biol*. 187:81-9.

Follit, J.A., L. Li, Y. Vucica, and G.J. Pazour. 2010. The cytoplasmic tail of fibrocystin contains a ciliary targeting sequence. *J Cell Biol*. 188:21-8.

Follit, J.A., J.T. San Agustin, F. Xu, J.A. Jonassen, R. Samtani, C.W. Lo, and G.J. Pazour. 2008. The Golgin GMAP210/TRIP11 anchors IFT20 to the Golgi complex. *PLoS Genet*. 4:e1000315.

Follit, J.A., R.A. Tuft, K.E. Fogarty, and G.J. Pazour. 2006. The intraflagellar transport protein IFT20 is associated with the Golgi complex and is required for cilia assembly. *Mol Biol Cell*. 17:3781-92.

Follit, J.A., F. Xu, B.T. Keady, and G.J. Pazour. 2009. Characterization of mouse IFT complex B. *Cell Motil Cytoskeleton*. 66:457-68.

Fouquet, J.P., B. Edde, M.L. Kann, A. Wolff, E. Desbruyeres, and P. Denoulet. 1994. Differential distribution of glutamylated tubulin during spermatogenesis in mammalian testis. *Cell Motil Cytoskeleton*. 27:49-58.

Garcia-Gonzalo, F.R., K.C. Corbit, M.S. Sirerol-Piquer, G. Ramaswami, E.A. Otto, T.R. Noriega, A.D. Seol, J.F. Robinson, C.L. Bennett, D.J. Josifova, J.M. Garcia-Verdugo, N. Katsanis, F. Hildebrandt, and J.F. Reiter.

2011. A transition zone complex regulates mammalian ciliogenesis and ciliary membrane composition. *Nat Genet*. 43:776-84.
Gerdes, J.M., Y. Liu, N.A. Zaghloul, C.C. Leitch, S.S. Lawson, M. Kato, P.A. Beachy, P.L. Beales, G.N. DeMartino, S. Fisher, J.L. Badano, and N. Katsanis. 2007. Disruption of the basal body compromises proteasomal function and perturbs intracellular Wnt response. *Nat Genet*. 39:1350-60.
Graser, S., Y.D. Stierhof, S.B. Lavoie, O.S. Gassner, S. Lamla, M. Le Clech, and E.A. Nigg. 2007. Cep164, a novel centriole appendage protein required for primary cilium formation. *J Cell Biol*. 179:321-30.
Haycraft, C.J., B. Banizs, Y. Aydin-Son, Q. Zhang, E.J. Michaud, and B.K. Yoder. 2005. Gli2 and Gli3 localize to cilia and require the intraflagellar transport protein polaris for processing and function. *PLoS Genet*. 1:e53.
Hidaka, K., N. Ashizawa, H. Endoh, M. Watanabe, and S. Fukumoto. 1995. Fine structure of the cilia in the pancreatic duct of WBN/Kob rat. *Int J Pancreatol*. 18:207-13.
Hildebrandt, F., T. Benzing, and N. Katsanis. 2011. Ciliopathies. *N Engl J Med*. 364:1533-43.
Hou, Y., G.J. Pazour, and G.B. Witman. 2004. A dynein light intermediate chain, D1bLIC, is required for retrograde intraflagellar transport. *Mol Biol Cell*. 15:4382-94.
Hoyer-Fender, S. 2010. Centriole maturation and transformation to basal body. *Semin Cell Dev Biol*. 21:142-7.
Hsu, S.H., X. Zhang, C. Yu, Z.J. Li, J.S. Wunder, C.C. Hui, and B.A. Alman. 2011. Kif7 promotes hedgehog signaling in growth plate chondrocytes by restricting the inhibitory function of Sufu. *Development*. 138:3791-801.
Huang, K., D.R. Diener, and J.L. Rosenbaum. 2009. The ubiquitin conjugation system is involved in the disassembly of cilia and flagella. *J Cell Biol*. 186:601-13.
Huangfu, D., and K.V. Anderson. 2005. Cilia and Hedgehog responsiveness in the mouse. *Proc Natl Acad Sci U S A*. 102:11325-30.
Huangfu, D., A. Liu, A.S. Rakeman, N.S. Murcia, L. Niswander, and K.V. Anderson. 2003. Hedgehog signalling in the mouse requires intraflagellar transport proteins. *Nature*. 426:83-7.
Hunnicutt, G.R., M.G. Kosfiszer, and W.J. Snell. 1990. Cell body and flagellar agglutinins in Chlamydomonas reinhardtii: the cell body plasma membrane is a reservoir for agglutinins whose migration to the flagella is regulated by a functional barrier. *J Cell Biol*. 111:1605-16.
Ikegami, K., S. Sato, K. Nakamura, L.E. Ostrowski, and M. Setou. 2010. Tubulin polyglutamylation is essential for airway ciliary function through the regulation of beating asymmetry. *Proc Natl Acad Sci U S A*. 107:10490-5.
Inglis, P.N., G. Ou, M.R. Leroux, and J.M. Scholey. 2007. The sensory cilia of Caenorhabditis elegans. *WormBook*:1-22.
Insinna, C., M. Humby, T. Sedmak, U. Wolfrum, and J.C. Besharse. 2009. Different roles for KIF17 and kinesin II in photoreceptor development and maintenance. *Dev Dyn*. 238:2211-22.
Insinna, C., N. Pathak, B. Perkins, I. Drummond, and J.C. Besharse. 2008. The homodimeric kinesin, Kif17, is essential for vertebrate photoreceptor sensory outer segment development. *Dev Biol*. 316:160-70.
Iomini, C., L. Li, J.M. Esparza, and S.K. Dutcher. 2009. Retrograde intraflagellar transport mutants identify complex A proteins with multiple genetic interactions in Chlamydomonas reinhardtii. *Genetics*. 183:885-96.
Iomini, C., K. Tejada, W. Mo, H. Vaananen, and G. Piperno. 2004. Primary cilia of human endothelial cells disassemble under laminar shear stress. *J Cell Biol*. 164:811-7.
Ishikawa, H., A. Kubo, and S. Tsukita. 2005. Odf2-deficient mother centrioles lack distal/subdistal appendages and the ability to generate primary cilia. *Nat Cell Biol*. 7:517-24.
Jacoby, M., J.J. Cox, S. Gayral, D.J. Hampshire, M. Ayub, M. Blockmans, E. Pernot, M.V. Kisseleva, P. Compere, S.N. Schiffmann, F. Gergely, J.H. Riley, D. Perez-Morga, C.G. Woods, and S. Schurmans. 2009. INPP5E mutations cause primary cilium signaling defects, ciliary instability and ciliopathies in human and mouse. *Nat Genet*. 41:1027-31.
Jauregui, A.R., K.C. Nguyen, D.H. Hall, and M.M. Barr. 2008. The Caenorhabditis elegans nephrocystins act as global modifiers of cilium structure. *J Cell Biol*. 180:973-88.
Jin, H., S.R. White, T. Shida, S. Schulz, M. Aguiar, S.P. Gygi, J.F. Bazan, and M.V. Nachury. 2010. The conserved Bardet-Biedl syndrome proteins assemble a coat that traffics membrane proteins to cilia. *Cell*. 141:1208-19.
Kaneshiro, E.S., D.F. Matesic, and K. Jayasimhulu. 1984. Characterizations of six ethanolamine sphingophospholipids from Paramecium cells and cilia. *J Lipid Res*. 25:369-77.
Kaya, K., C.S. Ramesha, and G.A. Thompson, Jr. 1984. On the formation of alpha-hydroxy fatty acids. Evidence for a direct hydroxylation of nonhydroxy fatty acid-containing sphingolipids. *J Biol Chem*. 259:3548-53.
Keady, B.T., R. Samtani, K. Tobita, M. Tsuchya, J.T. San Agustin, J.A. Follit, J.A. Jonassen, R. Subramanian, C.W. Lo, and G.J. Pazour. 2012. IFT25 Links the Signal-Dependent Movement of Hedgehog Components to Intraflagellar Transport. *Dev Cell*. 22:940-51.
Kim, J., J.E. Lee, S. Heynen-Genel, E. Suyama, K. Ono, K. Lee, T. Ideker, P. Aza-Blanc, and J.G. Gleeson. 2010. Functional genomic screen for modulators of ciliogenesis and cilium length. *Nature*. 464:1048-51.
Kim, S., N.A. Zaghloul, E. Bubenshchikova, E.C. Oh, S. Rankin, N. Katsanis, T. Obara, and L. Tsiokas. 2011. Nde1-mediated inhibition of ciliogenesis affects cell cycle re-entry. *Nat Cell Biol*. 13:351-60.

Kinzel, D., K. Boldt, E.E. Davis, I. Burtscher, D. Trumbach, B. Diplas, T. Attie-Bitach, W. Wurst, N. Katsanis, M. Ueffing, and H. Lickert. 2010. Pitchfork regulates primary cilia disassembly and left-right asymmetry. *Dev Cell*. 19:66-77.

Knodler, A., S. Feng, J. Zhang, X. Zhang, A. Das, J. Peranen, and W. Guo. 2010. Coordination of Rab8 and Rab11 in primary ciliogenesis. *Proc Natl Acad Sci U S A*. 107:6346-51.

Ko, H.W., R.X. Norman, J. Tran, K.P. Fuller, M. Fukuda, and J.T. Eggenschwiler. 2010. Broad-minded links cell cycle-related kinase to cilia assembly and hedgehog signal transduction. *Dev Cell*. 18:237-47.

Kobayashi, T., and B.D. Dynlacht. 2011. Regulating the transition from centriole to basal body. *J Cell Biol*. 193:435-44.

Kobayashi, T., W.Y. Tsang, J. Li, W. Lane, and B.D. Dynlacht. 2011. Centriolar kinesin Kif24 interacts with CP110 to remodel microtubules and regulate ciliogenesis. *Cell*. 145:914-25.

Kozminski, K.G., P.L. Beech, and J.L. Rosenbaum. 1995. The Chlamydomonas kinesin-like protein FLA10 is involved in motility associated with the flagellar membrane. *J Cell Biol*. 131:1517-27.

Kozminski, K.G., K.A. Johnson, P. Forscher, and J.L. Rosenbaum. 1993. A motility in the eukaryotic flagellum unrelated to flagellar beating. *Proc Natl Acad Sci U S A*. 90:5519-23.

Kubo, A., A. Yuba-Kubo, S. Tsukita, and M. Amagai. 2008. Sentan: a novel specific component of the apical structure of vertebrate motile cilia. *Mol Biol Cell*. 19:5338-46.

Kunitomo, H., and Y. Iino. 2008. Caenorhabditis elegans DYF-11, an orthologue of mammalian Traf3ip1/MIP-T3, is required for sensory cilia formation. *Genes Cells*. 13:13-25.

L'Hernault, S.W., and J.L. Rosenbaum. 1985. Chlamydomonas alpha-tubulin is posttranslationally modified by acetylation on the epsilon-amino group of a lysine. *Biochemistry*. 24:473-8.

Lechtreck, K.F., E.C. Johnson, T. Sakai, D. Cochran, B.A. Ballif, J. Rush, G.J. Pazour, M. Ikebe, and G.B. Witman. 2009a. The Chlamydomonas reinhardtii BBSome is an IFT cargo required for export of specific signaling proteins from flagella. *J Cell Biol*. 187:1117-32.

Lechtreck, K.F., S. Luro, J. Awata, and G.B. Witman. 2009b. HA-tagging of putative flagellar proteins in Chlamydomonas reinhardtii identifies a novel protein of intraflagellar transport complex B. *Cell Motil Cytoskeleton*. 66:469-82.

Li, A., M. Saito, J.Z. Chuang, Y.Y. Tseng, C. Dedesma, K. Tomizawa, T. Kaitsuka, and C.H. Sung. 2011. Ciliary transition zone activation of phosphorylated Tctex-1 controls ciliary resorption, S-phase entry and fate of neural progenitors. *Nat Cell Biol*. 13:402-11.

Li, C., P.N. Inglis, C.C. Leitch, E. Efimenko, N.A. Zaghloul, C.A. Mok, E.E. Davis, N.J. Bialas, M.P. Healey, E. Heon, M. Zhen, P. Swoboda, N. Katsanis, and M.R. Leroux. 2008. An essential role for DYF-11/MIP-T3 in assembling functional intraflagellar transport complexes. *PLoS Genet*. 4:e1000044.

Li, J.B., J.M. Gerdes, C.J. Haycraft, Y. Fan, T.M. Teslovich, H. May-Simera, H. Li, O.E. Blacque, L. Li, C.C. Leitch, R.A. Lewis, J.S. Green, P.S. Parfrey, M.R. Leroux, W.S. Davidson, P.L. Beales, L.M. Guay-Woodford, B.K. Yoder, G.D. Stormo, N. Katsanis, and S.K. Dutcher. 2004. Comparative genomics identifies a flagellar and basal body proteome that includes the BBS5 human disease gene. *Cell*. 117:541-52.

Liem, K.F., Jr., M. He, P.J. Ocbina, and K.V. Anderson. 2009. Mouse Kif7/Costal2 is a cilia-associated protein that regulates Sonic hedgehog signaling. *Proc Natl Acad Sci U S A*. 106:13377-82.

Liu, Q., G. Tan, N. Levenkova, T. Li, E.N. Pugh, Jr., J.J. Rux, D.W. Speicher, and E.A. Pierce. 2007. The proteome of the mouse photoreceptor sensory cilium complex. *Mol Cell Proteomics*. 6:1299-317.

Lucker, B.F., R.H. Behal, H. Qin, L.C. Siron, W.D. Taggart, J.L. Rosenbaum, and D.G. Cole. 2005. Characterization of the intraflagellar transport complex B core: direct interaction of the IFT81 and IFT74/72 subunits. *J Biol Chem*. 280:27688-96.

Marshall, W.F., H. Qin, M. Rodrigo Brenni, and J.L. Rosenbaum. 2005. Flagellar length control system: testing a simple model based on intraflagellar transport and turnover. *Mol Biol Cell*. 16:270-8.

Marszalek, J.R., P. Ruiz-Lozano, E. Roberts, K.R. Chien, and L.S. Goldstein. 1999. Situs inversus and embryonic ciliary morphogenesis defects in mouse mutants lacking the KIF3A subunit of kinesin-II. *Proc Natl Acad Sci U S A*. 96:5043-8.

Massinen, S., M.E. Hokkanen, H. Matsson, K. Tammimies, I. Tapia-Paez, V. Dahlstrom-Heuser, J. Kuja-Panula, J. Burghoorn, K.E. Jeppsson, P. Swoboda, M. Peyrard-Janvid, R. Toftgard, E. Castren, and J. Kere. 2011. Increased expression of the dyslexia candidate gene DCDC2 affects length and signaling of primary cilia in neurons. *PLoS One*. 6:e20580.

May, S.R., A.M. Ashique, M. Karlen, B. Wang, Y. Shen, K. Zarbalis, J. Reiter, J. Ericson, and A.S. Peterson. 2005. Loss of the retrograde motor for IFT disrupts localization of Smo to cilia and prevents the expression of both activator and repressor functions of Gli. *Dev Biol*. 287:378-89.

Mazelova, J., L. Astuto-Gribble, H. Inoue, B.M. Tam, E. Schonteich, R. Prekeris, O.L. Moritz, P.A. Randazzo, and D. Deretic. 2009. Ciliary targeting motif VxPx directs assembly of a trafficking module through Arf4. *EMBO J*. 28:183-92.

Mesland, D.A., J.L. Hoffman, E. Caligor, and U.W. Goodenough. 1980. Flagellar tip activation stimulated by membrane adhesions in Chlamydomonas gametes. *J Cell Biol*. 84:599-617.

Miki, H., Y. Okada, and N. Hirokawa. 2005. Analysis of the kinesin superfamily: insights into structure and function. *Trends Cell Biol*. 15:467-76.

Milenkovic, L., M.P. Scott, and R. Rohatgi. 2009. Lateral transport of Smoothened from the plasma membrane to the membrane of the cilium. *J Cell Biol*. 187:365-74.

Miyoshi, K., K. Kasahara, I. Miyazaki, and M. Asanuma. 2009. Lithium treatment elongates primary cilia in the mouse brain and in cultured cells. *Biochem Biophys Res Commun*. 388:757-62.

Miyoshi, K., K. Kasahara, I. Miyazaki, and M. Asanuma. 2011. Factors that influence primary cilium length. *Acta Med Okayama*. 65:279-85.

Moritz, O.L., B.M. Tam, L.L. Hurd, J. Peranen, D. Deretic, and D.S. Papermaster. 2001. Mutant rab8 Impairs docking and fusion of rhodopsin-bearing post-Golgi membranes and causes cell death of transgenic Xenopus rods. *Mol Biol Cell*. 12:2341-51.

Morsci, N.S., and M.M. Barr. 2011. Kinesin-3 KLP-6 Regulates Intraflagellar Transport in Male-Specific Cilia of Caenorhabditis elegans. *Curr Biol*. 21:1239-44.

Mukhopadhyay, S., Y. Lu, S. Shaham, and P. Sengupta. 2008. Sensory signaling-dependent remodeling of olfactory cilia architecture in C. elegans. *Dev Cell*. 14:762-74.

Mukhopadhyay, S., X. Wen, B. Chih, C.D. Nelson, W.S. Lane, S.J. Scales, and P.K. Jackson. 2010. TULP3 bridges the IFT-A complex and membrane phosphoinositides to promote trafficking of G protein-coupled receptors into primary cilia. *Genes Dev*. 24:2180-93.

Muresan, V., T. Abramson, A. Lyass, D. Winter, E. Porro, F. Hong, N.L. Chamberlin, and B.J. Schnapp. 1998. KIF3C and KIF3A form a novel neuronal heteromeric kinesin that associates with membrane vesicles. *Mol Biol Cell*. 9:637-52.

Muresan, V., and J.C. Besharse. 1994. Complex intermolecular interactions maintain a stable linkage between the photoreceptor connecting cilium axoneme and plasma membrane. *Cell Motil Cytoskeleton*. 28:213-30.

Muresan, V., A. Lyass, and B.J. Schnapp. 1999. The kinesin motor KIF3A is a component of the presynaptic ribbon in vertebrate photoreceptors. *J Neurosci*. 19:1027-37.

Mykytyn, K., R.F. Mullins, M. Andrews, A.P. Chiang, R.E. Swiderski, B. Yang, T. Braun, T. Casavant, E.M. Stone, and V.C. Sheffield. 2004. Bardet-Biedl syndrome type 4 (BBS4)-null mice implicate Bbs4 in flagella formation but not global cilia assembly. *Proc Natl Acad Sci U S A*. 101:8664-9.

Nachury, M.V., A.V. Loktev, Q. Zhang, C.J. Westlake, J. Peranen, A. Merdes, D.C. Slusarski, R.H. Scheller, J.F. Bazan, V.C. Sheffield, and P.K. Jackson. 2007. A core complex of BBS proteins cooperates with the GTPase Rab8 to promote ciliary membrane biogenesis. *Cell*. 129:1201-13.

Nauli, S.M., F.J. Alenghat, Y. Luo, E. Williams, P. Vassilev, X. Li, A.E. Elia, W. Lu, E.M. Brown, S.J. Quinn, D.E. Ingber, and J. Zhou. 2003. Polycystins 1 and 2 mediate mechanosensation in the primary cilium of kidney cells. *Nat Genet*. 33:129-37.

Nelsen, E.M. 1975. Regulation of tubulin during ciliary regeneration in non-growing Tetrahymena. *Exp Cell Res*. 94:152-8.

Nishimura, D.Y., M. Fath, R.F. Mullins, C. Searby, M. Andrews, R. Davis, J.L. Andorf, K. Mykytyn, R.E. Swiderski, B. Yang, R. Carmi, E.M. Stone, and V.C. Sheffield. 2004. Bbs2-null mice have neurosensory deficits, a defect in social dominance, and retinopathy associated with mislocalization of rhodopsin. *Proc Natl Acad Sci U S A*. 101:16588-93.

Nonaka, S., Y. Tanaka, Y. Okada, S. Takeda, A. Harada, Y. Kanai, M. Kido, and N. Hirokawa. 1998. Randomization of left-right asymmetry due to loss of nodal cilia generating leftward flow of extraembryonic fluid in mice lacking KIF3B motor protein. *Cell*. 95:829-37.

Novarino, G., N. Akizu, and J.G. Gleeson. 2011. Modeling human disease in humans: the ciliopathies. *Cell*. 147:70-9.

O'Hagan, R., B.P. Piasecki, M. Silva, P. Phirke, K.C. Nguyen, D.H. Hall, P. Swoboda, and M.M. Barr. 2011. The Tubulin Deglutamylase CCPP-1 Regulates the Function and Stability of Sensory Cilia in C. elegans. *Curr Biol*.

Omori, Y., T. Chaya, K. Katoh, N. Kajimura, S. Sato, K. Muraoka, S. Ueno, T. Koyasu, M. Kondo, and T. Furukawa. 2010. Negative regulation of ciliary length by ciliary male germ cell-associated kinase (Mak) is required for retinal photoreceptor survival. *Proc Natl Acad Sci U S A*. 107:22671-6.

Omori, Y., C. Zhao, A. Saras, S. Mukhopadhyay, W. Kim, T. Furukawa, P. Sengupta, A. Veraksa, and J. Malicki. 2008. Elipsa is an early determinant of ciliogenesis that links the IFT particle to membrane-associated small GTPase Rab8. *Nat Cell Biol*. 10:437-44.

Orozco, J.T., K.P. Wedaman, D. Signor, H. Brown, L. Rose, and J.M. Scholey. 1999. Movement of motor and cargo along cilia. *Nature*. 398:674.

Ostrowski, L.E., K. Blackburn, K.M. Radde, M.B. Moyer, D.M. Schlatzer, A. Moseley, and R.C. Boucher. 2002. A

proteomic analysis of human cilia: identification of novel components. *Mol Cell Proteomics*. 1:451-65.
Ou, G., O.E. Blacque, J.J. Snow, M.R. Leroux, and J.M. Scholey. 2005. Functional coordination of intraflagellar transport motors. *Nature*. 436:583-7.
Ou, G., M. Koga, O.E. Blacque, T. Murayama, Y. Ohshima, J.C. Schafer, C. Li, B.K. Yoder, M.R. Leroux, and J.M. Scholey. 2007. Sensory ciliogenesis in Caenorhabditis elegans: assignment of IFT components into distinct modules based on transport and phenotypic profiles. *Mol Biol Cell*. 18:1554-69.
Overgaard, C.E., K.M. Sanzone, K.S. Spiczka, D.R. Sheff, A. Sandra, and C. Yeaman. 2009. Deciliation is associated with dramatic remodeling of epithelial cell junctions and surface domains. *Mol Biol Cell*. 20:102-13.
Pan, J., and W.J. Snell. 2005. Chlamydomonas shortens its flagella by activating axonemal disassembly, stimulating IFT particle trafficking, and blocking anterograde cargo loading. *Dev Cell*. 9:431-8.
Pan, X., G. Ou, G. Civelekoglu-Scholey, O.E. Blacque, N.F. Endres, L. Tao, A. Mogilner, M.R. Leroux, R.D. Vale, and J.M. Scholey. 2006. Mechanism of transport of IFT particles in C. elegans cilia by the concerted action of kinesin-II and OSM-3 motors. *J Cell Biol*. 174:1035-45.
Papermaster, D.S., B.G. Schneider, and J.C. Besharse. 1985. Vesicular transport of newly synthesized opsin from the Golgi apparatus toward the rod outer segment. Ultrastructural immunocytochemical and autoradiographic evidence in Xenopus retinas. *Invest Ophthalmol Vis Sci*. 26:1386-404.
Patzke, S., S. Redick, A. Warsame, C.A. Murga-Zamalloa, H. Khanna, S. Doxsey, and T. Stokke. 2010. CSPP is a ciliary protein interacting with Nephrocystin 8 and required for cilia formation. *Mol Biol Cell*. 21:2555-67.
Pazour, G.J., N. Agrin, J. Leszyk, and G.B. Witman. 2005. Proteomic analysis of a eukaryotic cilium. *J Cell Biol*. 170:103-13.
Pazour, G.J., and R.A. Bloodgood. 2008. Targeting proteins to the ciliary membrane. *Curr Top Dev Biol*. 85:115-49.
Pazour, G.J., B.L. Dickert, and G.B. Witman. 1999. The DHC1b (DHC2) isoform of cytoplasmic dynein is required for flagellar assembly. *J Cell Biol*. 144:473-81.
Pazour, G.J., J.T. San Agustin, J.A. Follit, J.L. Rosenbaum, and G.B. Witman. 2002. Polycystin-2 localizes to kidney cilia and the ciliary level is elevated in orpk mice with polycystic kidney disease. *Curr Biol*. 12:R378-80.
Pazour, G.J., C.G. Wilkerson, and G.B. Witman. 1998. A dynein light chain is essential for the retrograde particle movement of intraflagellar transport (IFT). *J Cell Biol*. 141:979-92.
Peden, E.M., and M.M. Barr. 2005. The KLP-6 kinesin is required for male mating behaviors and polycystin localization in Caenorhabditis elegans. *Curr Biol*. 15:394-404.
Pedersen, L.B., M.S. Miller, S. Geimer, J.M. Leitch, J.L. Rosenbaum, and D.G. Cole. 2005. Chlamydomonas IFT172 is encoded by FLA11, interacts with CrEB1, and regulates IFT at the flagellar tip. *Curr Biol*. 15:262-6.
Perkins, L.A., E.M. Hedgecock, J.N. Thomson, and J.G. Culotti. 1986. Mutant sensory cilia in the nematode Caenorhabditis elegans. *Dev Biol*. 117:456-87.
Perrone, C.A., D. Tritschler, P. Taulman, R. Bower, B.K. Yoder, and M.E. Porter. 2003. A novel dynein light intermediate chain colocalizes with the retrograde motor for intraflagellar transport at sites of axoneme assembly in chlamydomonas and Mammalian cells. *Mol Biol Cell*. 14:2041-56.
Piao, T., M. Luo, L. Wang, Y. Guo, D. Li, P. Li, W.J. Snell, and J. Pan. 2009. A microtubule depolymerizing kinesin functions during both flagellar disassembly and flagellar assembly in Chlamydomonas. *Proc Natl Acad Sci U S A*. 106:4713-8.
Piperno, G., and K. Mead. 1997. Transport of a novel complex in the cytoplasmic matrix of Chlamydomonas flagella. *Proc Natl Acad Sci U S A*. 94:4457-62.
Piperno, G., E. Siuda, S. Henderson, M. Segil, H. Vaananen, and M. Sassaroli. 1998. Distinct mutants of retrograde intraflagellar transport (IFT) share similar morphological and molecular defects. *J Cell Biol*. 143:1591-601.
Pitaval, A., Q. Tseng, M. Bornens, and M. Thery. 2010. Cell shape and contractility regulate ciliogenesis in cell cycle-arrested cells. *J Cell Biol*. 191:303-12.
Porter, M.E., R. Bower, J.A. Knott, P. Byrd, and W. Dentler. 1999. Cytoplasmic dynein heavy chain 1b is required for flagellar assembly in Chlamydomonas. *Mol Biol Cell*. 10:693-712.
Pugacheva, E.N., S.A. Jablonski, T.R. Hartman, E.P. Henske, and E.A. Golemis. 2007. HEF1-dependent Aurora A activation induces disassembly of the primary cilium. *Cell*. 129:1351-63.
Qin, H., Z. Wang, D. Diener, and J. Rosenbaum. 2007. Intraflagellar transport protein 27 is a small G protein involved in cell-cycle control. *Curr Biol*. 17:193-202.
Quarmby, L.M. 2004. Cellular deflagellation. *Int Rev Cytol*. 233:47-91.
Ramamurthy, V., and M. Cayouette. 2009. Development and disease of the photoreceptor cilium. *Clin Genet*. 76:137-45.
Rana, A.A., J.P. Barbera, T.A. Rodriguez, D. Lynch, E. Hirst, J.C. Smith, and R.S. Beddington. 2004. Targeted deletion of the novel cytoplasmic dynein mD2LIC disrupts the embryonic organiser, formation of the body axes and specification of ventral cell fates. *Development*. 131:4999-5007.
Rasi, M.Q., J.D. Parker, J.L. Feldman, W.F. Marshall, and L.M. Quarmby. 2009. Katanin knockdown supports a role for microtubule severing in release of basal bodies before mitosis in Chlamydomonas. *Mol Biol Cell*. 20:379-88.

Reese, T.S. 1965. Olfactory Cilia in the Frog. *J Cell Biol*. 25:209-30.
Ringo, D.L. 1967. Flagellar motion and fine structure of the flagellar apparatus in Chlamydomonas. *J Cell Biol*. 33:543-71.
Rohatgi, R., L. Milenkovic, and M.P. Scott. 2007. Patched1 regulates hedgehog signaling at the primary cilium. *Science*. 317:372-6.
Rompolas, P., L.B. Pedersen, R.S. Patel-King, and S.M. King. 2007. Chlamydomonas FAP133 is a dynein intermediate chain associated with the retrograde intraflagellar transport motor. *J Cell Sci*. 120:3653-65.
Rosenbaum, J.L., and F.M. Child. 1967. Flagellar regeneration in protozoan flagellates. *J Cell Biol*. 34:345-64.
Rosenbaum, J.L., J.E. Moulder, and D.L. Ringo. 1969. Flagellar elongation and shortening in Chlamydomonas. The use of cycloheximide and colchicine to study the synthesis and assembly of flagellar proteins. *J Cell Biol*. 41:600-19.
Ross, A.J., H. May-Simera, E.R. Eichers, M. Kai, J. Hill, D.J. Jagger, C.C. Leitch, J.P. Chapple, P.M. Munro, S. Fisher, P.L. Tan, H.M. Phillips, M.R. Leroux, D.J. Henderson, J.N. Murdoch, A.J. Copp, M.M. Eliot, J.R. Lupski, D.T. Kemp, H. Dollfus, M. Tada, N. Katsanis, A. Forge, and P.L. Beales. 2005. Disruption of Bardet-Biedl syndrome ciliary proteins perturbs planar cell polarity in vertebrates. *Nat Genet*. 37:1135-40.
Rual, J.F., K. Venkatesan, T. Hao, T. Hirozane-Kishikawa, A. Dricot, N. Li, G.F. Berriz, F.D. Gibbons, M. Dreze, N. Ayivi-Guedehoussou, N. Klitgord, C. Simon, M. Boxem, S. Milstein, J. Rosenberg, D.S. Goldberg, L.V. Zhang, S.L. Wong, G. Franklin, S. Li, J.S. Albala, J. Lim, C. Fraughton, E. Llamosas, S. Cevik, C. Bex, P. Lamesch, R.S. Sikorski, J. Vandenhaute, H.Y. Zoghbi, A. Smolyar, S. Bosak, R. Sequerra, L. Doucette-Stamm, M.E. Cusick, D.E. Hill, F.P. Roth, and M. Vidal. 2005. Towards a proteome-scale map of the human protein-protein interaction network. *Nature*. 437:1173-8.
Rudiger, M., U. Plessmann, A.H. Rudiger, and K. Weber. 1995. Beta tubulin of bull sperm is polyglycylated. *FEBS Lett*. 364:147-51.
Santos, N., and J.F. Reiter. 2008. Building it up and taking it down: the regulation of vertebrate ciliogenesis. *Dev Dyn*. 237:1972-81.
Sarpal, R., S.V. Todi, E. Sivan-Loukianova, S. Shirolikar, N. Subramanian, E.C. Raff, J.W. Erickson, K. Ray, and D.F. Eberl. 2003. Drosophila KAP interacts with the kinesin II motor subunit KLP64D to assemble chordotonal sensory cilia, but not sperm tails. *Curr Biol*. 13:1687-96.
Satir, P., and S.T. Christensen. 2007. Overview of structure and function of mammalian cilia. *Annu Rev Physiol*. 69:377-400.
Schafer, J.C., C.J. Haycraft, J.H. Thomas, B.K. Yoder, and P. Swoboda. 2003. XBX-1 encodes a dynein light intermediate chain required for retrograde intraflagellar transport and cilia assembly in Caenorhabditis elegans. *Mol Biol Cell*. 14:2057-70.
Schafer, J.C., M.E. Winkelbauer, C.L. Williams, C.J. Haycraft, R.A. Desmond, and B.K. Yoder. 2006. IFTA-2 is a conserved cilia protein involved in pathways regulating longevity and dauer formation in Caenorhabditis elegans. *J Cell Sci*. 119:4088-100.
Schneider, L., C.A. Clement, S.C. Teilmann, G.J. Pazour, E.K. Hoffmann, P. Satir, and S.T. Christensen. 2005. PDGFRalphaalpha signaling is regulated through the primary cilium in fibroblasts. *Curr Biol*. 15:1861-6.
Sherwin, T., A. Schneider, R. Sasse, T. Seebeck, and K. Gull. 1987. Distinct localization and cell cycle dependence of COOH terminally tyrosinolated alpha-tubulin in the microtubules of Trypanosoma brucei brucei. *J Cell Biol*. 104:439-46.
Shida, T., J.G. Cueva, Z. Xu, M.B. Goodman, and M.V. Nachury. 2010. The major alpha-tubulin K40 acetyltransferase alphaTAT1 promotes rapid ciliogenesis and efficient mechanosensation. *Proc Natl Acad Sci U S A*. 107:21517-22.
Singla, V., and J.F. Reiter. 2006. The primary cilium as the cell's antenna: signaling at a sensory organelle. *Science*. 313:629-33.
Smith, L.A., N.O. Bukanov, H. Husson, R.J. Russo, T.C. Barry, A.L. Taylor, D.R. Beier, and O. Ibraghimov-Beskrovnaya. 2006. Development of polycystic kidney disease in juvenile cystic kidney mice: insights into pathogenesis, ciliary abnormalities, and common features with human disease. *J Am Soc Nephrol*. 17:2821-31.
Snow, J.J., G. Ou, A.L. Gunnarson, M.R. Walker, H.M. Zhou, I. Brust-Mascher, and J.M. Scholey. 2004. Two anterograde intraflagellar transport motors cooperate to build sensory cilia on C. elegans neurons. *Nat Cell Biol*. 6:1109-13.
Sohara, E., Y. Luo, J. Zhang, D.K. Manning, D.R. Beier, and J. Zhou. 2008. Nek8 regulates the expression and localization of polycystin-1 and polycystin-2. *J Am Soc Nephrol*. 19:469-76.
Song, L., and W.L. Dentler. 2001. Flagellar protein dynamics in Chlamydomonas. *J Biol Chem*. 276:29754-63.
Sorokin, S.P. 1968. Reconstructions of centriole formation and ciliogenesis in mammalian lungs. *J Cell Sci*. 3:207-30.
Souto-Padron, T., and W. de Souza. 1983. Freeze-fracture localization of filipin-cholesterol complexes in the plasma membrane of Trypanosoma cruzi. *J Parasitol*. 69:129-37.

Spektor, A., W.Y. Tsang, D. Khoo, and B.D. Dynlacht. 2007. Cep97 and CP110 suppress a cilia assembly program. *Cell*. 130:678-90.

Steinberg, R.H., and I. Wood. 1975. Clefts and microtubules of photoreceptor outer segments in the retina of the domestic cat. *J Ultrastruct Res*. 51:307-403.

Tachi, S., C. Tachi, and H.R. Lindner. 1974. Influence of ovarian hormones on formation of solitary cilia and behavior of the centrioles in uterine epithelial cells of the rat. *Biol Reprod*. 10:391-403.

Tam, L.W., N.F. Wilson, and P.A. Lefebvre. 2007. A CDK-related kinase regulates the length and assembly of flagella in Chlamydomonas. *J Cell Biol*. 176:819-29.

Tan, P.L., T. Barr, P.N. Inglis, N. Mitsuma, S.M. Huang, M.A. Garcia-Gonzalez, B.A. Bradley, S. Coforio, P.J. Albrecht, T. Watnick, G.G. Germino, P.L. Beales, M.J. Caterina, M.R. Leroux, F.L. Rice, and N. Katsanis. 2007. Loss of Bardet Biedl syndrome proteins causes defects in peripheral sensory innervation and function. *Proc Natl Acad Sci U S A*. 104:17524-9.

Taschner, M., S. Bhogaraju, M. Vetter, M. Morawetz, and E. Lorentzen. 2011. Biochemical Mapping of Interactions within the Intraflagellar Transport (IFT) B Core Complex: IFT52 BINDS DIRECTLY TO FOUR OTHER IFT-B SUBUNITS. *J Biol Chem*. 286:26344-52.

Thazhath, R., M. Jerka-Dziadosz, J. Duan, D. Wloga, M.A. Gorovsky, J. Frankel, and J. Gaertig. 2004. Cell context-specific effects of the beta-tubulin glycylation domain on assembly and size of microtubular organelles. *Mol Biol Cell*. 15:4136-47.

Thiel, C., K. Kessler, A. Giessl, A. Dimmler, S.A. Shalev, S. von der Haar, M. Zenker, D. Zahnleiter, H. Stoss, E. Beinder, R. Abou Jamra, A.B. Ekici, N. Schroder-Kress, T. Aigner, T. Kirchner, A. Reis, J.H. Brandstatter, and A. Rauch. 2011. NEK1 mutations cause short-rib polydactyly syndrome type majewski. *Am J Hum Genet*. 88:106-14.

Tran, P.V., C.J. Haycraft, T.Y. Besschetnova, A. Turbe-Doan, R.W. Stottmann, B.J. Herron, A.L. Chesebro, H. Qiu, P.J. Scherz, J.V. Shah, B.K. Yoder, and D.R. Beier. 2008. THM1 negatively modulates mouse sonic hedgehog signal transduction and affects retrograde intraflagellar transport in cilia. *Nat Genet*. 40:403-10.

Tsang, W.Y., C. Bossard, H. Khanna, J. Peranen, A. Swaroop, V. Malhotra, and B.D. Dynlacht. 2008. CP110 suppresses primary cilia formation through its interaction with CEP290, a protein deficient in human ciliary disease. *Dev Cell*. 15:187-97.

Tsao, C.C., and M.A. Gorovsky. 2008. Different effects of Tetrahymena IFT172 domains on anterograde and retrograde intraflagellar transport. *Mol Biol Cell*. 19:1450-61.

Verhey, K.J., and J. Gaertig. 2007. The tubulin code. *Cell Cycle*. 6:2152-60.

Vieira, O.V., K. Gaus, P. Verkade, J. Fullekrug, W.L. Vaz, and K. Simons. 2006. FAPP2, cilium formation, and compartmentalization of the apical membrane in polarized Madin-Darby canine kidney (MDCK) cells. *Proc Natl Acad Sci U S A*. 103:18556-61.

Wang, Q., J. Pan, and W.J. Snell. 2006. Intraflagellar transport particles participate directly in cilium-generated signaling in Chlamydomonas. *Cell*. 125:549-62.

Wang, Z., Z.C. Fan, S.M. Williamson, and H. Qin. 2009. Intraflagellar transport (IFT) protein IFT25 is a phosphoprotein component of IFT complex B and physically interacts with IFT27 in Chlamydomonas. *PLoS One*. 4:e5384.

Ward, H.H., U. Brown-Glaberman, J. Wang, Y. Morita, S.L. Alper, E.J. Bedrick, V.H. Gattone, 2nd, D. Deretic, and A. Wandinger-Ness. 2011. A conserved signal and GTPase complex are required for the ciliary transport of polycystin-1. *Mol Biol Cell*. 22:3289-305.

Ward, S., N. Thomson, J.G. White, and S. Brenner. 1975. Electron microscopical reconstruction of the anterior sensory anatomy of the nematode Caenorhabditis elegans.?2UU. *J Comp Neurol*. 160:313-37.

Watanabe, D., Y. Saijoh, S. Nonaka, G. Sasaki, Y. Ikawa, T. Yokoyama, and H. Hamada. 2003. The left-right determinant Inversin is a component of node monocilia and other 9+0 cilia. *Development*. 130:1725-34.

Webber, W.A., and J. Lee. 1975. Fine structure of mammalian renal cilia. *Anat Rec*. 182:339-43.

Wedaman, K.P., D.W. Meyer, D.J. Rashid, D.G. Cole, and J.M. Scholey. 1996. Sequence and submolecular localization of the 115-kD accessory subunit of the heterotrimeric kinesin-II (KRP85/95) complex. *J Cell Biol*. 132:371-80.

Westermann, S., and K. Weber. 2003. Post-translational modifications regulate microtubule function. *Nat Rev Mol Cell Biol*. 4:938-47.

Wicks, S.R., C.J. de Vries, H.G. van Luenen, and R.H. Plasterk. 2000. CHE-3, a cytosolic dynein heavy chain, is required for sensory cilia structure and function in Caenorhabditis elegans. *Dev Biol*. 221:295-307.

Wilson, C.W., C.T. Nguyen, M.H. Chen, J.H. Yang, R. Gacayan, J. Huang, J.N. Chen, and P.T. Chuang. 2009. Fused has evolved divergent roles in vertebrate Hedgehog signalling and motile ciliogenesis. *Nature*. 459:98-102.

Wloga, D., A. Camba, K. Rogowski, G. Manning, M. Jerka-Dziadosz, and J. Gaertig. 2006. Members of the NIMA-related kinase family promote disassembly of cilia by multiple mechanisms. *Mol Biol Cell*. 17:2799-810.

Yang, Z., E.A. Roberts, and L.S. Goldstein. 2001. Functional analysis of mouse kinesin motor Kif3C. *Mol Cell Biol*.

21:5306-11.
Yoder, B.K., X. Hou, and L.M. Guay-Woodford. 2002. The polycystic kidney disease proteins, polycystin-1, polycystin-2, polaris, and cystin, are co-localized in renal cilia. *J Am Soc Nephrol*. 13:2508-16.
Yokoyama, R., E. O'Toole, S. Ghosh, and D.R. Mitchell. 2004. Regulation of flagellar dynein activity by a central pair kinesin. *Proc Natl Acad Sci U S A*. 101:17398-403.
Zaghloul, N.A., and N. Katsanis. 2009. Mechanistic insights into Bardet-Biedl syndrome, a model ciliopathy. *J Clin Invest*. 119:428-37.
Zhang, Q., D. Nishimura, S. Seo, T. Vogel, D.A. Morgan, C. Searby, K. Bugge, E.M. Stone, K. Rahmouni, and V.C. Sheffield. 2011. Bardet-Biedl syndrome 3 (Bbs3) knockout mouse model reveals common BBS-associated phenotypes and Bbs3 unique phenotypes. *Proc Natl Acad Sci U S A*. 108:20678-83.
Zhang, Q., S. Seo, K. Bugge, E.M. Stone, and V.C. Sheffield. 2012. BBS proteins interact genetically with the IFT pathway to influence SHH-related phenotypes. *Hum Mol Genet*.
Zhao, C., Y. Omori, K. Brodowska, P. Kovach, and J. Malicki. 2012. Kinesin-2 family in vertebrate ciliogenesis. *Proc Natl Acad Sci U S A*.
Zwaal, R.R., J.E. Mendel, P.W. Sternberg, and R.H. Plasterk. 1997. Two neuronal G proteins are involved in chemosensation of the Caenorhabditis elegans Dauer-inducing pheromone. *Genetics*. 145:715-27.

Chapter 2

MRK and MOK regulate cilia length and intraflagellar transport in renal epithelial cells

Joost R. Broekhuis[1], Kristen J. Verhey[2], and Gert Jansen[1]

[1] Department of Cell Biology, Erasmus MC, PO Box 2040, 3000 CA, Rotterdam, the Netherlands [2] Department of Cell and Developmental Biology, University of Michigan Medical School, Ann Arbor, Michigan 48109, U.S.A.

Abstract

Primary cilia are microtubule-based organelles, which have important sensory functions. A wide variety exists in cilia length and morphology, probably reflecting their specific functions in different tissues. Cilia length and morphology are thought to be regulated by several signaling pathways. Cilia are build and maintained by a specialized transport mechanism, known as intraflagellar transport (IFT). During IFT, motor proteins transport multimeric protein complexes along the microtubule axoneme, delivering proteins to the distal tip or returning them to the cell body. Here, we show that MRK and MOK, two members of the *ros* cross-hybridizing kinase family (RCK), localize to the primary cilium, and negatively regulate cilia length in IMCD-3 cells. To analyze whether MRK and/or MOK regulate IFT, we generated IMCD-3 clones stably expressing fluorescently tagged components of the IFT machinery: KIF3B, KIF17, IFT43, IFT20, and BBS8. We found that these proteins all moved at ~0.45 μm/s in anterograde and retrograde direction. Knockdown of MRK increased anterograde IFT velocity, but did not affect retrograde IFT, correlating with delivery of more axonemal precursors at the distal tip, and cilium lengthening. Previous studies have shown that the mTOR pathway modulates cilia length, and that MRK phosphorylates Raptor, a subunit of mTORC1. We found that the mTOR inhibitor rapamycin can block all effects of MRK and MOK depletion, indicating MRK and MOK act through the mTOR pathway. In summary, we show that MRK and MOK are important signaling proteins in regulating cilia length, IFT, and possibly cilia function.

Introduction

Primary cilia are microtubule-based protrusions that can be found on the surface of almost all vertebrate cells, and function as sensory organelles. Defects in cilia structure or length have been associated with many genetic diseases, collectively called ciliopathies (Hildebrandt et al., 2011). The assembly and maintenance of primary cilia depends on intraflagellar transport (IFT). IFT is a microtubule-based transport mechanism that brings cargo to the tip of the cilium, and back to the cell body (Pedersen and Rosenbaum, 2008). IFT particles are composed of motor proteins, kinesins (kinesin-II and KIF17/OSM-3), which mediate anterograde transport, dynein (cytoplasmic dynein 2), which mediates retrograde transport, and adaptor complexes (complex A, complex B, and the BBsome) (Pedersen and Rosenbaum, 2008).

In vertebrates, a wide variety in both cilia length and morphology exists, most likely to better support cilium function in specific tissues. Moreover, primary cilia length is not fixed, but may vary in a well regulated manner. Several classes of signaling molecules have been shown to modulate cilia length (Avasthi and Marshall, 2011; Miyoshi et al., 2011). How elongation and shortening of cilia is achieved mechanistically is not completely understood, but it has been shown to be accompanied by changes in IFT dynamics (Besschetnova et al., 2010; Burghoorn et al., 2007; Burghoorn et al., 2010; Engel et al., 2009).

The family of *ros* cross-hybridizing kinases (RCKs), a small family of kinases (Manning et al., 2002), are characterized by a MAP kinase-like Thr-Xaa-Tyr (TXY) motif in their activation loop, and an overall structure similar to Cdks (Miyata et al., 1999). In *Chlamydomonas* (LF4), *Leishmania* (LmxMPK9), *C. elegans* (*dyf-5*), and mouse (MAK) RCKs have been identified that negatively regulate cilia length (Bengs et al., 2005; Berman et al., 2003; Burghoorn et al., 2007; Omori et al., 2010). In addition, *dyf-5* affects the *C. elegans* IFT machinery (Burghoorn et al., 2007). The sensory cilia of *C. elegans'* amphid neurons can be divided in a middle segment, which has nine microtubule doublets, and a distal segment, which has nine microtubule singlets (Ward et al., 1975). In the middle segment of wild type animals IFT particles are transported by kinesin-II and OSM-3 together, and in the distal segment only by OSM-3 (Snow et al., 2004). However, in *dyf-5* mutant animals kinesin-II and OSM-3 no longer move together, and the IFT complex travels with kinesin-II. In addition, kinesin-II can move into the distal segment in *dyf-5* mutant animals. Together these data suggest that DYF-5 plays a role in the undocking of kinesin II from IFT particles and in the docking of OSM-3 onto IFT particles.

In mammals, the RCK family contains three members: MAK/RCK (male germ cell-associated kinase/ *ros* cross-hybridizing kinase) (Bladt and Birchmeier, 1993; Xia et al., 2002), MRK/ICK (MAK-related kinase/intestinal cell kinase) (Abe et al., 1995; Togawa et al., 2000), and MOK/ RAGE (MAPK/MAK/MRK overlapping kinase/renal tumor antigen) (Miyata et al., 1999; Van Den Eynde et al., 1999). Recently, it was shown that MAK is expressed in photoreceptor cells, where it localizes to the connecting cilium and outer-segment axoneme (Omori et al., 2010). In retina of *Mak* knock out mice the cilia are elongated, and several IFT markers mislocalized (Omori et al., 2010). In addition, photoreceptors of *Mak* knock out mice degenerate over time (Omori et al., 2010). In line with the phenotype of KO mice, mutations in MAK have been found in patients with Retinitis Pigmentosa, a ciliopathy characterized by apoptotic death of photoreceptor cells (Ozgul et al., 2011; Tucker et al., 2011). MRK has been associated with endocrine-cerebro-osteodysplasia (ECO) (Lahiry et al., 2009). ECO is a lethal recessive disorder with multiple anomalies involving the endocrine, cerebral, and skeletal systems. The ciliopathies

Jeune syndrome, short-rib polydactyly, and Sensenbrenner syndrome are also characterized by skeletal anomalies (Waters and Beales, 2011).

Here, we investigate whether MRK and MOK also have a ciliary function. We show that both MRK and MOK localize to the primary cilium in cultured renal epithelial cells (IMCD-3). Using knockdown and overexpression experiments, we demonstrate that both MRK and MOK negatively regulate cilia length. To analyze whether MRK and/or MOK regulate IFT, we generated IMCD-3 clones stably expressing fluorescently tagged KIF3B, KIF17, IFT43, IFT20, or BBS8. We found that these proteins all move at ~0.45 μm/s in anterograde and in retrograde direction. In IMCD-3 cells depleted of MRK we observed that the anterograde velocity of all tested GFP-tagged IFT markers increased. Remarkably, treating the IMCD-3 cells with the mTOR inhibitor rapamycin completely blocked all effects of MRK and MOK knockdown, indicating MRK and MOK act through the mTOR pathway.

Results

MRK and MOK localize to the primary cilium

To investigate whether MRK and MOK function in the primary cilium, we first determined their subcellular localization pattern. We generated N- and C-terminal GFP-fusion constructs for MRK and MOK and expressed these constructs in IMCD-3 cells. Both MRK and MOK localized to the primary cilium in serum-starved IMCD-3 cells (Figure 1A, 1B). In addition, we observed two spots at the ciliary base, which co-localized with the centrosomal marker centrin-2 (Figure 1A, 1B). MRK and MOK also localized to the nucleus, which is in line with previous observations (Fu et al., 2005; Yang et al., 2002). C-terminally tagged MRK and MOK gave similar subcellular localization patterns (data not shown). Live imaging of these cells showed movement of MRK and MOK inside the cilium in anterograde and retrograde direction (data not shown), suggesting that MRK and MOK associate with the IFT complex. Together these data indicate that both MRK and MOK function in the primary cilium.

MRK and MOK negatively regulate cilia length

Because MAK, as well as orthologues in other model organisms, act as negative regulators of cilia length we expected that MRK and MOK would also negatively regulate cilia length. RT-PCR showed that IMCD-3 cells express MRK and MOK, but do not express MAK (data not shown). To knockdown MRK we used two non-overlapping lentiviral shRNA's targeted against MRK, shMRK #01 and shMRK #02. Immunoblotting showed that these shRNA's effectively reduced MRK expression (Figure 2A). Measurement of cilia length showed that cilia of IMCD-3 cells depleted of MRK were ~60% longer than those of control cells (Figure 2B, 2D). Two

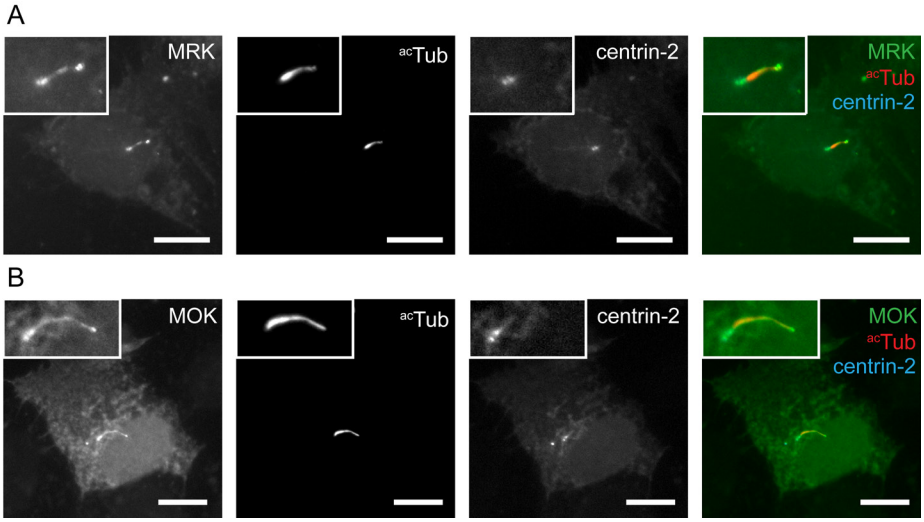

Figure 1. MRK and MOK localize to the primary cilium. IMCD-3 cells expressing GFP-MRK and CFP-centrin-2 (A), or GFP-MOK and CFP-centrin-2 (B), were serum-starved for 48 hours, fixed with paraformaldehyde, and immunostained for acetylated tubulin (acTub). Insets show enlargements of the region containing the cilium. Scale bars, 10 μm.

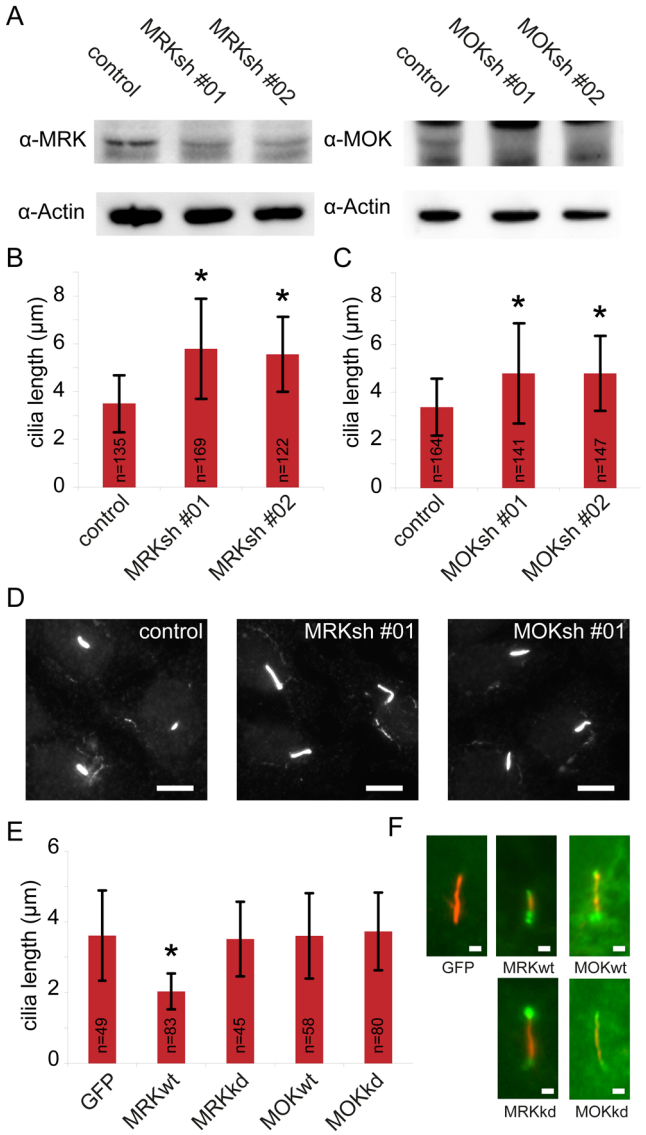

Figure 2. MRK and MOK control cilia length. (A) Immunoblot of cell lysates of IMCD-3 cells transduced with shRNA's targeting MRK and MOK, Actin was used as loading control. (B) Average length of primary cilia of IMCD-3 cells depleted of MRK. (C) Average length of primary cilia of IMCD-3 cells depleted of MOK. (D) Immunofluorescence images of IMCD-3 cells expressing the control shRNA, MRKsh #01, or MOKsh #01 stained with anti-acetylated tubulin. Scale bar, 10 µm. (E) Average length of primary cilia of IMCD-3 cells overexpressing GFP-C1, wild type (wt) GFP-MRK, kinase-dead (kd) GFP-MRK, wt GFP-MOK, or kd GFP-MOK. (F) Immunofluorescence images of IMCD-3 cells expressing GFP-C1, wt GFP-MRK, kd GFP-MRK, wt GFP-MOK, or kd GFP-MOK stained with anti-acetylated tubulin. Scale bar, 1 µm. Statistically significant differences compared to control cells are indicated with a black asterisk. Error bars indicate SD.

independent lentiviral shRNA's targeted against MOK, shMOK #01 and shMOK #02 reduced MOK expression, as judged by immunoblotting (Figure 2A). Cilia length measurements showed that depletion of MOK resulted in a ~40% elongation of cilium length (Figure 2C, 2D). Neither knockdown of MRK nor MOK affected the percentage of IMCD-3 cells that formed cilia after 48 hours of serum starvation (data not shown).

In addition, we analyzed the effect of overexpression of N-terminal GFP-fusions of wild type MRK and MOK, and N-terminal GFP-fusions of kinase-dead MRK and MOK, on cilia length. To generate kinase-dead mutant constructs we replaced an essential lysine in the ATP-binding pocket for a methionine, making the protein inactive (Xia et al., 2002). Transfected IMCD-3 cells were serum starved for 48 hours, and cilia length was determined by anti-acetylated tubulin immunostaining. Cells transfected with GFP-MRK had ~40% shorter cilia compared to cells transfected with an empty GFP vector (Figure 2E, 2F). Conversely, overexpression of kinase-dead GFP-MRK did not affect cilia length (Figure 2E, 2F), indicating that kinase activity of MRK is necessary for the negative regulation of cilia length by MRK. Overexpression of GFP-MOK did not affect cilia length (Figure 2E, 2F).

Together, these data suggest that MRK and MOK can negatively regulate cilia length in IMCD-3 cells, where the effects of MRK on cilia length are more profound than those of MOK.

MRK regulates IFT

Since mutation of *dyf-5* affects IFT in *C. elegans*, we determined whether reduced expression of MRK and/or MOK affects IFT in cultured mammalian cells. In *C. elegans* anterograde IFT is mediated by two ciliary kinesins, kinesin-II and OSM-3 (Snow et al., 2004). In vertebrates, kinesin-II appears to be the 'core' ciliary kinesin (Verhey et al., 2011), while OSM-3's vertebrate orthologue KIF17 acts in a cell type specific manner (Insinna et al., 2008). Using immunofluorescence, we confirmed that KIF17 is expressed and localizes to the primary cilium in IMCD-3 cells (data no shown). To visualize IFT for all IFT subcomplexes, we generated clonal lines stably expressing the following GFP fusions: IFT43-YFP (complex A), IFT20-GFP (complex B), mCit-KIF3B (kinesin-II), KIF17-mCit (KIF17), and GFP-BBS8 (BBSome). All five markers localized to the primary cilia (Figure 3A), and moved in both anterograde and retrograde direction along the microtubule axis (Figure 3B*)*.

First, we determined the velocities of the IFT components in IMCD-3 cells expressing a control shRNA. All five IFT markers moved in the anterograde direction at 0.40-0.45 μm/s, and in the retrograde direction at 0.39-0.46 μm/s (Figure 3C). Next, we reduced the expression of MRK in the cells stably expressing each of the five IFT markers. The average anterograde velocities of all tested IFT markers were significantly increased with an average of 35% in cells depleted of MRK (Figure 3C). In contrast, there were no significant effects on retrograde velocities of any of the tested IFT markers (Figure 3C). An increase of the anterograde velocity of the IFT machinery while retrograde IFT velocity is not affected would result in the delivery of more material at the distal tip, which would explain the elongation of primary cilia in MRK-depleted IMCD-3 cells. Depletion of MOK also yields longer primary cilia, however in contrast to MRK, depletion of MOK did not significantly affect anterograde or retrograde IFT velocity. Perhaps the effect of depletion of MOK on cilia length is achieved by effects on other IFT parameters, for example the number of transport events, particle size, or cargo types.

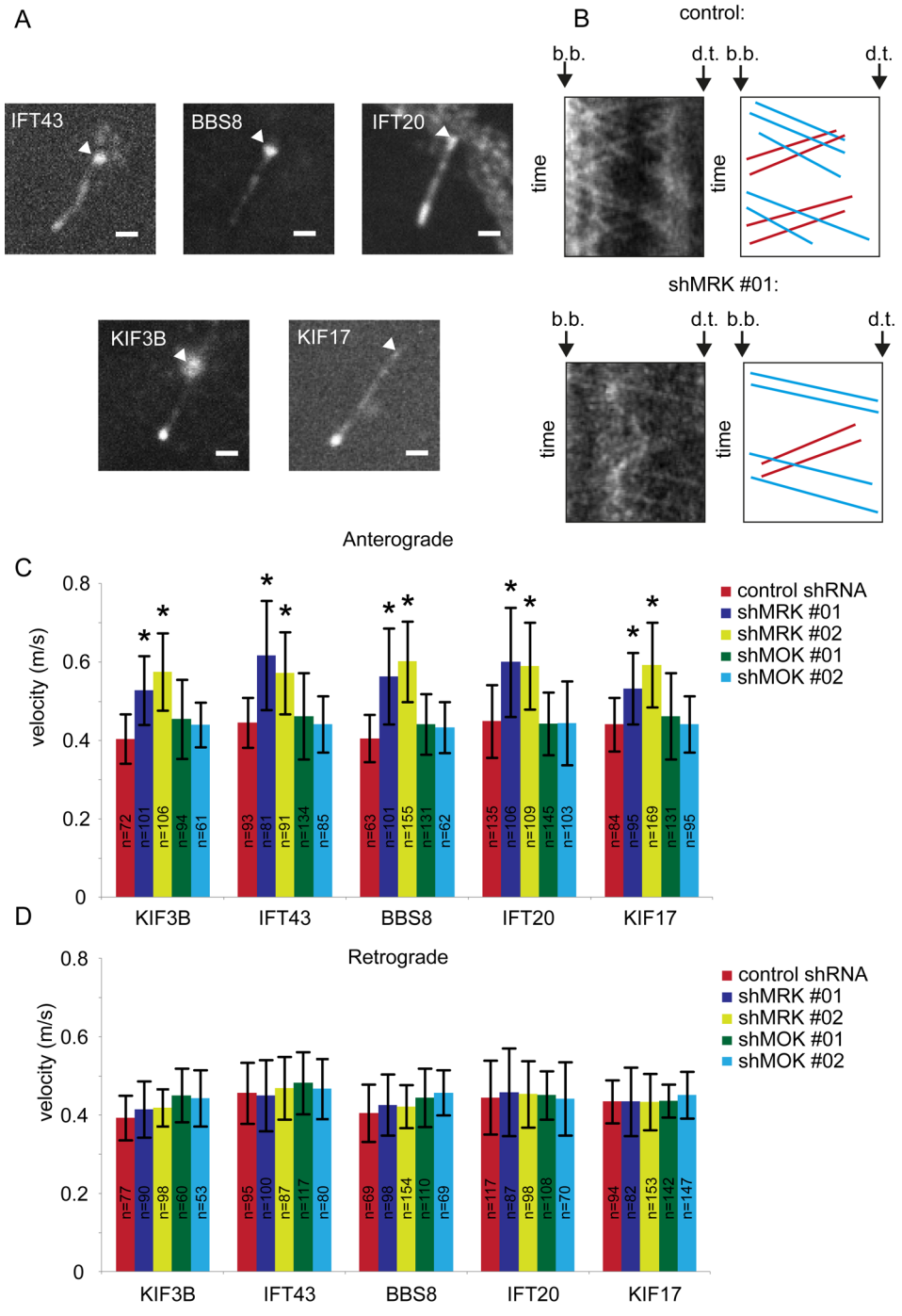
A
IFT43
BBS8
IFT20
KIF3B
KIF17
B
control:
b.b.
d.t.
b.b.
d.t.
time
time
shMRK #01:
b.b.
d.t.
b.b.
d.t.
time
time
Anterograde
C
velocity (m/s)
0.8
0.6
0.4
0.2
0
control shRNA
shMRK #01
shMRK #02
shMOK #01
shMOK #02
n=72 n=101 n=106 n=94 n=61
n=93 n=81 n=91 n=134 n=85
n=63 n=101 n=155 n=131 n=62
n=135 n=106 n=109 n=145 n=103
n=84 n=95 n=169 n=131 n=95
KIF3B
IFT43
BBS8
IFT20
KIF17
D
Retrograde
velocity (m/s)
0.8
0.6
0.4
0.2
0
control shRNA
shMRK #01
shMRK #02
shMOK #01
shMOK #02
n=77 n=90 n=98 n=60 n=53
n=95 n=100 n=87 n=117 n=80
n=69 n=98 n=154 n=110 n=69
n=117 n=87 n=98 n=108 n=70
n=94 n=82 n=153 n=142 n=147
KIF3B
IFT43
BBS8
IFT20
KIF17

Figure 3. Depletion of MRK results in increased anterograde IFT velocity. (A) Fluorescence images of the cilia of IMCD-3 cells stably expressing mCit-Kif3b, IFT43-YFP, GFP-BBS8, IFT20-GFP, and Kif17-mCit. The basal body is indicated with an arrowhead. Scale bar, 1 μm. (B) Representative examples of kymographs of IFT43-YFP in control cells and in cells depleted of MRK. The basal body and the distal tip of the cilium are indicated with b.b. and d.t., respectively. In the corresponding drawings the anterograde trajectories are shown in blue, and retrograde trajectories are shown in red. (C) Average anterograde and retrograde velocities of IFT components in control cells, and cells depleted of MRK and MOK. Statistically significant differences compared to the velocity of the same IFT component in IMCD-3 control cells are indicated with a black asterisk. Error bars indicate SD.

MRK and MOK act through mTOR

Primary cilia are highly dynamic structures, whose length is tightly regulated by several signaling pathways (Avasthi and Marshall, 2011; Miyoshi et al., 2011). An increase in intracellular cyclic AMP (cAMP) results in an elongation of primary cilia, as well as an increase in the anterograde velocity of IFT particles (Besschetnova et al., 2010). Since these effects are similar to the effect observed upon MRK depletion, we wondered whether MRK (and possibly MOK) function in the same pathway. We treated control cells, cells depleted of MRK, and cells depleted of MOK with forskolin (which increases cAMP levels), and measured cilia length and IFT velocities. Addition of forskolin to control cells increased cilia length (Figure 4A, 4B), as shown previously (Besschetnova et al., 2010). Interestingly, forskolin treatment of cells depleted of MRK, resulted in an additional increase of cilia length (Figure 4A, 4B). These data suggest that the effect of MRK depletion on cilia length is independent of the cAMP pathway. Depletion of MOK in forskolin-treated cells did not result in significantly longer cilia (Figure 4A, 4B), suggesting that MOK depletion and forskolin affect the same pathway. Depletion of MRK or treatment with forskolin resulted in increased anterograde IFT velocity of IFT20-GFP (Figure 4C). However, depletion of MRK and treatment with forskolin at the same time did not result in an additional increase of the anterograde IFT velocity of IFT20-GFP (Figure 4C). This could mean that MRK and cAMP act in the same pathway in the regulation of IFT, but that in addition cilium length is modulated by other mechanisms.

Cilium length and function are also regulated by the mTOR pathway (Yuan et al., 2012). Interestingly, MRK has been shown to phosphorylate Raptor (Wu et al., 2012), a component of mTOR Complex 1 (mTORC1) (Kim et al., 2002). To investigate whether MRK and MOK act through the mTOR pathway, we treated control cells, and cells expressing shMRK #01, or shMOK #01 with rapamycin, an inhibitor of mTOR. Rapamycin treatment of cells depleted of MRK and MOK completely blocked cilia elongation, while cilia length in control cells was not affected (Figure 4D, 4E). Rapamycin treatment also suppressed the effect of MRK depletion on the anterograde IFT velocity of IFT20-GFP (Figure 4F). Together our data indicate that MRK and MOK function in the same pathway as mTOR, most likely upstream of mTOR.

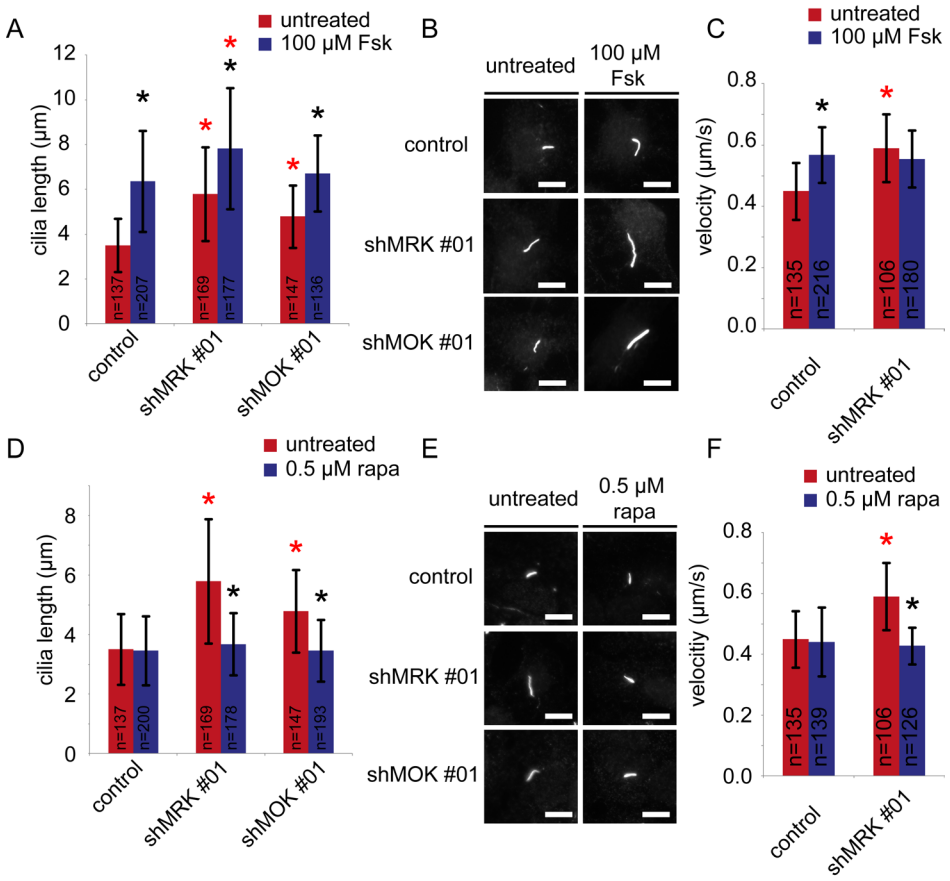

Figure 4. MRK and MOK act through mTOR. (A) Average length of primary cilia of IMCD-3 cells expressing a control shRNA, shMRK #01, or shMOK #01, untreated or treated with 100 µM forskolin (Fsk) for 24 hours. (B) Immunofluorescence images of IMCD-3 cells expressing a control shRNA, MRKsh #01, or MOKsh #01, untreated or forskolin-treated, stained with anti-acetylated tubulin. (C) Average anterograde velocity of IFT20-GFP in IMCD-3 control cells, and cells depleted of MRK, untreated and forskolin-treated. (D) Average length of primary cilia of IMCD-3 cells expressing a control shRNA, shMRK #01, or shMOK #01, untreated or treated with 0.5 µM rapamycin (rapa) for 24 hours. (E) Immunofluorescence images of IMCD-3 cells expressing a control shRNA, MRKsh #01, or MOKsh #01, untreated or rapamycin-treated, stained with anti-acetylated tubulin. (F) Average anterograde velocity of IFT20-GFP in IMCD-3 control cells, and cells depleted of MRK, untreated and rapamycin-treated. Statistically significant differences compared to the untreated cells are indicated with a black asterisk, and to the control shRNA are indicated with a red asterisk. Error bars indicate SD. Scale bar, 10 µm.

Discussion

In this study we show that the *ros* cross-hybridizing kinases (RCKs) MRK and MOK function in the regulation of primary cilia length. Both MRK and MOK localize to the primary cilium in cultured renal epithelial cells. Our knockdown experiments indicate that MRK and MOK negatively regulate cilia length. Overexpression of MRK resulted in shorter primary cilia, while overexpression of MOK did not affect cilia length. Depletion of MRK resulted in increased anterograde IFT velocities of components of all the IFT subcomplexes, while retrograde velocity was not affected. The effect of MRK depletion on cilia length was independent of cAMP signaling, but the effect of forskolin and MRK depletion on IFT were not additive. Depletion of MOK in forskolin-treated cells did not lead to further cilia length increase. Using an inhibitor of mTOR, rapamycin, we showed that the effects of both MRK and MOK on cilia length and IFT require the mTOR pathway.

Regulation of cilium length by IFT

Elongation of cilia is thought to be achieved by increased delivery of axonemal subunits at the distal tip by the anterograde IFT system. Our work showing that depletion of MRK increases anterograde IFT velocity and cilia length is in agreement with this theory. In addition, an increase of axonemal precursors at the distal tip could be achieved by altering other IFT parameters. For example, in *Chlamydomonas* it has been shown that during flagellar regeneration IFT particle size increases, while IFT velocity decreases. In fully elongated flagella the particle size decreases again, and IFT velocity increases. These data suggest that in short, elongating flagella IFT particles form long and slow moving trains, while in long, fully elongated flagella IFT particles form short and fast moving particles. Since MOK did regulate cilia length, but did not affect anterograde IFT velocity, it could be that particle size, or other IFT parameters such IFT frequency or cargo selection are altered, resulting in an influx of material at the distal tip. Unfortunately, it proved to be impossible to accurately and reproducible measure these parameters in our imaging setup.

Signaling cascade by which MRK and MOK regulate cilia length

MRK can be phosporylated and activated by CCRK (cell cycle-related kinase). CCRK is the vertebrate orthologue of *Chlamydomonas'* long flagella 2 (*lf2*) and *C. elegans' dyf-19*. *Chlamydomonas* cells containing a mutant allele of *lf2* form extra long flagella (Asleson and Lefebvre, 1998). Mutations in *dyf-19* resulted in the abnormal distribution of some IFT proteins, but did not significantly affect cilia length (Phirke et al., 2011). In zebrafish, CCRK acts together with its binding partner Bromi to regulate ciliary assembly (Ko et al., 2010). Downstream, MRK has been shown to phosphorylate Raptor (Wu et al., 2012), a component of mTORC1 (Kim et al., 2002). Recently, the mTOR pathway has been linked to cilia length regulation (Yuan et al., 2012). mTOR exists in at least two molecular complexes, mTORC1 and mTORC2, which are defined by the presence of either Raptor (mTORC1) or Rictor (mTORC2). Raptor is a scaffolding protein that recruits S6K1 and 4EBP1 to mTORC1 (Nojima et al., 2003). After subsequent phosphorylation by mTOR, S6K1 and 4EBP1 promote mRNA translation and ribosome biogenesis (Ma and Blenis, 2009). Thus, modulation of cilia length by mTOR is probably achieved by regulation of protein synthesis (Yuan et al., 2012). Our observation that

treatment with rapamycin suppresses all effects of depletion of MRK and MOK on cilia length and IFT, and the finding that MRK phosphorylates Raptor, make it likely that MRK and possibly MOK act in a cilia length regulating pathway, which involves Raptor and mTOR. Whether this pathway also involves CCRK remains to be determined. It is unclear where this pathway acts. Both the downstream target Raptor and the upstream regulator CCRK have never been shown to localize to the ciliary compartment. In addition, it remains unclear how such a signaling cascade could increase anterograde IFT velocities. Possibly, changes in protein synthesis as a result of modulation of the mTOR pathway could affect IFT kinetics. An alternative pathway might involve retinitis pigmentosa 1 (RP1), since the third RCK, MAK, negatively regulates cilia length by acting through RP1 (Omori et al., 2010). RP1 is a microtubule-associated protein, which positively regulates cilia length, and can be phosphorylated by MAK (Omori et al., 2010). However, in IMCD-3 cells MRK and MOK probably do not act through RP1, because it is exclusively expressed in photoreceptor cells (Sullivan et al., 1999). Interestingly, increased expression of a close relative of RP1, DCDC2, has also been shown to positively regulate cilia length (Massinen et al., 2011). Further studies are required to better understand the molecular mechanisms behind the regulation cilia length and IFT by MRK and MOK.

Concluding remarks

Cilia length and morphology vary extensively between different tissues. These differences are important for the specific functions of cilia, since inappropriate elongation of cilia hinders the biological processes in which cilia function (Niggemann et al., 1992; Yuan et al., 2012). Several ciliopathies arise from defects in cilia length control. For example, MAK, negative regulator of cilia length and close relative of MRK and MOK, has been linked to the retina-specific ciliopathy retinitis pigmentosa (Ozgul et al., 2011; Tucker et al., 2011). Also Juvenile Cystic Kidney Disease and Meckel–Gruber Syndrome have been linked to the long cilia phenotype (Sohara et al., 2008; Tammachote et al., 2009). MRK has been linked to endocrine-cerebro-osteodysplasia (ECO), which has ciliopathy-like symptoms (Lahiry et al., 2009). Previously reported data have identified a number of signaling proteins that play an important role in controlling cilia length. Here we show that MRK and MOK function in the mTOR pathway to regulate cilia length, and we provide evidence that regulation of cilia length is achieved by modulation of IFT.

Material and methods

Antibodies and plasmids

The following primary antibodies were used: mouse monoclonal anti-acetylated tubulin (Sigma; immunofluorescence (IF), 1:1000), rabbit polyclonal anti-MRK (Gift from Zheng Fu; Western blot (WB), 1:500), rabbit polyclonal anti-MOK (Cosmo Bio Co., Ltd.; WB, 1:1000), and anti-actin (Millipore; WB, 1:5000). The following secondary antibodies were used: alexa594-conjugated anti-mouse (Invitrogen; IF, 1:1000), HRP-conjugated anti-rabbit (Dako; WB, 1:5000), and HRP-conjugated anti-mouse (Amersham; WB, 1:10000).

IFT43-YFP was a gift from Heleen Arts, and IFT20-GFP was a gift from Gregory Pazour. GFP-MRK was generated by PCR amplifying the MRK open reading frame (ORF) from mouse MRK cDNA (IMAGE clone 4224269) and subcloning it into the EcoRI and KpnI sites of pEGFP-C1. GFP-MOK was generated by PCR amplifying from the MOK ORF from mouse MOK cDNA (a gift from Yoshihiko Miyata) and subcloning it into the SalI and SacII sites of pEGFP-C1. GFP-BBS8 was generated by PCR amplifying the BBS8 ORF from the mouse BBS8 cDNA (IMAGE clone 4527657) and subcloning it into the KpnI and ApaI sites of pEGFP-C1. CFP-centrin-2 was generated by PCR amplifying the centrin-2 ORF from IMCD-3 cDNA and subcloning it into the KpnI and BamHI sites of pECFP-N1. The coding sequence of mouse KIF3B (IMAGE clone 8862410) was subcloned by PCR into the pmCit-C1 vector (equivalent to Clontech pEGFP-C1 except that EGFP was replaced with a monomeric version of mCitrine) using Xho I and EcoRI restriction sites engineered into the 5' and 3' PCR primers, respectively. The plasmid was confirmed by sequencing in both directions. A single mutation was found which changed Valine 34 to Alanine. This mutation does not change the motility of KIF3B (KJV, unpublished). Kif17-mCit has been described previously (Hammond et al., 2010).

To make a kinase-dead GFP-MRK construct site-directed mutagenesis was used to change the codon of an essential lysine residue at a.a. position 33 into a methionine codon. To make a kinase-dead GFP-MOK construct site-directed mutagenesis was used to change the codon of an essential lysine residue at a.a. position 35 into a methionine codon. The shRNA clones, non-target control shRNA, shMRK #01 (targeting sequence (T.S.), CACAACCACGAGGCGGTGTAA), shMRK #02 (T.S., CCAGTGAAATTGACACAATTT), shMOK #01 (T.S., CTGGTTCTCTTGCACTAATAT), and shMOK #02 (T.S., GCCGGAGAATATCCTAGTAAA) were obtained from the TRC lentivirus-based shRNA library (Sigma). For additional information, see SI Materials and Methods.

Cell culture and transfections

IMCD-3 cells (CRC-212, ATCC) were grown in DMEM/F10 medium supplemented with 10% FCS, penicillin (100 U/ml) and streptomycin (100 µg/ml). For transient transfections IMCD-3 cells, at 60% confluency, were transfected with FuGENE 6 (Roche), and serum starved for 48 hours to induce ciliogenesis.

To generate clonal IMCD-3 cell lines that stably express GFP-tagged IFT complex components, IMCD-3 cells were first transfected with linearized FP-fusion constructs. After 48 hours, G418 (500 µg/ml) was used to select transfected cells. After two weeks, the viable cells were sorted on a FACS Aria II cell sorter (Becton-Dickinson) to select the GFP-positive cells. Individual

cells were seeded in a 96-well plate and cultured until there were enough cells to confirm the FP-construct expression levels and subcellular localization by fluorescence microscopy.

Immunofluorescence and microscopy

IMCD-3 cells were fixed with 4% PFA, permeabilized with 0.15% Triton X-100 in PBS, and blocked with blocking buffer (1% BSA and 0.05% Tween-20 in 1x PBS) for 45 minutes at room temperature (R.T.). Cells were incubated with primary antibodies (in blocking buffer) for 1 h at R.T., and washed three times with PBS tween (0.05% Tween-20 in 1x PBS). Cells were incubated with fluorescent-conjugated secondary antibodies (in blocking buffer) for 45 minutes at R.T., and washed three times with PBS tween. After the washing steps the cells were washed with 70% ethanol for 1 minute and 100% ethanol for 1 minute. The samples were air-dried and mounted on a microscope slide with mounting solution (20 mM Tris HCl pH 8, 0.2 M DABCO, 90% glycerol). Subcellular localization studies and cilia length measurements were performed using a Zeiss Imager Z1 microscope with a 63x (NA 1.4) objective.

Retroviral expression

Third-generation lentiviruses were packaged in HEK293T cells by transient co-transfection, with Lipofectamine 2000 (Invitrogen), of pMDg/RRE, pRSVREV, pMD.9, and pLKO.1-puro containing non-target control shRNA, shMRK #01, shMRK #02, shMOK #01, or shMOK #02. IMCD-3 cells growing at 40% confluency were transduced with lentiviruses. Forty-eight hours after transduction, the transduced cells were serum-starved in the presence of 5 μg/ml puromycin. After 48 hours of serum starvation cells were either harvested for protein extraction or used to determine cilia length or IFT velocities.

Western Blot Analysis

IMCD-3 cells were harvested in lysis buffer (50 mM Tris pH 6.8, 5 mM EDTA, 5% glycerol, 2% SDS, 1% β-mercaptoethanol, and Protease Inhibitor Cocktail (Roche)). Lysates were centrifuged at 13.200 rpm for 1 min at 4 °C. Supernatants were collected, and 1x Laemmli loading buffer was added. The protein samples were separated on SDS-PAGE gels and then transferred to a nitrocellulose transfer membrane (Whatman). Membranes were probed with primary antibodies, washed three times with PBST (0.25% Tween-20 in 1x PBS), probed with HRP-conjugated secondary antibodies, washed three times with PBST, and finally the membranes were exposed to chemiluminescence reagent (Amersham). Chemiluminescence was detected with Alliance 2.7 (UVItec).

Imaging of intraflagellar transport in cultured cells

Clonal IMCD-3 cells stably expressing mCit-KIF3B, IFT43-YFP, GFP-BBS8, IFT20-GFP, or KIF17-mCit were grown on 18 mm cover slips. Prior to analysis glass slide were inversed onto a 24 mm cover slip, and placed in a live-cell imaging chamber. Time-lapse movies were acquired on a spinning-disc microscope (CSU-X1-A1; Yokogawa) equipped with 100× 1.49 NA oil objective (Nikon) and an EMCCD camera (QuantEM 512SC; Roper Scientific), installed on an inverted research microscope (Eclipse Ti-E; Nikon), and controlled with MetaMorph 7.5 software (Molecular Devices). To determine the IFT particles' velocities, kymographs were generated in ImageJ with the Kymograph plugin, written by J. Rietdorf.

Statistical analysis

P values were derived from one-way ANOVA analysis, followed by a Bonferroni post-hoc test, using SPSS. In all figures the criteria for statistical significance was defined as $P < 0.001$.

References

Abe, S., T. Yagi, S. Ishiyama, M. Hiroe, F. Marumo, and Y. Ikawa. 1995. Molecular cloning of a novel serine/threonine kinase, MRK, possibly involved in cardiac development. *Oncogene*. 11:2187-95.

Asleson, C.M., and P.A. Lefebvre. 1998. Genetic analysis of flagellar length control in Chlamydomonas reinhardtii: a new long-flagella locus and extragenic suppressor mutations. *Genetics*. 148:693-702.

Avasthi, P., and W.F. Marshall. 2011. Stages of ciliogenesis and regulation of ciliary length. *Differentiation*.

Bengs, F., A. Scholz, D. Kuhn, and M. Wiese. 2005. LmxMPK9, a mitogen-activated protein kinase homologue affects flagellar length in Leishmania mexicana. *Mol Microbiol*. 55:1606-15.

Berman, S.A., N.F. Wilson, N.A. Haas, and P.A. Lefebvre. 2003. A novel MAP kinase regulates flagellar length in Chlamydomonas. *Curr Biol*. 13:1145-9.

Besschetnova, T.Y., E. Kolpakova-Hart, Y. Guan, J. Zhou, B.R. Olsen, and J.V. Shah. 2010. Identification of signaling pathways regulating primary cilium length and flow-mediated adaptation. *Curr Biol*. 20:182-7.

Bladt, F., and C. Birchmeier. 1993. Characterization and expression analysis of the murine rck gene: a protein kinase with a potential function in sensory cells. *Differentiation*. 53:115-22.

Burghoorn, J., M.P. Dekkers, S. Rademakers, T. de Jong, R. Willemsen, and G. Jansen. 2007. Mutation of the MAP kinase DYF-5 affects docking and undocking of kinesin-2 motors and reduces their speed in the cilia of Caenorhabditis elegans. *Proc Natl Acad Sci U S A*. 104:7157-62.

Burghoorn, J., M.P. Dekkers, S. Rademakers, T. de Jong, R. Willemsen, P. Swoboda, and G. Jansen. 2010. Dauer pheromone and G-protein signaling modulate the coordination of intraflagellar transport kinesin motor proteins in C. elegans. *J Cell Sci*. 123:2077-84.

Engel, B.D., W.B. Ludington, and W.F. Marshall. 2009. Intraflagellar transport particle size scales inversely with flagellar length: revisiting the balance-point length control model. *J Cell Biol*. 187:81-9.

Fu, Z., M.J. Schroeder, J. Shabanowitz, P. Kaldis, K. Togawa, A.K. Rustgi, D.F. Hunt, and T.W. Sturgill. 2005. Activation of a nuclear Cdc2-related kinase within a mitogen-activated protein kinase-like TDY motif by autophosphorylation and cyclin-dependent protein kinase-activating kinase. *Mol Cell Biol*. 25:6047-64.

Hammond, J.W., T.L. Blasius, V. Soppina, D. Cai, and K.J. Verhey. 2010. Autoinhibition of the kinesin-2 motor KIF17 via dual intramolecular mechanisms. *J Cell Biol*. 189:1013-25.

Hildebrandt, F., T. Benzing, and N. Katsanis. 2011. Ciliopathies. *N Engl J Med*. 364:1533-43.

Insinna, C., N. Pathak, B. Perkins, I. Drummond, and J.C. Besharse. 2008. The homodimeric kinesin, Kif17, is essential for vertebrate photoreceptor sensory outer segment development. *Dev Biol*. 316:160-70.

Kim, D.H., D.D. Sarbassov, S.M. Ali, J.E. King, R.R. Latek, H. Erdjument-Bromage, P. Tempst, and D.M. Sabatini. 2002. mTOR interacts with raptor to form a nutrient-sensitive complex that signals to the cell growth machinery. *Cell*. 110:163-75.

Ko, H.W., R.X. Norman, J. Tran, K.P. Fuller, M. Fukuda, and J.T. Eggenschwiler. 2010. Broad-minded links cell cycle-related kinase to cilia assembly and hedgehog signal transduction. *Dev Cell*. 18:237-47.

Lahiry, P., J. Wang, J.F. Robinson, J.P. Turowec, D.W. Litchfield, M.B. Lanktree, G.B. Gloor, E.G. Puffenberger, K.A. Strauss, M.B. Martens, D.A. Ramsay, C.A. Rupar, V. Siu, and R.A. Hegele. 2009. A multiplex human syndrome implicates a key role for intestinal cell kinase in development of central nervous, skeletal, and endocrine systems. *Am J Hum Genet*. 84:134-47.

Ma, X.M., and J. Blenis. 2009. Molecular mechanisms of mTOR-mediated translational control. *Nat Rev Mol Cell Biol*. 10:307-18.

Manning, G., D.B. Whyte, R. Martinez, T. Hunter, and S. Sudarsanam. 2002. The protein kinase complement of the human genome. *Science*. 298:1912-34.

Massinen, S., M.E. Hokkanen, H. Matsson, K. Tammimies, I. Tapia-Paez, V. Dahlstrom-Heuser, J. Kuja-Panula, J. Burghoorn, K.E. Jeppsson, P. Swoboda, M. Peyrard-Janvid, R. Toftgard, E. Castren, and J. Kere. 2011. Increased expression of the dyslexia candidate gene DCDC2 affects length and signaling of primary cilia in neurons. *PLoS One*. 6:e20580.

Miyata, Y., M. Akashi, and E. Nishida. 1999. Molecular cloning and characterization of a novel member of the MAP kinase superfamily. *Genes Cells*. 4:299-309.

Miyoshi, K., K. Kasahara, I. Miyazaki, and M. Asanuma. 2011. Factors that influence primary cilium length. *Acta Med Okayama*. 65:279-85.

Niggemann, B., A. Muller, A. Nolte, N. Schnoy, and U. Wahn. 1992. Abnormal length of cilia--a cause of primary ciliary dyskinesia--a case report. *Eur J Pediatr*. 151:73-5.

Nojima, H., C. Tokunaga, S. Eguchi, N. Oshiro, S. Hidayat, K. Yoshino, K. Hara, N. Tanaka, J. Avruch, and K. Yonezawa. 2003. The mammalian target of rapamycin (mTOR) partner, raptor, binds the mTOR substrates p70 S6 kinase and 4E-BP1 through their TOR signaling (TOS) motif. *J Biol Chem*. 278:15461-4.

Omori, Y., T. Chaya, K. Katoh, N. Kajimura, S. Sato, K. Muraoka, S. Ueno, T. Koyasu, M. Kondo, and T. Furukawa. 2010. Negative regulation of ciliary length by ciliary male germ cell-associated kinase (Mak) is required for retinal photoreceptor survival. *Proc Natl Acad Sci U S A*. 107:22671-6.

Ozgul, R.K., A.M. Siemiatkowska, D. Yucel, C.A. Myers, R.W. Collin, M.N. Zonneveld, A. Beryozkin, E. Banin, C.B. Hoyng, L.I. van den Born, C. The European Retinal Disease, R. Bose, W. Shen, D. Sharon, F.P. Cremers, B.J. Klevering, A.I. den Hollander, and J.C. Corbo. 2011. Exome Sequencing and cis-Regulatory Mapping Identify Mutations in MAK, a Gene Encoding a Regulator of Ciliary Length, as a Cause of Retinitis Pigmentosa. *Am J Hum Genet*. 89:253-264.

Pedersen, L.B., and J.L. Rosenbaum. 2008. Intraflagellar transport (IFT) role in ciliary assembly, resorption and signalling. *Curr Top Dev Biol*. 85:23-61.

Phirke, P., E. Efimenko, S. Mohan, J. Burghoorn, F. Crona, M.W. Bakhoum, M. Trieb, K. Schuske, E.M. Jorgensen, B.P. Piasecki, M.R. Leroux, and P. Swoboda. 2011. Transcriptional profiling of C. elegans DAF-19 uncovers a ciliary base-associated protein and a CDK/CCRK/LF2p-related kinase required for intraflagellar transport. *Dev Biol*.

Snow, J.J., G. Ou, A.L. Gunnarson, M.R. Walker, H.M. Zhou, I. Brust-Mascher, and J.M. Scholey. 2004. Two anterograde intraflagellar transport motors cooperate to build sensory cilia on C. elegans neurons. *Nat Cell Biol*. 6:1109-13.

Sohara, E., Y. Luo, J. Zhang, D.K. Manning, D.R. Beier, and J. Zhou. 2008. Nek8 regulates the expression and localization of polycystin-1 and polycystin-2. *J Am Soc Nephrol*. 19:469-76.

Sullivan, L.S., J.R. Heckenlively, S.J. Bowne, J. Zuo, W.A. Hide, A. Gal, M. Denton, C.F. Inglehearn, S.H. Blanton, and S.P. Daiger. 1999. Mutations in a novel retina-specific gene cause autosomal dominant retinitis pigmentosa. *Nat Genet*. 22:255-9.

Tammachote, R., C.J. Hommerding, R.M. Sinders, C.A. Miller, P.G. Czarnecki, A.C. Leightner, J.L. Salisbury, C.J. Ward, V.E. Torres, V.H. Gattone, 2nd, and P.C. Harris. 2009. Ciliary and centrosomal defects associated with mutation and depletion of the Meckel syndrome genes MKS1 and MKS3. *Hum Mol Genet*. 18:3311-23.

Togawa, K., Y.X. Yan, T. Inomoto, S. Slaugenhaupt, and A.K. Rustgi. 2000. Intestinal cell kinase (ICK) localizes to the crypt region and requires a dual phosphorylation site found in map kinases. *J Cell Physiol*. 183:129-39.

Tucker, B.A., T.E. Scheetz, R.F. Mullins, A.P. Deluca, J.M. Hoffmann, R.M. Johnston, S.G. Jacobson, V.C. Sheffield, and E.M. Stone. 2011. Exome sequencing and analysis of induced pluripotent stem cells identify the cilia-related gene male germ cell-associated kinase (MAK) as a cause of retinitis pigmentosa. *Proc Natl Acad Sci U S A*.

Van Den Eynde, B.J., B. Gaugler, M. Probst-Kepper, L. Michaux, O. Devuyst, F. Lorge, P. Weynants, and T. Boon. 1999. A new antigen recognized by cytolytic T lymphocytes on a human kidney tumor results from reverse strand transcription. *J Exp Med*. 190:1793-800.

Verhey, K.J., J. Dishinger, and H.L. Kee. 2011. Kinesin motors and primary cilia. *Biochem Soc Trans*. 39:1120-5.

Ward, S., N. Thomson, J.G. White, and S. Brenner. 1975. Electron microscopical reconstruction of the anterior sensory anatomy of the nematode Caenorhabditis elegans.?2UU. *J Comp Neurol*. 160:313-37.

Waters, A.M., and P.L. Beales. 2011. Ciliopathies: an expanding disease spectrum. *Pediatr Nephrol*. 26:1039-56.

Wu, D., J.R. Chapman, L. Wang, T.E. Harris, J. Shabanowitz, D.F. Hunt, and Z. Fu. 2012. Intestinal cell kinase (ICK) promotes activation of the mTOR complex 1 (mTORC1) through phosphorylation of raptor Thr-908. *J Biol Chem*.

Xia, L., D. Robinson, A.H. Ma, H.C. Chen, F. Wu, Y. Qiu, and H.J. Kung. 2002. Identification of human male germ cell-associated kinase, a kinase transcriptionally activated by androgen in prostate cancer cells. *J Biol Chem*. 277:35422-33.

Yang, T., Y. Jiang, and J. Chen. 2002. The identification and subcellular localization of human MRK. *Biomol Eng*. 19:1-4.

Yuan, S., J. Li, D.R. Diener, M.A. Choma, J.L. Rosenbaum, and Z. Sun. 2012. Target-of-rapamycin complex 1 (Torc1) signaling modulates cilia size and function through protein synthesis regulation. *Proc Natl Acad Sci U S A*.

Chapter 3

Identification of MRK and MOK interacting proteins

Joost R. Broekhuis[1], V.H. Linh Nguyen[1], Dick H.W. Dekkers[2], Jeroen Demmers[2], and Gert Jansen[1]

[1] Department of Cell Biology, Erasmus MC, PO Box 2040, 3000 CA, Rotterdam, the Netherlands
[2] Proteomics Center, Erasmus MC, Dr Molewaterplein 50, 3015 GE Rotterdam, the Netherlands

Abstract

Primary cilia are microtubule-based organelles, which have important sensory functions. Primary cilia are dynamic organelles, and their length can be modulated by several signaling molecules. MRK and MOK are two kinases that can negatively regulate cilia length in cultured renal epithelial cells, and MRK also modulates intraflagellar transport. However, the molecular mechanisms by which MRK and MOK regulate cilia length are not clear. To gain more insight in the function of MRK and MOK we sought to identify proteins that interact with MRK and MOK using a proteomic approach. Our analysis revealed a range of MRK and/or MOK binding proteins, including centrosomal proteins, proteins involved in microtubule-based motor transport, and signal transduction. In addition, we compared the proteins found in the mass spectrometry analysis with proteins found in the ciliary proteome and with proteins containing the MRK phosphorylation consensus sequence (R-P-X-S/T-P). The proteins found using this approach provide a source for future experiments aiming to determine the ciliary function of MRK and MOK.

Introduction

Primary cilia are microtubule-based organelles found on the surface of most eukaryotic cells. They have specialized sensory functions, including chemosensation, mechanosensation, and photosensation (Satir and Christensen, 2008). A wide variety of cilia lengths and morphologies exists, probably reflecting their specific functions in different types of tissues and organisms. Several signaling proteins regulate cilia and morphology (Avasthi and Marshall, 2011). Among the signaling proteins that modulate cilia length is a small family of kinases, the RCKs (*ros* cross-hybridizing kinases). Members of the RCK family have been shown to negatively regulate cilia length in *Chlamydomonas*, *Leishmania*, *C. elegans*, and mice (Bengs et al., 2005; Berman et al., 2003; Burghoorn et al., 2007; Omori et al., 2010).

The mammalian genomes harbor three members of the RCK family: MAK/RCK (male germ cell-associated kinase/*ros* cross-hybridizing kinase) (Bladt and Birchmeier, 1993; Xia et al., 2002), MRK/ICK (MAK-related kinase/intestinal cell kinase) (Abe et al., 1995; Togawa et al., 2000), and MOK/RAGE (MAPK/MAK/MRK overlapping kinase/renal tumor antigen) (Miyata et al., 1999; Van Den Eynde et al., 1999). Several proteins have been found to interact with the different RCK members. Co-immunoprecipitation assays showed that MAK, which regulates cilia length in mouse photoreceptors (Omori et al., 2010), associates with and phosporylates the microtubule-associated protein (MAP) RP1 (Omori et al., 2010). A yeast two-hybrid screen showed that MRK interacts with CCRK (cell cycle-related kinase), Raptor (regulatory-associated protein of mTOR), PP5 (protein phosphatase 5), and Scythe (Fu et al., 2006). Of these four proteins, CCRK is the only protein with a known ciliary function. The CCRK homologue in *Chlamydomonas*, LF2 (long flagella 2), is a negative regulator of cilia length (Tam et al., 2007). In zebrafish, CCRK, together with Bromi, regulates ciliary membrane and axonemal growth (Ko et al., 2010). The other three proteins do not immediately appear to have a ciliary function. Raptor is an mTOR scaffold protein (Yonezawa et al., 2004). Interestingly, the mTOR pathway was recently shown to be involved in the modulation of cilia length (Yuan et al., 2012). Protein phosphatase 5 (PP5) is a negative regulator of growth arrest (Zuo et al., 1998; Zuo et al., 1999) and Scythe is an inhibitor of apoptosis (Desmots et al., 2005). Co-immunoprecipitation assays showed that MOK binds the molecular chaperones Cdc37, HSC70, HSP90, HSP70, and HSP60 (Miyata et al., 2001). No other binding partners have been reported for MOK.

Regulation of cilia length is complex process, involving several signaling pathways, as well as structural proteins (Avasthi and Marshall, 2011; Miyoshi et al., 2011). To gain more insight in how RCK kinases regulate cilia length, we sought to identify proteins that associate with MRK and/or MOK using a proteomics approach. MS analysis of proteins co-purified with tagged MRK and MOK identified various potential MRK and MOK interacting proteins.

Results

Identification of MRK and MOK binding partners in HEK293T cells using a biotinylation-proteomics approach

We chose to perform our pull-down assays in HEK293T cells, because of their high transfection efficiency. Although some groups have reported that HEK293T can generate primary cilia (Gerdes et al., 2007; Kinzel et al., 2010; van Rooijen et al., 2008), we did not observe any ciliated HEK293T cells after 48 hours of serum-starvation (data not shown). However, HEK293T cells do express MRK and MOK (data not shown), as well as most IFT complex proteins (Boldt et al., 2011). Triple tagged MRK and MOK constructs were generated by fusing GFP, a V5 tag, and a biotinylation tag (bio-tag) to their C-terminal end. In addition to wild type MRK and MOK, we also generated triple tagged kinase-dead MRK and MOK. In kinase-dead mutant constructs an essential lysine in the ATP-binding pocket was changed into a methionine, making the protein inactive (Xia et al., 2002). Each of the resulting constructs were transiently expressed together with birA, a bacterial protein–biotin ligase (Driegen et al., 2005), in HEK293T cells. Biotinylated MRK and MOK were recovered from the HEK293T extracts using magnetic streptavidin beads. MRK/MOK and co-precipitated proteins were resolved on SDS-PAGE followed by Coomassie staining (Figure 1A). The (co)-purified proteins were subjected to MS analysis. This analysis identified numerous potential binding partners of MRK and MOK. After exclusion of aspecifically binding proteins (proteins that were pulled-down with GFP-Bio), MS analysis identified 89 potential binding partners for wild type MOK, 262 potential binding partners for kinase-dead MOK, 416 potential binding partners for wild type MRK, and 341 potential binding partners for kinase-dead MRK.

Comparison of candidate proteins with ciliary proteome database

To select the candidate binding partners of MRK and MOK relevant to cilia, we decided to compare our MS results with the ciliary proteome database (http://www.ciliaproteome.org). The ciliary proteome (Gherman et al., 2006) provides an overview of candidate ciliary proteins by combining several proteomic (Andersen et al., 2003; Keller et al., 2005; Liu et al., 2007; Ostrowski et al., 2002; Pazour et al., 2005) and genomic studies (Avidor-Reiss et al., 2004; Blacque et al., 2005; Broadhead et al., 2006; Efimenko et al., 2005; Li et al., 2004). Proteins that are present (according to the ciliary proteome database) in at least two of these proteomic/genomic studies, as well as in our mass spec results are shown in table 1. This reduced the list of candidate binding partners to 66 proteins. It is important to note that with this approach cytosolic proteins that directly interact with MOK and MRK might not be taken into account. These proteins could still play an important role in how MRK and MOK regulate cilia length and IFT. This list of candidates comprises proteins that have been described to function in a variety of processes. At first glance some process do not appear to be compatible with a ciliary function (for examples transcription and translation), while others function in processes which are compatible with a ciliary function (for example centrosomal proteins and proteins involved MT-based transport).

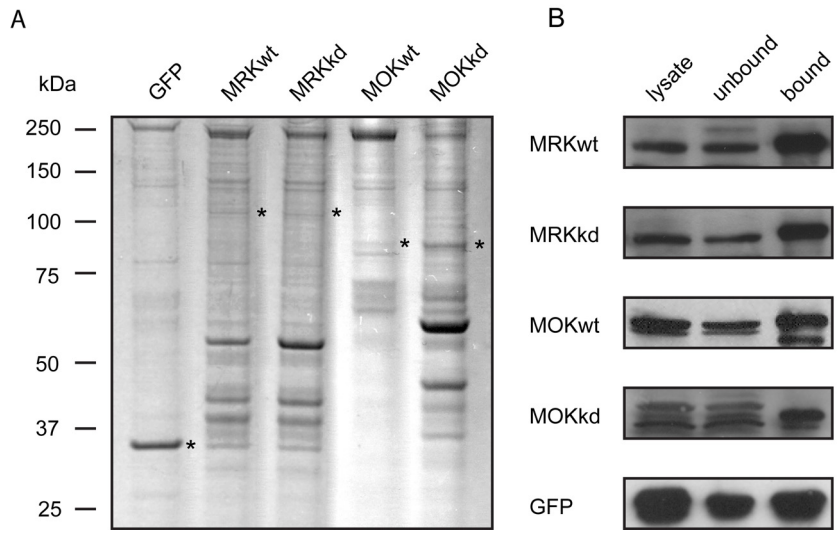

Figure 1. Purification of MRK and MOK, and their binding partners. (A) Coomassie stained SDS-PAGE gel with (co)-purified proteins from pull-down assays in HEK293T with GFP-Bio (GFP), MRKwt-GFP-Bio (MRKwt), MRKkd-GFP-Bio (MRKkd), MOKwt-GFP-Bio (MOKwt), and MOKkd-GFP-Bio (MOKkd). The proteins used as baits are indicated with asterisks. (B) Western blot analysis of the lysate, unbound, and bound fractions of pull down assays in HEK293T visualizing MRKwt, MRKkd, MOKwt, MOKkd, and GFP with anti-GFP.

Identification of proteins containing R-P-X-S/T-P, the MRK phosphorylation consensus sequence

Protein kinases recognize specific amino acid sequences surrounding the site of phosphorylation (Songyang et al., 1996), which can be useful for identifying protein substrates. Using a positional scanning peptide array method, R-P-X-S/T-P was identified as the preferred phosphorylation consensus sequence recognized by MRK (Fu et al., 2006). We performed a BLAST search for this consensus sequence in both the human and mouse genomes. This search yielded 84 proteins containing the MRK phosphorylation consensus sequence. Several of these proteins had already been described to have a ciliary function. The most interesting one is RP1, a MT-associated protein that positively regulates cilia length, and which is the downstream target of the third RCK, MAK (Omori et al., 2010). The BLAST search also yielded three basal body-associated proteins: Centrosomal protein 110kDa/Centriolin, centrosomal protein 350kDa, and rootletin. In addition, two ciliary dynein subunits were found, axonemal dynein heavy chain 1 and axonemal dynein heavy chain 3. However, these dyneins do not function in IFT, but instead function in the coordinated beating of motile cilia (Lee, 2011). MRK has been found to phosphorylate Raptor (Fu et al., 2009), an associated component of mTOR (Kim et al., 2002). Surprisingly, the phosporylation site of Raptor for MRK was R-P-G-T-T (Wu et al., 2012), which is slightly different from the MRK phosphorylation consensus sequence (a nonpolar a.a proline is replaced for a polar a.a. threonine). This suggests that minor deviations of the phosphorylation consensus sequence

are possible. When comparing the proteins containing the MRK phosphorylation consensus sequence with the candidate binding partners from the pull-down experiments we found two proteins that were present in both: nuclear mitotic apparatus protein 1 (NUMA1) and ankyrin repeat domain-containing protein 17 (ANKRD17). Intriguingly, both proteins are also present in the ciliary proteome. It would be interesting to further examine this interaction.

Discussion

Mass spectrometry analysis

Here we used a biotinylation-proteomics approach to identify the molecular partners of MRK and MOK, in order to learn more about their function. For this approach, the biotin ligase from *Escherichia coli* (birA) was used to biotinylate proteins containing a short (15 amino acids) peptide sequence, the bio-tag (Driegen et al., 2005). In HEK293T cells transfected with tagged MRK/MOK (and birA) we observed high expression of these fluorescent proteins (data not shown), however biotinylated wild type and kinase-dead MRK and MOK were not efficiently pulled down from HEK293T cells. A possible explanation would be that not all bio-tagged MRK and MOK is efficiently biotinylated, for example because bio-tagged MRK/MOK and birA reside in different cellular compartments in the cell. Western blot analysis revealed that there was still a considerable amount of tagged MRK and MOK present in the unbound fractions (Figure 1B), supporting this idea. Perhaps, pull down experiments with beads coated with an antibody, such as anti-GFP or anti-V5, would be more efficient.

Centrosomal proteins

Among the proteins that co-purified with MRK were four centrosomal proteins: centrosomal protein 164kDa (Cep164), pericentrin (Pcnt), centrosomal protein 170kDa (Cep170), and CDK5 regulatory subunit associated protein 2 (CDK5RAP2). Cep164 localizes to the distal appendages of the basal body, and in the absence of Cep164, hTERT-RPE1 cells fail to form primary cilia (Graser et al., 2007). Pcnt is an integral component of the centrosome, and can act as a multifunctional scaffold for numerous proteins and protein complexes (Doxsey et al., 1994; Takahashi et al., 2002; Zimmerman et al., 2004). Interestingly, Pcnt depletion disrupts basal body localization of IFT proteins and the cation channel polycystin-2 (PC2), and inhibits primary cilia assembly in hTERT-RPE1 cells (Jurczyk et al., 2004). Cep170 associates with subdistal appendages, and depletion of Cep170 perturbs cytoskeletal organization and cell shape (Guarguaglini et al., 2005). CDK5RAP2 functions in gamma-tubulin attachment to centrosomes (Fong et al., 2008). Three additional centrosomal proteins were found to have the preferred MRK phosphorylation consensus sequence: Centriolin, Centrosome-associated protein 350 (Cep350), and Rootletin. Centriolin interacts with proteins of the vesicle-targeting exocyst complexes and vesicle-fusion SNARE complexes (Gromley et al., 2005), as well as with Hook2 (Szebenyi et al., 2007), a member of the Hook family of proteins which function in the positioning of cellular structures. Cep350 has been described to function in MT anchoring (Yan et al., 2006). Rootletin is a structural component of the ciliary rootlet (Yang et al., 2002), but has also been described to act as a scaffolding protein for kinesin-1 vesicular cargos (Yang and Li, 2005). In *C. elegans*, the amphid cilia of *che-10* (homologue of rootletin) mutants degenerate, leaving dendrites with bulb-shaped endings, filled with protein accumulations (Perkins et al., 1986). MRK and MOK both localize to the basal body and it is very well possible that MRK and MOK regulate the entry of specific ciliary proteins at this location.

Microtubule–based transport & other microtubule-associated proteins

Intraflagellar transport is a microtubule motor protein-based transport system. Molecular motors use microtubules to transport cargo to particular locations. Typically, adaptor and

scaffold proteins are used to bind cargo to the motor proteins. MOK and MRK both undergo transport in the cilium, but MRK also affects the anterograde velocity of IFT particles. Thus, an interaction of MRK and MOK with components of molecular transport machineries could be explained in different ways. Dynein light chain 1/LC8 was co-purified with kinase-dead MOK. Dynein light chain 1 is part of cytoplasmic dynein 2 (Rompolas et al., 2007), the dynein motor complex responsible for retrograde IFT. Additionally, it has been shown that Nde1 negatively regulates ciliary length by tethering dynein light chain 1 at the basal body (Kim et al., 2011). Tubulin tyrosine ligase-like family member 3 (TTLL3) was found in the IPs of both wild type and kinase-dead MRK. Posttranslational modifications (PTMs) of microtubules can alter the affinities of motor proteins. TTLL3 acts as a tubulin glycine ligase and depletion of TTLL3 shortens the ciliary axoneme (Wloga et al., 2009). Two other proteins associated with microtubule-based motor transport found in the MS analysis are nuclear distribution gene C (NudC) and intraflagellar transport 74 (IFT74). NudC mediates the interaction between dynein and dynactin complexes with kinesin-1, when these complexes are transported in an anterograde direction (Yamada et al., 2010). IFT74 is a peripheral complex B protein. In *C. elegans*, *ift-74* mutants show marginal defects in cilia formation, thus *ift-74* is not absolutely required for ciliogenesis (Kobayashi et al., 2007). Modulation of the MT motor protein-based transport system inside the cilium, but also towards the cilium, could alter the delivery of proteins to the distal tip, and thus explain the function of MRK and MOK as negative regulators of cilia length.

Signal transduction

MRK and MOK are kinases, and probably function in a signaling cascade. In the MS analysis of the co-purified proteins multiple signaling components were found: several subunits of protein phosphatase 1 (PP1), three G protein subunits, a subunit of a cAMP-dependent protein kinase, and MAK. PP1 is a major serine/threonine-protein phosphatase involved in various cellular processes (Shi, 2009). One of these is the modulation of sperm motility (Fardilha et al., 2011), a process where MAK also functions in (Shinkai et al., 2002). Membrane-associated G proteins are heterotrimeric proteins, consisting of α, β, and γ subunit. The three G protein subunits that co-purified with MRK/MOK have not been described to have a ciliary function. cAMP-dependent protein kinase type II-alpha regulatory subunit (PRKAR2A) has been shown to interact with GSK-3β (Tanji et al., 2002), a component of the mTOR pathways and a negative regulator of cilia length (Miyoshi et al., 2009). Finally, MAK co-purified with MRK, which could mean that RCKs can form heterodimers, or function together in a bigger complex.

Others

In addition to IFT, the cilium also relies on vesicular-mediated transport for its formation and its function (Emmer et al., 2010; Nachury et al., 2010; Pazour and Bloodgood, 2008). ADP-ribosylation factor 1 (ARF1), RAB1A, RAB10, RAP2C, ADP-ribosylation factor 6 (ARF6), Ras-related protein R-Ras (RRAS), and golgin B1 were co-purified with MRK and/or MOK. Of these proteins, Rab10 is the only protein that has been described to have a ciliary function (Babbey et al., 2010). Since subcellular localization studies suggest that neither MRK nor MOK associate with vesicles it is unclear why they would associate with proteins involved in vesicular-mediated transport.

The proteins of the 14-3-3 family are scaffolding proteins that anchor different signaling proteins (Bustos, 2012). 14-3-3ε, 14-3-3γ, and 14-3-3θ co-purified with both MRK and MOK. These three proteins could act as scaffolding proteins for MRK and MOK, bringing them in close proximity with upstream or downstream signaling proteins.

NME1 and NME2, which can form hexamers (Janin et al., 2000), are nucleoside diphosphate kinases (NDPKs). These kinases catalyze the exchange of phosphate groups between different nucleoside diphosphates. Several members have already been shown to localize to primary cilia and sperm flagella, but their function in the cilium is still unknown. Interestingly, NME1 has been shown to interact with Aurora A kinase, which regulates the disassembly of cilia (Kinzel et al., 2010).

The presence of NUMA1 and ANKRD17 in the MS analysis of proteins that co-purified with MRK and/or MOK was particularly interesting because they contain MRK's preferred phosphorylation consensus sequence. NuMA plays a central role in spindle maintenance by physically tethering microtubules to centrosomes and by focusing spindle microtubules at the poles (Gaglio et al., 1995; Gordon et al., 2001; Kallajoki et al., 1991; Merdes et al., 1996). ANKRD17 is ubiquitously expressed and binds Cyclin E/Cdk2 (Deng et al., 2009; Wang et al., 2012), a key regulator of the G_1-S transition.

Material and methods

Plasmids

GFPbio was generated by PCR amplification of the V5-bio-tag from PK-bio (Gift from Eric Soler) and subcloning into the BsrGI and NotI sites of pEGFP-N1 (Clontech). MOKwt-GFP-bio was generated by subcloning the V5-bio-tag from GFP-bio into the BsrGI and NotI sites of MOKwt-GFP. MOKwt-GFP had previously been generated by PCR amplification of the MOK ORF from mouse MOK cDNA (a gift from Yoshihiko Miyata) and subcloning it into the NheI and HindIII sites of pEGFP-N1. MOKkd-GFPbio was generated by replacing MOKwt from MOKwt-GFPbio with MOKkd from MOKkd-GFP using the NheI and HindIII sites. MOKkd-GFP had previously been generated by changing the codon of an essential lysine residue at a.a. position 33 into a methionine codon using site-directed mutagenesis. To make a kinase-dead GFP-MOK construct, site-directed mutagenesis was used to change the codon of an essential lysine residue at a.a. position 35 into a methionine codon. MRKwt-GFPbio was generated by replacing MOKwt from MOKwt-GFPbio with MRKwt from MRKwt-GFP using the AgeI and EcoRI sites. MRKwt-GFP had previously been generated by PCR amplification of the MRK open reading frame (ORF) from mouse MRK cDNA (purchased from ImaGenes) and subcloning it into the NheI and HindIII sites of pEGFP-N1. MRKkd-GFPbio was generated by replacing MOKwt from MOKwt-GFPbio with MRKkd from MRKkd-GFP using the AgeI and EcoRI sites. MRKkd-GFP had previously been generated by changing the codon of an essential lysine residue at a.a. position 35 into a methionine codon using site-directed mutagenesis. HA-birA was a gift from Dies Meijer.

Cell culture and transfections

HEK293T cells were grown in DMEM/F10 medium supplemented with 10% FCS, penicillin (100 U/ml) and streptomycin (100 µg/ml). For pull-down experiments, four 14-cm plates with HEK293T cells, at a confluency of 80%, were transfected using Lipofectamine 2000 (Invitrogen).

Pull-down

For pull-downs, HEK293 cells transfected with the bio-tagged bait protein and birA were harvested one day after transfection. Harvested cells were washed once with 1x PBS, and lysed with lysis buffer (20 mM Tris pH 7.5, 150 mM KCl, 0.2% Triton X-100, 10% glycerol, and Protease Inhibitor Cocktail (Roche)) for 30 minutes on ice. Cell lysates were centrifuged for 10 minutes at 16.000 g. Supernatant was incubated with streptavidin-coated beads (Dynabeads M-280 Streptavidin, Invitrogen) for two hours at room temperature, which had been blocked for 30 minutes at room temperature with blocking buffer (20 mM Tris pH 7.5, 150 mM KCl, 20% glycerol, and 1 µg/µl chicken egg albumin). Afterwards, the beads were washed six times with wash buffer (20 mM Tris pH 7.5, 150 mM KCl, 0.1% Triton X-100, 10% glycerol, and Protease Inhibitor Cocktail (Roche). Finally, purified proteins were eluted in 50 µl 1x PBS by boiling for 5 minutes. Proteins were resolved on a pre-cast polyacrylamide gel (NuPAGE Novex 4–12% Bis-Tris Gels, Invitrogen), and stained using Colloidal Blue Staining Kit (Invitrogen).

Western Blot Analysis

The lysate, unbound, and bound fractions, obtained during the pull-downs, were separated on SDS-PAGE gels and then transferred to a nitrocellulose transfer membrane (Whatman). Membranes were probed with rabbit polyclonal anti-GFP (Abcam; 1:1000), washed three times with PBST (0.25% Tween-20 in 1x PBS), probed with HRP-conjugated anti-rabbit (Dako; WB, 1:5000), washed three times with PBST, and finally the membranes were exposed to chemiluminescence reagent (Amersham). Chemiluminescence was detected with Alliance 2.7 (UVItec).

Mass spectrometry

One-dimensional SDS-PAGE gel lanes were cut into 2-mm slices using an automatic gel slicer and subjected to in-gel reduction with dithiothreitol, alkylation with iodoacetamide, and digestion with trypsin (sequencing grade; Promega), as described previously (Wilm et al., 1996). Nanoflow liquid chromatography-tandem mass spectrometry was performed on an 1100 series capillary liquid chromatography system (Agilent Technologies) coupled to an LTQ-Orbitrap mass spectrometer (Thermo) operating in positive mode and equipped with a nanospray source. Peptide mixtures were trapped on a ReproSil C18 reversed-phase column (column dimensions, 1.5 cm by 100 µm, packed in-house; Dr Maisch GmbH) at a flow rate of 8 µl/min. Peptide separation was performed on a ReproSil C18 reversed-phase column (column dimensions, 15 cm by 50 µm, packed in-house; Dr Maisch GmbH) using a linear gradient from 0 to 80% B buffer (A buffer is 0.1 M acetic acid, and B buffer is 80% [vol/vol] acetonitrile-0.1 M acetic acid) for 70 min and at a constant flow rate of 200 nl/min using a splitter. The column eluent was directly sprayed into the electrospray ionization source of the mass spectrometer. Mass spectra were acquired in continuum mode; fragmentation of the peptides was performed in data-dependent mode. Peak lists were automatically created from raw data files using Mascot Distiller software (version 2.0; MatrixScience). The Mascot search algorithm (version 2.2) was used for searching against the International Protein Index database (IPI_human_20110407.fasta). Peptide tolerance was typically set to 10 ppm, and the fragment ion tolerance was set to 0.8 Da. A maximum number of two missed cleavages by trypsin were allowed, and carbamidomethylated cysteine and oxidized methionine were set as fixed and variable modifications, respectively. The Mascot score cutoff value for a positive protein hit was set to 40. Individual peptide tandem mass spectrometry spectra with Mascot scores <40 were checked manually and either interpreted as valid identifications or discarded. Proteins present in the negative control (GFPbio) were omitted from the initial analysis.

References

Abe, S., T. Yagi, S. Ishiyama, M. Hiroe, F. Marumo, and Y. Ikawa. 1995. Molecular cloning of a novel serine/threonine kinase, MRK, possibly involved in cardiac development. *Oncogene*. 11:2187-95.

Andersen, J.S., C.J. Wilkinson, T. Mayor, P. Mortensen, E.A. Nigg, and M. Mann. 2003. Proteomic characterization of the human centrosome by protein correlation profiling. *Nature*. 426:570-4.

Avasthi, P., and W.F. Marshall. 2011. Stages of ciliogenesis and regulation of ciliary length. *Differentiation*.

Avidor-Reiss, T., A.M. Maer, E. Koundakjian, A. Polyanovsky, T. Keil, S. Subramaniam, and C.S. Zuker. 2004. Decoding cilia function: defining specialized genes required for compartmentalized cilia biogenesis. *Cell*. 117:527-39.

Babbey, C.M., R.L. Bacallao, and K.W. Dunn. 2010. Rab10 associates with primary cilia and the exocyst complex in renal epithelial cells. *Am J Physiol Renal Physiol*. 299:F495-506.

Bengs, F., A. Scholz, D. Kuhn, and M. Wiese. 2005. LmxMPK9, a mitogen-activated protein kinase homologue affects flagellar length in Leishmania mexicana. *Mol Microbiol*. 55:1606-15.

Berman, S.A., N.F. Wilson, N.A. Haas, and P.A. Lefebvre. 2003. A novel MAP kinase regulates flagellar length in Chlamydomonas. *Curr Biol*. 13:1145-9.

Blacque, O.E., E.A. Perens, K.A. Boroevich, P.N. Inglis, C. Li, A. Warner, J. Khattra, R.A. Holt, G. Ou, A.K. Mah, S.J. McKay, P. Huang, P. Swoboda, S.J. Jones, M.A. Marra, D.L. Baillie, D.G. Moerman, S. Shaham, and M.R. Leroux. 2005. Functional genomics of the cilium, a sensory organelle. *Curr Biol*. 15:935-41.

Bladt, F., and C. Birchmeier. 1993. Characterization and expression analysis of the murine rck gene: a protein kinase with a potential function in sensory cells. *Differentiation*. 53:115-22.

Boldt, K., D.A. Mans, J. Won, J. van Reeuwijk, A. Vogt, N. Kinkl, S.J. Letteboer, W.L. Hicks, R.E. Hurd, J.K. Naggert, Y. Texier, A.I. den Hollander, R.K. Koenekoop, J. Bennett, F.P. Cremers, C.J. Gloeckner, P.M. Nishina, R. Roepman, and M. Ueffing. 2011. Disruption of intraflagellar protein transport in photoreceptor cilia causes Leber congenital amaurosis in humans and mice. *J Clin Invest*. 121:2169-80.

Broadhead, R., H.R. Dawe, H. Farr, S. Griffiths, S.R. Hart, N. Portman, M.K. Shaw, M.L. Ginger, S.J. Gaskell, P.G. McKean, and K. Gull. 2006. Flagellar motility is required for the viability of the bloodstream trypanosome. *Nature*. 440:224-7.

Burghoorn, J., M.P. Dekkers, S. Rademakers, T. de Jong, R. Willemsen, and G. Jansen. 2007. Mutation of the MAP kinase DYF-5 affects docking and undocking of kinesin-2 motors and reduces their speed in the cilia of Caenorhabditis elegans. *Proc Natl Acad Sci U S A*. 104:7157-62.

Bustos, D.M. 2012. The role of protein disorder in the 14-3-3 interaction network. *Mol Biosyst*. 8:178-84.

Deng, M., F. Li, B.A. Ballif, S. Li, X. Chen, L. Guo, and X. Ye. 2009. Identification and functional analysis of a novel cyclin e/cdk2 substrate ankrd17. *J Biol Chem*. 284:7875-88.

Desmots, F., H.R. Russell, Y. Lee, K. Boyd, and P.J. McKinnon. 2005. The reaper-binding protein scythe modulates apoptosis and proliferation during mammalian development. *Mol Cell Biol*. 25:10329-37.

Doxsey, S.J., P. Stein, L. Evans, P.D. Calarco, and M. Kirschner. 1994. Pericentrin, a highly conserved centrosome protein involved in microtubule organization. *Cell*. 76:639-50.

Driegen, S., R. Ferreira, A. van Zon, J. Strouboulis, M. Jaegle, F. Grosveld, S. Philipsen, and D. Meijer. 2005. A generic tool for biotinylation of tagged proteins in transgenic mice. *Transgenic Res*. 14:477-82.

Efimenko, E., K. Bubb, H.Y. Mak, T. Holzman, M.R. Leroux, G. Ruvkun, J.H. Thomas, and P. Swoboda. 2005. Analysis of xbx genes in C. elegans. *Development*. 132:1923-34.

Emmer, B.T., D. Maric, and D.M. Engman. 2010. Molecular mechanisms of protein and lipid targeting to ciliary membranes. *J Cell Sci*. 123:529-36.

Fardilha, M., S.L. Esteves, L. Korrodi-Gregorio, S. Pelech, E.S.O.A. da Cruz, and E.S.E. da Cruz. 2011. Protein phosphatase 1 complexes modulate sperm motility and present novel targets for male infertility. *Mol Hum Reprod*. 17:466-77.

Fong, K.W., Y.K. Choi, J.B. Rattner, and R.Z. Qi. 2008. CDK5RAP2 is a pericentriolar protein that functions in centrosomal attachment of the gamma-tubulin ring complex. *Mol Biol Cell*. 19:115-25.

Fu, Z., J. Kim, A. Vidrich, T.W. Sturgill, and S.M. Cohn. 2009. Intestinal cell kinase, a MAP kinase-related kinase, regulates proliferation and G1 cell cycle progression of intestinal epithelial cells. *Am J Physiol Gastrointest Liver Physiol*. 297:G632-40.

Fu, Z., K.A. Larson, R.K. Chitta, S.A. Parker, B.E. Turk, M.W. Lawrence, P. Kaldis, K. Galaktionov, S.M. Cohn, J. Shabanowitz, D.F. Hunt, and T.W. Sturgill. 2006. Identification of yin-yang regulators and a phosphorylation consensus for male germ cell-associated kinase (MAK)-related kinase. *Mol Cell Biol*. 26:8639-54.

Gaglio, T., A. Saredi, and D.A. Compton. 1995. NuMA is required for the organization of microtubules into aster-like mitotic arrays. *J Cell Biol*. 131:693-708.

Gerdes, J.M., Y. Liu, N.A. Zaghloul, C.C. Leitch, S.S. Lawson, M. Kato, P.A. Beachy, P.L. Beales, G.N. DeMartino, S.

Fisher, J.L. Badano, and N. Katsanis. 2007. Disruption of the basal body compromises proteasomal function and perturbs intracellular Wnt response. *Nat Genet*. 39:1350-60.

Gherman, A., E.E. Davis, and N. Katsanis. 2006. The ciliary proteome database: an integrated community resource for the genetic and functional dissection of cilia. *Nat Genet*. 38:961-2.

Gordon, M.B., L. Howard, and D.A. Compton. 2001. Chromosome movement in mitosis requires microtubule anchorage at spindle poles. *J Cell Biol*. 152:425-34.

Graser, S., Y.D. Stierhof, S.B. Lavoie, O.S. Gassner, S. Lamla, M. Le Clech, and E.A. Nigg. 2007. Cep164, a novel centriole appendage protein required for primary cilium formation. *J Cell Biol*. 179:321-30.

Gromley, A., C. Yeaman, J. Rosa, S. Redick, C.T. Chen, S. Mirabelle, M. Guha, J. Sillibourne, and S.J. Doxsey. 2005. Centriolin anchoring of exocyst and SNARE complexes at the midbody is required for secretory-vesicle-mediated abscission. *Cell*. 123:75-87.

Guarguaglini, G., P.I. Duncan, Y.D. Stierhof, T. Holmstrom, S. Duensing, and E.A. Nigg. 2005. The forkhead-associated domain protein Cep170 interacts with Polo-like kinase 1 and serves as a marker for mature centrioles. *Mol Biol Cell*. 16:1095-107.

Janin, J., C. Dumas, S. Morera, Y. Xu, P. Meyer, M. Chiadmi, and J. Cherfils. 2000. Three-dimensional structure of nucleoside diphosphate kinase. *J Bioenerg Biomembr*. 32:215-25.

Jurczyk, A., A. Gromley, S. Redick, J. San Agustin, G. Witman, G.J. Pazour, D.J. Peters, and S. Doxsey. 2004. Pericentrin forms a complex with intraflagellar transport proteins and polycystin-2 and is required for primary cilia assembly. *J Cell Biol*. 166:637-43.

Kallajoki, M., K. Weber, and M. Osborn. 1991. A 210 kDa nuclear matrix protein is a functional part of the mitotic spindle; a microinjection study using SPN monoclonal antibodies. *EMBO J*. 10:3351-62.

Keller, L.C., E.P. Romijn, I. Zamora, J.R. Yates, 3rd, and W.F. Marshall. 2005. Proteomic analysis of isolated chlamydomonas centrioles reveals orthologs of ciliary-disease genes. *Curr Biol*. 15:1090-8.

Kim, D.H., D.D. Sarbassov, S.M. Ali, J.E. King, R.R. Latek, H. Erdjument-Bromage, P. Tempst, and D.M. Sabatini. 2002. mTOR interacts with raptor to form a nutrient-sensitive complex that signals to the cell growth machinery. *Cell*. 110:163-75.

Kim, S., N.A. Zaghloul, E. Bubenshchikova, E.C. Oh, S. Rankin, N. Katsanis, T. Obara, and L. Tsiokas. 2011. Nde1-mediated inhibition of ciliogenesis affects cell cycle re-entry. *Nat Cell Biol*. 13:351-60.

Kinzel, D., K. Boldt, E.E. Davis, I. Burtscher, D. Trumbach, B. Diplas, T. Attie-Bitach, W. Wurst, N. Katsanis, M. Ueffing, and H. Lickert. 2010. Pitchfork regulates primary cilia disassembly and left-right asymmetry. *Dev Cell*. 19:66-77.

Ko, H.W., R.X. Norman, J. Tran, K.P. Fuller, M. Fukuda, and J.T. Eggenschwiler. 2010. Broad-minded links cell cycle-related kinase to cilia assembly and hedgehog signal transduction. *Dev Cell*. 18:237-47.

Kobayashi, T., K. Gengyo-Ando, T. Ishihara, I. Katsura, and S. Mitani. 2007. IFT-81 and IFT-74 are required for intraflagellar transport in C. elegans. *Genes Cells*. 12:593-602.

Lee, L. 2011. Mechanisms of mammalian ciliary motility: Insights from primary ciliary dyskinesia genetics. *Gene*. 473:57-66.

Li, J.B., J.M. Gerdes, C.J. Haycraft, Y. Fan, T.M. Teslovich, H. May-Simera, H. Li, O.E. Blacque, L. Li, C.C. Leitch, R.A. Lewis, J.S. Green, P.S. Parfrey, M.R. Leroux, W.S. Davidson, P.L. Beales, L.M. Guay-Woodford, B.K. Yoder, G.D. Stormo, N. Katsanis, and S.K. Dutcher. 2004. Comparative genomics identifies a flagellar and basal body proteome that includes the BBS5 human disease gene. *Cell*. 117:541-52.

Liu, Q., G. Tan, N. Levenkova, T. Li, E.N. Pugh, Jr., J.J. Rux, D.W. Speicher, and E.A. Pierce. 2007. The proteome of the mouse photoreceptor sensory cilium complex. *Mol Cell Proteomics*. 6:1299-317.

Merdes, A., K. Ramyar, J.D. Vechio, and D.W. Cleveland. 1996. A complex of NuMA and cytoplasmic dynein is essential for mitotic spindle assembly. *Cell*. 87:447-58.

Miyata, Y., M. Akashi, and E. Nishida. 1999. Molecular cloning and characterization of a novel member of the MAP kinase superfamily. *Genes Cells*. 4:299-309.

Miyata, Y., Y. Ikawa, M. Shibuya, and E. Nishida. 2001. Specific association of a set of molecular chaperones including HSP90 and Cdc37 with MOK, a member of the mitogen-activated protein kinase superfamily. *J Biol Chem*. 276:21841-8.

Miyoshi, K., K. Kasahara, I. Miyazaki, and M. Asanuma. 2009. Lithium treatment elongates primary cilia in the mouse brain and in cultured cells. *Biochem Biophys Res Commun*. 388:757-62.

Miyoshi, K., K. Kasahara, I. Miyazaki, and M. Asanuma. 2011. Factors that influence primary cilium length. *Acta Med Okayama*. 65:279-85.

Nachury, M.V., E.S. Seeley, and H. Jin. 2010. Trafficking to the ciliary membrane: how to get across the periciliary diffusion barrier? *Annu Rev Cell Dev Biol*. 26:59-87.

Omori, Y., T. Chaya, K. Katoh, N. Kajimura, S. Sato, K. Muraoka, S. Ueno, T. Koyasu, M. Kondo, and T. Furukawa. 2010. Negative regulation of ciliary length by ciliary male germ cell-associated kinase (Mak) is required for

retinal photoreceptor survival. *Proc Natl Acad Sci U S A*. 107:22671-6.
Ostrowski, L.E., K. Blackburn, K.M. Radde, M.B. Moyer, D.M. Schlatzer, A. Moseley, and R.C. Boucher. 2002. A proteomic analysis of human cilia: identification of novel components. *Mol Cell Proteomics*. 1:451-65.
Pazour, G.J., N. Agrin, J. Leszyk, and G.B. Witman. 2005. Proteomic analysis of a eukaryotic cilium. *J Cell Biol*. 170:103-13.
Pazour, G.J., and R.A. Bloodgood. 2008. Targeting proteins to the ciliary membrane. *Curr Top Dev Biol*. 85:115-49.
Perkins, L.A., E.M. Hedgecock, J.N. Thomson, and J.G. Culotti. 1986. Mutant sensory cilia in the nematode Caenorhabditis elegans. *Dev Biol*. 117:456-87.
Rompolas, P., L.B. Pedersen, R.S. Patel-King, and S.M. King. 2007. Chlamydomonas FAP133 is a dynein intermediate chain associated with the retrograde intraflagellar transport motor. *J Cell Sci*. 120:3653-65.
Satir, P., and S.T. Christensen. 2008. Structure and function of mammalian cilia. *Histochem Cell Biol*. 129:687-93.
Shi, Y. 2009. Serine/threonine phosphatases: mechanism through structure. *Cell*. 139:468-84.
Shinkai, Y., H. Satoh, N. Takeda, M. Fukuda, E. Chiba, T. Kato, T. Kuramochi, and Y. Araki. 2002. A testicular germ cell-associated serine-threonine kinase, MAK, is dispensable for sperm formation. *Mol Cell Biol*. 22:3276-80.
Songyang, Z., K.P. Lu, Y.T. Kwon, L.H. Tsai, O. Filhol, C. Cochet, D.A. Brickey, T.R. Soderling, C. Bartleson, D.J. Graves, A.J. DeMaggio, M.F. Hoekstra, J. Blenis, T. Hunter, and L.C. Cantley. 1996. A structural basis for substrate specificities of protein Ser/Thr kinases: primary sequence preference of casein kinases I and II, NIMA, phosphorylase kinase, calmodulin-dependent kinase II, CDK5, and Erk1. *Mol Cell Biol*. 16:6486-93.
Szebenyi, G., B. Hall, R. Yu, A.I. Hashim, and H. Kramer. 2007. Hook2 localizes to the centrosome, binds directly to centriolin/CEP110 and contributes to centrosomal function. *Traffic*. 8:32-46.
Takahashi, M., A. Yamagiwa, T. Nishimura, H. Mukai, and Y. Ono. 2002. Centrosomal proteins CG-NAP and kendrin provide microtubule nucleation sites by anchoring gamma-tubulin ring complex. *Mol Biol Cell*. 13:3235-45.
Tam, L.W., N.F. Wilson, and P.A. Lefebvre. 2007. A CDK-related kinase regulates the length and assembly of flagella in Chlamydomonas. *J Cell Biol*. 176:819-29.
Tanji, C., H. Yamamoto, N. Yorioka, N. Kohno, K. Kikuchi, and A. Kikuchi. 2002. A-kinase anchoring protein AKAP220 binds to glycogen synthase kinase-3beta (GSK-3beta) and mediates protein kinase A-dependent inhibition of GSK-3beta. *J Biol Chem*. 277:36955-61.
Togawa, K., Y.X. Yan, T. Inomoto, S. Slaugenhaupt, and A.K. Rustgi. 2000. Intestinal cell kinase (ICK) localizes to the crypt region and requires a dual phosphorylation site found in map kinases. *J Cell Physiol*. 183:129-39.
Van Den Eynde, B.J., B. Gaugler, M. Probst-Kepper, L. Michaux, O. Devuyst, F. Lorge, P. Weynants, and T. Boon. 1999. A new antigen recognized by cytolytic T lymphocytes on a human kidney tumor results from reverse strand transcription. *J Exp Med*. 190:1793-800.
van Rooijen, E., R.H. Giles, E.E. Voest, C. van Rooijen, S. Schulte-Merker, and F.J. van Eeden. 2008. LRRC50, a conserved ciliary protein implicated in polycystic kidney disease. *J Am Soc Nephrol*. 19:1128-38.
Wang, Y., X. Tong, G. Li, J. Li, M. Deng, and X. Ye. 2012. Ankrd17 positively regulates RIG-I-like receptor (RLR)-mediated immune signaling. *Eur J Immunol*. 42:1304-15.
Wilm, M., A. Shevchenko, T. Houthaeve, S. Breit, L. Schweigerer, T. Fotsis, and M. Mann. 1996. Femtomole sequencing of proteins from polyacrylamide gels by nano-electrospray mass spectrometry. *Nature*. 379:466-9.
Wloga, D., D.M. Webster, K. Rogowski, M.H. Bre, N. Levilliers, M. Jerka-Dziadosz, C. Janke, S.T. Dougan, and J. Gaertig. 2009. TTLL3 Is a tubulin glycine ligase that regulates the assembly of cilia. *Dev Cell*. 16:867-76.
Wu, D., J.R. Chapman, L. Wang, T.E. Harris, J. Shabanowitz, D.F. Hunt, and Z. Fu. 2012. Intestinal cell kinase (ICK) promotes activation of the mTOR complex 1 (mTORC1) through phosphorylation of raptor Thr-908. *J Biol Chem*.
Xia, L., D. Robinson, A.H. Ma, H.C. Chen, F. Wu, Y. Qiu, and H.J. Kung. 2002. Identification of human male germ cell-associated kinase, a kinase transcriptionally activated by androgen in prostate cancer cells. *J Biol Chem*. 277:35422-33.
Yamada, M., S. Toba, T. Takitoh, Y. Yoshida, D. Mori, T. Nakamura, A.H. Iwane, T. Yanagida, H. Imai, L.Y. Yu-Lee, T. Schroer, A. Wynshaw-Boris, and S. Hirotsune. 2010. mNUDC is required for plus-end-directed transport of cytoplasmic dynein and dynactins by kinesin-1. *EMBO J*. 29:517-31.
Yan, X., R. Habedanck, and E.A. Nigg. 2006. A complex of two centrosomal proteins, CAP350 and FOP, cooperates with EB1 in microtubule anchoring. *Mol Biol Cell*. 17:634-44.
Yang, J., and T. Li. 2005. The ciliary rootlet interacts with kinesin light chains and may provide a scaffold for kinesin-1 vesicular cargos. *Exp Cell Res*. 309:379-89.
Yang, J., X. Liu, G. Yue, M. Adamian, O. Bulgakov, and T. Li. 2002. Rootletin, a novel coiled-coil protein, is a structural component of the ciliary rootlet. *J Cell Biol*. 159:431-40.
Yonezawa, K., C. Tokunaga, N. Oshiro, and K. Yoshino. 2004. Raptor, a binding partner of target of rapamycin. *Biochem Biophys Res Commun*. 313:437-41.

Yuan, S., J. Li, D.R. Diener, M.A. Choma, J.L. Rosenbaum, and Z. Sun. 2012. Target-of-rapamycin complex 1 (Torc1) signaling modulates cilia size and function through protein synthesis regulation. *Proc Natl Acad Sci U S A*.

Zimmerman, W.C., J. Sillibourne, J. Rosa, and S.J. Doxsey. 2004. Mitosis-specific anchoring of gamma tubulin complexes by pericentrin controls spindle organization and mitotic entry. *Mol Biol Cell*. 15:3642-57.

Zuo, Z., N.M. Dean, and R.E. Honkanen. 1998. Serine/threonine protein phosphatase type 5 acts upstream of p53 to regulate the induction of p21(WAF1/Cip1) and mediate growth arrest. *J Biol Chem*. 273:12250-8.

Zuo, Z., G. Urban, J.G. Scammell, N.M. Dean, T.K. McLean, I. Aragon, and R.E. Honkanen. 1999. Ser/Thr protein phosphatase type 5 (PP5) is a negative regulator of glucocorticoid receptor-mediated growth arrest. *Biochemistry*. 38:8849-57.

Table 1: Selection of MOK and MRK interacting proteins, which are also present in the cilia proteome (Gherman et al., 2006)

		MRKwt		MRKkd		MOKwt		MOKkd	
Protein	**accession**	**emPAI value**	**Mascot score**	**emPAI value**	**Mascot score**	**emPAI value**	**Mascot score**	**emPAI value**	**Mascot score**
MAK-related kinase	IPI00414132	1.74	856	1.74	776	-	-	-	-
MAPK/MAK/MRK overlapping kinase	IPI00398648	-	-	-	-	0.57	366	0.75	384
Centrosomal proteins									
Centrosomal protein 164kD	IPI00007293	0.22	549	0.29	436	-	-	-	-
Pericentrin	IPI00479143	0.09	456	0.18	839	-	-	-	-
Centrosomal protein 170kDa	IPI00186194	0.13	280	0.09	207	-	-	-	-
CDK5 regulatory subunit associated protein 2	IPI00329038	-	-	0.03	125	-	-	-	-
MT motor transport & other MT associated proteins									
Dynein light chain 1/LC8	IPI00019329	-	-	-	-	-	-	1.63	148
Tubulin tyrosine ligase-like family member 3	IPI00554811	0.71	142	0.71	160	-	-	-	-
Nuclear distribution gene C	IPI00550746	0.45	172	0.21	110	-	-	0.45	173
Intraflagellar transport 74	IPI00018090	0.3	301	-	-	-	-	-	-
Signal transduction									
Guanine nucleotide-binding protein G(i), alpha-2 subunit	IPI00748145	-	-	1.62	641	-	-	0.3	212
Protein phosphatase 1, catalytic subunit, beta isozyme	IPI00218236	1.13	232	0.94	229	-	-	0.76	284
Protein phosphatase 1, catalytic subunit, gamma isozyme	IPI00005705	0.94	189	0.61	186	-	-	0.94	308
Protein phosphatase 1, catalytic subunit, alpha isozyme	IPI00027423	-	-	0.58	190	-	-	0.73	260
Guanine nucleotide-binding protein G(I)/G(S)/G(T) subunit beta-2	IPI00003348	-	-	-	-	-	-	0.6	284
Protein kinase, cAMP-dependent, catalytic, alpha	IPI00217960	-	-	0.43	208	-	-	-	-
Guanine nucleotide-binding protein subunit beta-2-like 1	IPI00848226	-	-	-	-	-	-	0.22	120
Protein phosphatase 1, regulatory (inhibitor) subunit 10	IPI00298731	-	-	0.2	171	-	-	-	-
Protein kinase, cAMP-dependent, regulatory, type II. alpha	IPI00063234	0.18	116	-	-	-	-	-	-

Male germ cell-associated kinase	IPI00025489	0.5	328	0.09	111	-	-	-	-
Vesicle-mediated transport									
ADP-ribosylation factor 1	IPI00215914	3.6	431	2.28	368	-	-	1.34	265
RAB1A. member RAS oncogene family	IPI00005719	0.86	262	-	-	-	-	-	-
RAB10. member RAS oncogene family	IPI00016513	0.86	184	-	-	-	-	-	-
RAP2C. member of RAS oncogene family	IPI00009607	0.96	251	0.65	128	-	-	-	-
ADP-ribosylation factor 6	IPI00215920	-	-	0.42	111	-	-	-	-
Ras-related protein R-Ras	IPI00020418	-	-	0.38	124	-	-	-	-
Golgin B1	IPI00063234	-	-	0.02	111	-	-	-	-
Scaffold proteins									
14-3-3 epsilon	IPI00000816	1.07	383	1.34	326	0.98	276	-	-
14-3-3 gamma	IPI00220642	0.46	204	0.87	217	-	-	-	-
14-3-3 theta	IPI00018146	-	-	-	-	0.43	119	0.29	115
Actin skeleton									
Myosin, heavy chain 9, non-muscle	IPI00019502	3.07	531	-	-	0.05	198	-	-
Coronin, actin binding protein, 1B	IPI00007058	-	-	0.22	120	-	-	-	-
Myosin, heavy chain 11, smooth muscle	IPI00020501	-	-	-	-	-	-	0.07	187
Myosin ID	IPI00329719	-	-	-	-	-	-	0.17	268
Apoptosis									
Serpin peptidase inhibitor, clade B (ovalbumin). member 3	IPI00022204	-	-	-	-	0.57	290	-	-
Glutathione S-transferase pi 1	IPI00219757	-	-	-	-	0.76	185	-	-
Transcription & Translation									
Ribosomal protein S10	IPI00008438	6.73	508	-	-	-	-	-	-
Ribosomal protein S19	IPI00215780	3.55	366	-	-	-	-	-	-
Peptidylprolyl isomerase A (cyclophilin A)	IPI00419585	0.78	162	-	-	1.47	189	-	-
Ribosomal protein S6	IPI00021840	-	-	-	-	-	-	0.85	301
Ribosomal protein S9	IPI00221088	-	-	-	-	0.8	158	-	-

DEAD (Asp-Glu-Ala-Asp) box polypeptide 5	IPI00017617	0.6	481	0.87	623	-	-	-	-
DEAD (Asp-Glu-Ala-Asp) box polypeptide 17	IPI00651653	-	-	0.72	482	-	-	-	-
Nascent polypeptide-associated complex alpha subunit	IPI00023748	-	-	0.57	195	-	-	0.57	188
DEAD (Asp-Glu-Ala-Asp) box polypeptide 20	IPI00005904	0.22	222	-	-	-	-	-	-
Aspartyl-tRNA synthetase	IPI00216951	0.13	130	-	-	-	-	-	-
Molecular chaperones									
Heat shock 70kDa protein 5 (glucose-regulated protein. 78kDa)	IPI00003362	1.12	843	-	-	-	-	-	-
Heat shock 27kDa protein 1	IPI00025512	-	-	0.86	142	1.06	190	0.86	150
Heat shock 70kDa protein 9 (mortalin)	IPI00007765	0.8	597	-	-	-	-	-	-
Cell division cycle 37	IPI00300659	0.62	240	0.38	266	-	-	-	-
Other & Unknown									
RAN. member RAS oncogene family	IPI00643041	-	-	1.75	275	-	-	-	-
NME1-NME2 readthrough	IPI00012048	1.74	211	1.24	154	1.58	148	0.92	267
S100 calcium binding protein, zeta	IPI00031091	-	-	-	-	-	-	1.2	320
Peroxiredoxin 4	IPI00011937	0.42	134	0.59	139	-	-	-	-
Exosome component 1	IPI00032823	-	-	0.63	120	-	-	-	-
ATP-binding cassette, sub-family F (GCN20). member 2	IPI00005045	0.42	188	-	-	-	-	-	-
Prohibitin 2	IPI00027252	-	-	-	-	0.35	114	-	-
Cell division cycle 73, Paf1/RNA polymerase II complex component	IPI00300659	0.35	275	-	-	-	-	-	-
ATP synthase subunit beta	IPI00303476	0.21	252	0.21	129	-	-	-	-
Stomatin (EPB72)-like 2	IPI00334190	0.2	108	-	-	-	-	-	-
Monooxygenase, DBH-like 1	IPI00419596	0.11	108	-	-	-	-	-	-
Zinc finger CCCH-type, antiviral 1	IPI00332936	-	-	0.1	120	-	-	-	-
Nuclear mitotic apparatus protein 1	IPI00006196	0.13	383	0.05	140	-	-	-	-
Damage-specific DNA binding protein 1, 127kDa	IPI00293464	-	-	-	-	0.08	107	-	-
5-azacytidine induced 1	IPI00298883	0.03	104	0.09	220	-	-	-	-
Ankyrin repeat domain 17	IPI00783186	0.03	127	-	-	-	-	-	-

Chapter 4

SQL-1, homologue of the Golgi protein GMAP210, modulates Intraflagellar Transport in *C. elegans*

Joost R. Broekhuis[1], Suzanne Rademakers[1], Jan Burghoorn[1], and Gert Jansen[1]

[1]Department of Cell Biology, Erasmus MC, PO Box 2040, 3000 CA, Rotterdam, the Netherlands

Abstract

Primary cilia are microtubule-based organelles, which have an important sensory function. For their function they rely on the delivery of specific proteins, both by intracellular trafficking and intraflagellar transport (IFT). In *C. elegans'* cilia anterograde IFT is mediated by kinesin-II and OSM-3. Previously, we have shown that expression of a dominant active G protein α subunit (GPA-3QL) in amphid channel neurons affects the coordination of kinesin-II and OSM-3 and cilia length, suggesting that environmental signals can affect IFT and cilia length. Here, we show that mutation of *sql-1* (suppressor of *gpa-3QL – 1*), which encodes the homologue of the mammalian Golgi protein GMAP-210, can suppress the *gpa-3QL* cilia length phenotype. SQL-1 localizes to the Golgi apparatus, where it is required for maintaining Golgi organization. Loss of *sql-1* by itself does not affect cilia length, while overexpression of *sql-1* results in longer cilia. Using live imaging of fluorescently tagged IFT proteins, we show that in *sql-1* mutants OSM-3 moves faster, kinesin-II moves slower, and that some complex A and B proteins move at an intermediate velocity, while others move at the same velocity as OSM-3. This indicates that mutation of *sql-1* destabilizes the IFT complex. Finally, we show that simultaneous inactivation of *sql-1* and activation of *gpa-3QL* affects the velocity of OSM-3. In summary, we show that in *C. elegans* the Golgin protein SQL-1 plays an important role in maintaining the stability of the IFT complex.

Introduction

Primary cilia are microtubule-based protrusions that can be found on the surface of almost all vertebrate cells, and have important sensory functions. Cilia dysfunction has been associated with a number of genetic diseases, collectively called ciliopathies (Hildebrandt et al., 2011). Many ciliopathies affect various tissues and are caused by defects in proteins that play a role in transport to the cilium or within the cilium. Often these mutations do not completely block ciliogenesis, but rather result in changes in cilia morphology and/or localization of signaling proteins in cilia.

A large diversity in cilia lengths and morphologies exists, probably reflecting the specialized functions cilia can have in different tissues and/or organisms. However, little is known about how this diversity is achieved. Different types of signaling molecules, including second messengers (Abdul-Majeed et al., 2012; Besschetnova et al., 2010; Mukhopadhyay et al., 2008; Ou et al., 2009), kinases (Berman et al., 2003; Burghoorn et al., 2007; Miyoshi et al., 2009; Omori et al., 2010; Tam et al., 2007; Wang et al., 2006) and G proteins (Burghoorn et al., 2010) have been shown to regulate cilia length and cilia morphology. Since these signaling pathways also regulate transport, both in and toward the cilium, it is likely that these transport processes play a role in regulating cilium length and morphology (Silverman and Leroux, 2009).

Ciliary proteins often originate from the Golgi apparatus (Emmer et al., 2010; Pazour and Bloodgood, 2008). A number of small GTPases, including Arf4, Arl6 and Rab8 (Jin et al., 2010; Mazelova et al., 2009; Nachury et al., 2007; Wiens et al., 2010), are involved in budding of vesicles from the Golgi apparatus and fusion at the ciliary base. In the absence of components of the multimeric BBSome complex, which is composed of 7 Bardet-Biedl Syndrome (BBS) proteins (Nachury et al., 2007), the GPCRs rhodopsin, Sstr3, and Mchr1 (Abd-El-Barr et al., 2007; Berbari et al., 2008; Nishimura et al., 2004), fail to reach the cilium, indicating that the BBSome functions in trafficking of (G-protein coupled) receptors to the cilium. However, whether the BBSome functions in vesicular transport, cargo selection, or vesicle docking and fusion is not completely clear.

Once inside the cilium, signaling proteins and structural proteins are transported by intraflagellar transport (IFT). During this process, IFT particles, multimeric protein complexes consisting of ~20 proteins, carry cargo along the microtubule axis of the cilium, towards the distal tip and back. Movement of the IFT particle is powered by kinesin-2 motors (anterograde transport) and cytosolic dynein 2 (retrograde transport) (Rosenbaum and Witman, 2002). IFT particles are organized in two distinct subcomplexes, complex A and complex B (Cole and Snell, 2009). Complex A has been implicated in retrograde transport and complex B in anterograde transport. In addition, proteins that are part of the BBSome have been observed moving in the cilium, with similar velocities as components of the IFT complex (Blacque et al., 2004; Nachury et al., 2007), suggesting that the BBSome associates with or is part of the IFT complex.

GMAP210 was recently found to play a role in vesicular transport from the Golgi to the cilium (Follit et al., 2008). It belongs to the Golgin family, whose members are characterized by a large number of coiled-coil domains, and function in maintaining the organization and position of the Golgi apparatus (Short et al., 2005). GMAP210 localizes to the cis-Golgi network (Rios et al., 1994), and is important for Golgi integrity (Rios et al., 2004). Interestingly, GMAP210 was found to anchor IFT20 to the Golgi apparatus. IFT20 is proposed to function as an adaptor

protein for targeting vesicles to the cilium. In addition, IFT20 is a complex B protein (Follit et al., 2006). In line with its novel role in vesicular trafficking to the cilium, absence of GMAP210 results in reduced levels of ciliary polycystin-2 (Follit et al., 2008). GMAP210 knockout mice die at birth, most likely due to heart and lung defects (Follit et al., 2008). Both heart and lung are among the organs affected in ciliopathy patients (Cardenas-Rodriguez and Badano, 2009).

The sensory cilia of *C. elegans'* amphid neurons provide an excellent model to study the regulation of cilia morphology. They can be divided in a middle segment, which has nine microtubule doublets, and a distal segment, which has nine microtubule singlets (Perkins et al., 1986; Ward et al., 1975). In the middle segment the IFT complex is transported by two members of the kinesin-2 family, kinesin-II and OSM-3. At the end of the middle segment kinesin-II dissociates from the complex, which leaves OSM-3 to transport the IFT complex in the distal segment (Snow et al., 2004). We have previously shown that in animals carrying a dominant active mutant *gpa-3* sensory Gα subunit, *gpa-3QL,* the coordination of kinesin-II and OSM-3 in cilia is affected, and the sensory cilia are shorter (Burghoorn et al., 2010). Interestingly, exposure of animals to dauer pheromone (a continuously secreted compound that at high concentration induces an alternative larval stage, the dauer larva (Golden and Riddle, 1982)), affects the coordination of kinesin-II and OSM-3 very similarly as *gpa-3QL* (Burghoorn et al., 2010). IFT measurements on *gpa-3* mutant animals exposed to dauer pheromone suggest that *gpa-3* functions in the pathway by which the pheromone affects IFT. Together these results suggest that environmental cues transduced via GPA-3 can modulate IFT.

To find out how *gpa-3* regulates IFT and cilia length we performed a screen for suppressors of the *gpa-3QL* cilia defect. We identified and characterized one of the mutants, *sql-1*, and found that *sql-1* encodes the *C. elegans'* orthologue of the mammalian Golgin protein GMAP210. We show that SQL-1 is ubiquitously expressed and localizes to the Golgi apparatus. In *sql-1* mutants the Golgi structure seems disorganized, in line with the function of Golgin proteins. In addition, s*ql-1* affects the stability of the IFT machinery, resulting in a partial separation of kinesin-II and OSM-3, and transport of the IFT complex predominantly by OSM-3.

Results

sql-1 encodes the *C. elegans* orthologue of mammalian GMAP210

A subset of the amphid neurons of wild type *C. elegans* can take up fluorescent dyes (e.g. DiO) from the environment (Hedgecock et al., 1985). However, animals with ciliary defects lose this ability. Among the mutations that result in such a dye filling defect is a dominant active mutation of the sensory Gα subunit *gpa-3*, *gpa-3QL* (Zwaal et al., 1997). We performed a forward genetic screen for mutations that suppress the dye filling defect of *gpa-3QL* animals. Using SNP-mapping (Wicks et al., 2001), the mutation in *gj202*, one of the mutants (Figure 1A), was mapped to a region of chromosome III. Injection of a combination of long-range PCR fragments spanning 35 kbp restored the *gpa-3QL* dye filling defect. This region was predicted to encode three genes, Y111B2A.4, Y111B2A.5, and Y111B2A.26. Using RT-PCR we found that these three predicted genes were actually a single gene spanning 18 exons, which we named *sql-1* (suppressor of *gpa-3QL* – 1). *sql-1(gj202)* contains an A>T nonsense mutation in exon 8 that introduces a premature stop codon (Figure 1B).

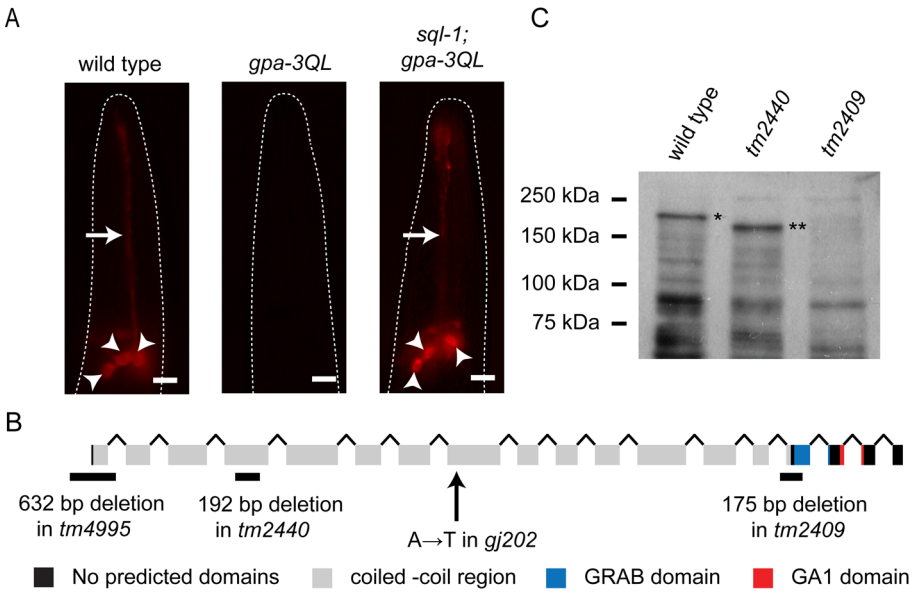

Figure 1. Identification of *sql-1*. (A) DiO dye filling of wild type, *gpa-3QL*, and *sql-1(gj202); gpa-3QL* animals. The dye filling defect of *gpa-3QL* animals is suppressed in *sql-1(gj202); gpa3QL*. DiO dye filling stains 6 pairs of amphid neurons. The cell bodies (indicated with an arrowhead) and dendrites (indicated with an arrow) of some of these are in the focal plane of this picture. Anterior is towards the top. Outlines of the worms are indicated with a dotted line. Scale bar, 10 µm. (B) Schematic representation of the *sql-1* gene structure. Coding exons are indicated as colored boxes. The coiled-coil region is shown in grey, the GRAB domain in blue, the GA-1 domain in red, and regions with no predicted domains in black. The position of the missense mutation in *sql-1 (gj202)* animals is indicated with an arrow, and the deletions of *sql-1(tm2409)*, *sql-1(tm2440)*, and *sql-1(tm4995)* animals are indicated with black bars. (C) Immunoblotting of whole worm lysates collected from wild type, *sql-1(tm2440)*, and *sql-1(tm2409)* animals, with an antibody raised against the N-terminal end of SQL-1. * marks wild type SQL-1 , ** marks truncated SQL-1 in *tm2440* animals.

sql-1 encodes the *C. elegans* orthologue of mammalian GMAP210, a member of the family of Golgin proteins (Short et al., 2005). At the a.a. level SQL-1 shows 12% identity to mouse GMAP210. Both SQL-1 and GMAP210 consist of predominantly coiled-coil domains; a.a. 5-1116 in SQL-1 and a.a. 64-1768 in GMAP210. The remaining 153 a.a. polypeptide of mammalian GMAP210 contains a GRAB (GRIP-related Arf-binding) domain, which is necessary for Golgi localization and might bind small GTPases, as well as a GA-1 motif, with unknown function (Gillingham et al., 2004; Short et al., 2005). The last 201 amino acids of mammalian GMAP210 have also been shown to interact with γ-tubulin (Infante et al., 1999; Rios et al., 2004). *C. elegans'* SQL-1 contains regions with high similarity to the GRAB (56% homology) and GA-1 domains (61% homology), suggesting these domains are conserved. The first 38 a.a. of GMAP210 contain an ALPS (ArfGAP-1 lipid-packing sensor) motif (Drin et al., 2007), which can also mediate Golgi targeting (Cardenas et al., 2009), but this motif is not present in *C. elegans'* SQL-1. Finally, mammalian GMAP210 has been shown to bind IFT20, and the IFT20-binding site was mapped to residues 1180-1319 of GMAP210 (Follit et al., 2008). It was suggested that the IFT20-binding site was not conserved in *C. elegans* (Follit et al., 2008). However, in SQL-1 we found a region with 39% similarity (16% identity) to the IFT20 binding region of mammalian GMAP210. To determine whether this interaction is conserved in *C. elegans* we performed co-IP assays on animals expressing GFP-tagged IFT-20. We found that anti-SQL-1 antibodies were unable to bring down IFT-20::GFP, and anti-GFP antibodies failed to bring down endogenous SQL-1 (Figure S1A, S1B). In addition, we determined the subcellular localization of IFT-20 using a full length *ift-20::gfp* fusion construct. In the ciliated neurons IFT-20::GFP localized to the cilia, transition zone, dendrites, and cell body. In the cilia we observed IFT-20::GFP positive particles, but in the transition zone, dendrites, and cell body we only observed a diffuse signal (Figure S1C). The localization pattern of IFT-20::GFP in *sql-1* mutant animals was identical to that of wild type animals. These data suggest that in *C. elegans* SQL-1 and IFT-20 do not physically interact, and that IFT-20 does not localize to the Golgi apparatus. Possibly, IFT-20's function in the Golgi apparatus is not conserved in *C. elegans*.

Initially, two deletion mutants were obtained from the NBP-Japan, *sql-1(tm2409)*, and *sql-1(tm2440)*. In the *sql-1(tm2440)* strain 192 bp of exon 4 was deleted, resulting in the loss of 64 a.a. of SQL-1 (Figure 1B). Western blot analysis, using antibodies raised against the N- and C-terminal parts of the SQL-1 protein, showed that the *sql-1(tm2440)* strain indeed expressed a smaller SQL-1 protein (Figure 1C, Figure S2A). *sql-1(tm2440); gpa-3QL* animals were dye filling defective, thus the deletion in *sql-1(tm2440)* did not suppress the dye filling defect of *gpa-3QL* animals (data not shown). The *sql-1(tm2409)* strain carries a 175 bp deletion, starting in intron 14 and ending in exon 15. RT-PCR showed that this resulted in the loss of exon 15, a frameshift in exon 16, and an early stop (data not shown). We could not detect the truncated SQL-1 protein of *sql-1(tm2409)* animals on a Western blot (expected molecular weight 137 kDa), or in immunofluorescence (Figure 1C, Figure S2A, S2B), indicating *sql-1(tm2409)* is a null allele. In *sql-1(tm2409); gpa-3QL* mutants the dye filling defect caused by *gpa-3QL* was suppressed (data not shown). Recently, we obtained a third deletion mutant, *tm4995*. The *sql-1(tm4955)* strain carries a 632 bp deletion, which removes exon 1 suggesting it might be a null allele. However, we could detect *sql-1* mRNA in the animals using RT-PCR with primers located in exons 3 and 8 (data not shown). Conversely, we could not detect a truncated SQL-1 protein on Western blot, or with immunofluorescence (data not shown). This suggests that *sql-1(tm4995)* is a null allele. *sql-1(tm4955);gpa-3QL* animals did show dye filling (data not shown). In addition to the loss-of-function mutants, we generated animals that contain extra copies of the *sql-1* gene, *sql-1XS*. Western blot analysis showed that *sql-1XS* animals (*gj2077)* expressed approximately

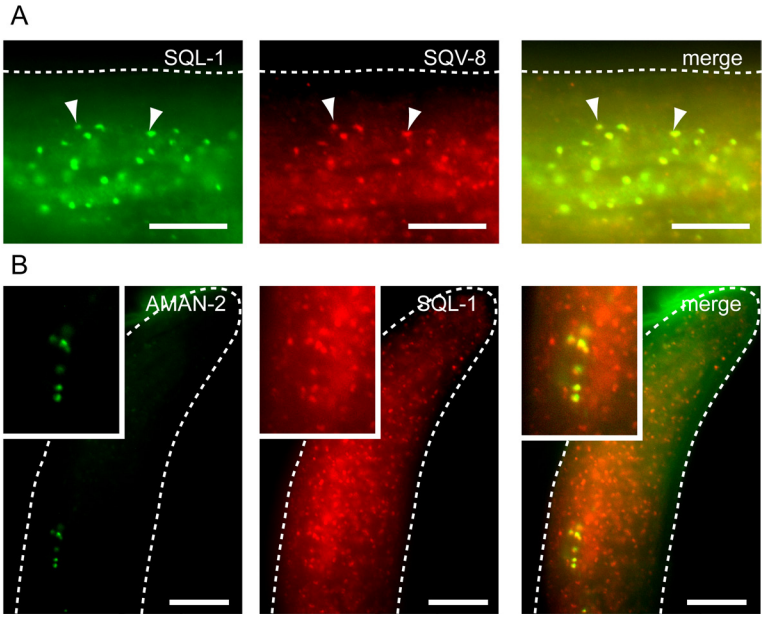

Figure 2. SQL-1 localizes to the Golgi apparatus. (A) Immunofluorescence images of wild type animals expressing SQL-1::GFP (green) stained with anti-SQV-8 (red) to mark the Golgi apparatus. Outline of the worm is indicated with a dotted line. Scale bar, 10 µm. (B) Immunofluorescence images of wild type animals expressing the Golgi marker AMAN-2::YFP (green) in the ASI neurons stained with anti-SQL-1 (red). Anterior is towards the top. Outlines of the worm is indicated with a dotted line. Scale bar, 10 µm.

three times more SQL-1 than wild type animals (data not shown). Overexpression of *sql-1* did not affect dye filling. All loss-of-function and overexpression animals were healthy and showed no apparent phenotype.

SQL-1 is ubiquitously expressed, and localizes to the Golgi apparatus

To determine the expression pattern and subcellular localization of SQL-1, two different antibodies were raised against SQL-1, one against an N-terminal part (a.a. 106-737) of SQL-1, and one against a C-terminal part (a.a. 519-1328). Immunofluorescence on wild type animals showed a spotted pattern throughout the whole body (Figure S2B), suggesting SQL-1 is ubiquitously expressed. A similar pattern was seen in *sql-1(tm2440)* animals (Figure S2B), but no immunoreactivity could be detected in *sql-1(tm2409)* and *sql-1(tm4995)* animals (Figure S2B, data not shown), confirming the specificity of the antibodies.

To confirm the localization pattern determined in the immunofluorescence experiments, we generated animals that expressed full length SQL-1 fused to GFP, p_{sql-1}*::sql-1::GFP* animals. In these animals we observed spots throughout their bodies (Figure 2A), similar to the pattern observed with SQL-1 Abs. Since the homologue of SQL-1, GMAP210, localizes to the Golgi apparatus (Rios et al., 1994), we stained p_{sql-1}*::sql-1::GFP* animals with an antibody against the glucuronyl transferase SQV-8, which stains the Golgi apparatus (Hadwiger et al., 2010).

This showed co-localization of SQL-1 and SQV-8 (Figure 2A). Both the immunofluorescence data and GFP fusion confirm that SQL-1 localizes to the Golgi apparatus. Interestingly, also an N-terminal (a.a. 1-302) SQL-1::GFP fusion localized to spots throughout the animal (data not shown), suggesting that perhaps SQL-1 contains an N-terminal region that mediates Golgi localization. However, this GFP-fusion is more abundant in the cytosol than the full length SQL-1 GFP-fusion (data not shown).

Mutation of *sql-1* suppresses the dye-filling defect of *gpa-3QL* animals, and therefore we analyzed the expression and subcellular localization of SQL-1 in neurons. We generated animals that express ed the Golgi marker AMAN-2, an alpha-mannosidase, tagged with YFP only in one pair of ciliated sensory neurons, the ASI neurons (p_{gpa-4}*::aman-2::YFP*), or in a subset of inter- and motor neurons (p_{glr-1}*::aman-2::YFP*). Staining of these animals with α-SQL-1 Ab indeed showed co-localization of AMAN-2::YFP and SQL-1 in the cell bodies of the ASI neurons (Figure 2B), and in the cell bodies of *glr-1* expressing neurons (data not shown). In p_{gpa-4}*::sql-1::GFP* animals, we observed SQL-1::GFP in the Golgi apparatus, and sometimes SQL-1 spots in the dendrites (data not shown). These SQL-1 spots were immobile, and were never observed in close proximity of the cilium. Together these data show that SQL-1 localizes to the Golgi apparatus in *C. elegans'* ciliated sensory neurons.

sql-1 is required for maintaining Golgi apparatus structure, but is not required for normal GPA-3 localization

Knock-down of GMAP210 has been shown to result in the dispersion of the Golgi membranes (Rios et al., 2004; Yadav et al., 2009). However, no defects were observed in the Golgi apparatus of GMAP210 mutant mice (Follit et al., 2008). We wondered whether the absence of SQL-1 affects the integrity of the Golgi apparatus in *C. elegans*.

To investigate this we visualized the Golgi apparatus specifically in the ASI neurons using AMAN-2::GFP in wild type and *sql-1(tm2409)* animals. In wild type animals we observed clear AMAN-2::GFP structures in the ASI cells (Figure 3A, 3B). However, in the majority of the *sql-1(tm2409)* animals the AMAN-2::GFP signal was more fragmented or even diffuse (Figure 3A, 3B). These results suggest that loss of function of *sql-1* affects the organization of the Golgi apparatus.

One way to explain the suppression of the dye filling defect in *sql-1(tm2409); gpa-3QL* animals is a trafficking defect of dominant active GPA-3QL protein, caused by the absence of the Golgi protein SQL-1. Therefore we used immunofluorescence to visualize the localization of GPA-3. In both wild type and *sql-1(tm2409)* animals GPA-3 can be observed at the ciliary membrane at comparable levels (Figure 3C), showing that *sql-1* is not required for ciliary localization of GPA-3. In *gpa-3QL* and *sql-1; gpa-3QL* animals α-GPA-3 staining is much stronger, showing GPA-3QL localization in the cilia, dendrite, and cell bodies. However, we observed no obvious differences in the levels of GPA-3QL staining in the cilia of *gpa-3QL* and *sql-1; gpa-3QL* animals (data not shown). Together these data suggest that suppression of the Dyf phenotype in *sql-1(tm2409); gpa-3QL* animals is not caused by absence of ciliary GPA-3QL.

Mutation of *sql-1* regulates cilia length, and acts cell-autonomously

It was previously shown that the cilia of the ADF, ASH, ASI, ASK, and ADL neurons of adult

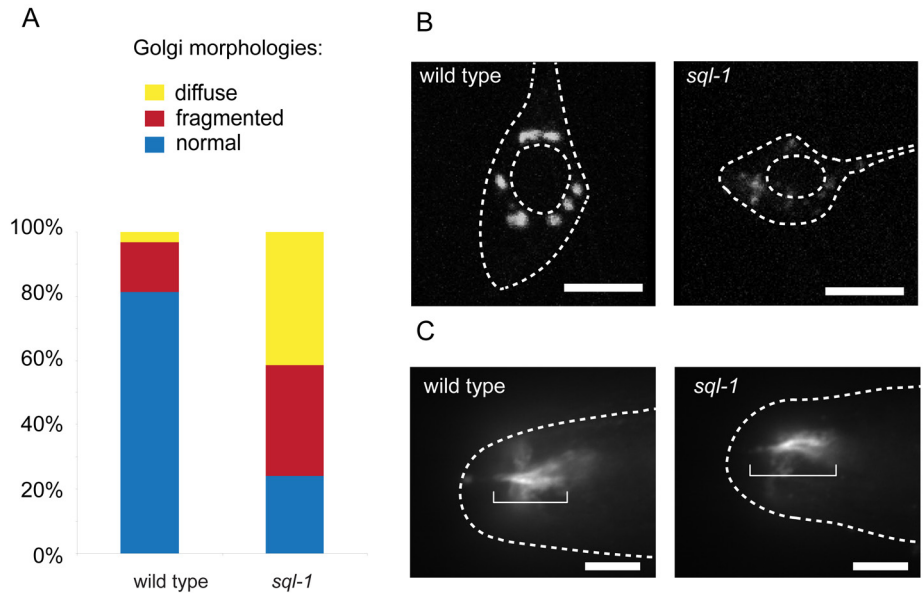

Figure 3. SQL-1 is required to maintain Golgi organization. (A) Percentage of wild type and *sql-1(tm2409)* animals that have distinct Golgi-membranes (normal), fragmentation of the Golgi-membranes (fragmented), or diffuse AMAN-2::GFP fluorescence (diffuse). The Golgi apparatus was visualized in the ASI neurons using AMAN-2::GFP. (B) ASI neurons of wild type and *sql-1(tm2409)* animals expressing AMAN-2::YFP. Outline of the cells and nuclei are indicated with a dotted line. Scale bar, 5 µm. (C) Immunofluorescence images of wild type and *sql-1(tm2409)* animals stained with anti-GPA-3. Sensory cilia are indicated with a bracket. Anterior is towards the left. Outlines of the worms are indicated with a dotted line. Scale bar, 5 µm.

gpa-3QL animals are shorter than those of wild-type adult animals (Burghoorn et al., 2010), explaining the dye filling defect. To determine if *sql-1* mutation affects cilia length of *gpa-3QL* animals, we visualized cilia using an ASI neuron specific *gpa-4::gfp* construct, and a *gpa-15::gfp* construct expressed in ASH, ASK, and ADL neurons (Jansen et al., 1999). Cilium length of *gpa-3QL* animals was restored to approximately wild type length in *sql-1(tm2409)*; *gpa-3QL* animals (Figure 4A, 4B).

To determine if *sql-1* levels themselves regulate cilium length we visualized cilia of *sql-1(tm2409)* and *sql-1XS* animals. Cilium length in *sql-1(tm2409)* animals is comparable to cilium length in wild type animals (Figure 4A, 4B). Interestingly, the cilia of ASI neurons of animals that overexpress SQL-1, *sql-1XS*, were significantly longer than those of wild-type animals (Figure 4A). To test if this effect on cilia length depends on either of the two kinesins we measured ASI lengths in *osm-3; sql-1XS* and *kap-1; sql-1XS* animals. *osm-3; sql-1XS* animals had longer cilia than *osm-3* animals (Figure 4A), suggesting that *osm-3* is not required for cilia lengthening in *sql-1XS* animals. However, loss of *kap-1* completely suppressed cilia lengthening as a result of *sql-1* overexpression (Figure 4A), indicating that kinesin-II is required for this effect.

To further confirm the specificity of suppression of the Dyf phenotype in *gpa-3QL* animals by

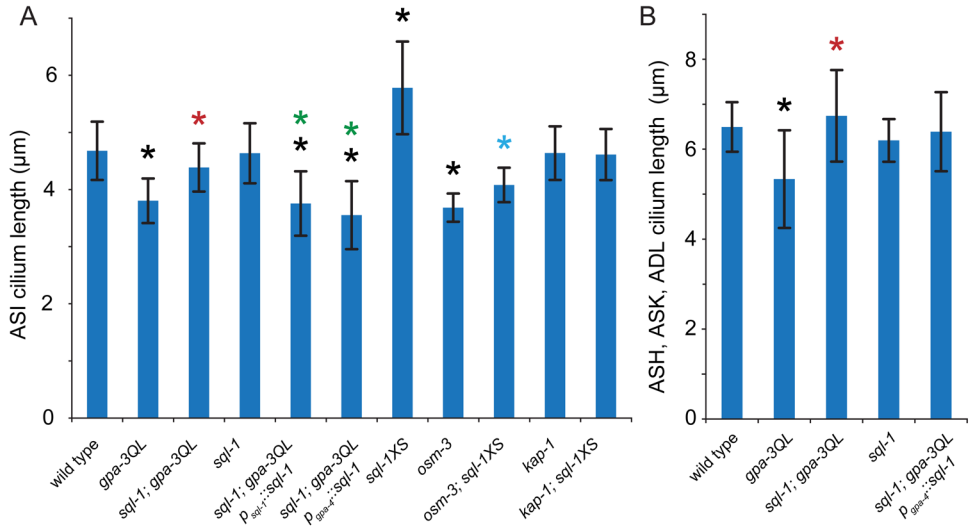

Figure 4. *sql-1* regulates cilia length. Average length of sensory cilia of the ASI neurons (A), and ASH, ASK, ADL neurons (B) in various genetic backgrounds. Statistically significant differences ($p < 0.001$) compared to cilia length in wild type animals are indicated in black, compared to cilia length in *gpa-3QL* animals in red, compared to cilia length in *sql-1; gpa-3QL* animals in green, and compared to cilia length in *osm-3* animals in blue. Statistical analysis was performed using an ANOVA, followed by a Bonferroni post hoc test. Error bars indicate SD.

the loss of SQL-1 we re-introduced the *sql-1* gene in *sql-1(tm2409); gpa-3QL* animals. This resulted in a decrease of the length of the cilia of the ASI neurons, comparable to the length of ASI cilia in *gpa-3QL* animals (Figure 4A). In addition, while expression of wild type *sql-1* specifically in the ASI neurons of *sql-1; gpa-3QL* animals did rescue ASI cilia length it did not affect the length of the cilia of ASH, ASK, and ADL. This suggests that *sql-1* acts cell-autonomously.

Mutation of *sql-1* partially uncouples kinesin-II and OSM-3

We previously hypothesized that the decrease of cilia length in *gpa-3QL* animals was the result of the partial uncoupling of kinesin-II and OSM-3 observed in the *gpa-3QL* animals (Burghoorn et al., 2010). To determine whether *sql-1* also affects the IFT machinery, we examined the motility of the two ciliary kinesins KAP-1 (mammalian homologue KAP3) and OSM-3 (KIF17), two complex A proteins CHE-11 (IFT140), DAF-10 (IFT22), two complex B proteins OSM-1 (IFT172) and CHE-13 (IFT57), and the dynein motor subunit XBX-1 (D2LIC) in *sql-1(tm2409)* animals as well as in wild type animals. In wild type animals all IFT proteins were transported at approximately 0.7 µm/s in the middle segments (Table 1), and at approximately 1.15 µm/s in the distal segments (Table S1). These speeds are consistent with published data (Snow et al., 2004). However, in the middle segments of *sql-1(tm2409)* animals kinesin-II moved at 0.59 µm/s, and OSM-3 at 0.89 µm/s (Table 1). Since the two kinesins moved with different velocities it is not possible that they were in the same complex at all time. CHE-11::GFP (complex A), OSM-1::GFP (complex B) and XBX-1::GFP (dynein) moved at similar velocities as OSM-3 in the middle segments of *sql-1(tm2409)* animals (Table 1), which implies that these associate

with IFT particles transported by OSM-3. Interestingly, DAF-10::GFP (complex A) and CHE-13::GFP (complex B) both moved at 0.67 µm/s in the middle segments of *sql-1(tm2409)* animals (Table 1). In the distal segments of *sql-1(tm2409)* animals, all examined IFT markers moved at a velocity of 1.15 µm/s, just as in wild type animals (Table S1).

To exclude that the any of these effects were caused by changes in the intrinsic velocities of kinesin-II or OSM-3, we decided to measure how the absence of SQL-1 affects IFT motility in *osm-3* and *kap-1* mutant backgrounds. In *sql-1(tm2409); osm-3* animals KAP-1::GFP (kinesin-II), DAF-10::GFP (complex A), CHE-13::GFP (complex B), and XBX-1::GFP (cargo) moved at 0.49-0.52 µm/s (Table 1), similar to the velocities observed in *osm-3* animals. In *kap-1; sql-1(tm2409)* animals OSM-3::GFP, DAF-10::GFP (complex A), CHE-13::GFP (complex B), and XBX-1::GFP (dynein) moved at the 1.00-1.19 µm/s (Table 1), similar to velocities observed in *kap-1* animals. These data indicate that the intrinsic velocities of the kinesins are not altered in *sql-1* mutant animals.

Together these data suggest that in *sql-1(tm2409)* animals kinesin-II and OSM-3 are partially separated. Moreover, the IFT complex also appears to dissociate. Of the tested IFT markers CHE-11, OSM-1, and XBX-1 predominantly travel with OSM-3, and DAF-10 and CHE-13 remain associated with the kinesin-II/OSM-3 complex. An alternative explanation would be that DAF-10 and CHE-13 associate with all three possible particles (the slow kinesin-II particle, the fast OSM-3 particle and the kinesin-II/OSM-3 complex), averaging in a velocity of 0.7 µm/s. To distinguish between these two possibilities we plotted the distributions of the speeds of CHE-13::GFP and DAF-10::GFP IFT events, where the presence of CHE-13 and DAF-10 in three particle types would show as additional peaks, or at least a wider distribution. However, the distributions of the CHE-11::GFP and DAF-10::GFP IFT events in wild type and *sql-1(tm2409)* animals (Figure S3) were very similar, suggesting that CHE-11 and DAF-10 were only present in the kinesin-II/OSM-3 transported particles.

It is not clear how SQL-1 affects IFT. Because of GMAP210's function in sorting or transport of proteins destined for the ciliary membrane, a possible explanation could be a defect in trafficking of ciliary proteins in the dendrite. Therefore, we visualized RAB-8 (a small GTPase involved in protein trafficking in the dendrite (Kaplan et al., 2010)) in the dendrites of the ciliated neurons. In *sql-1(tm2409)* animals we did not observe significant differences in the localization of GFP::RAB-8, or in the motility and frequency of transport events of GFP::RAB-8 positive particles, compared to wild type animals (data not shown).

OSM-3::GFP speed is affected in *sql-1; gpa-3QL* double mutant

Since in *gpa-3QL*, *gpa-3* and *sql-1(tm2409)* animals IFT is affected, we decided to examine IFT in double mutants, to study their genetic interaction. In the middle segments of *sql-1(tm2409); gpa-3* animals KAP-1::GFP and XBX-1::GFP moved at velocities similar to those observed in *sql-1* or *gpa-3* single mutant animals, OSM-3::GFP moved at the same speed as in *sql-1(tm2409)* animals (Table 1). These data suggest that *gpa-3* and *sql-1* function in the same genetic pathway.

In the middle segments of *sql-1(tm2409); gpa-3QL* animals KAP-1::GFP, DAF-10::GFP, and CHE-13::GFP moved at velocities similar to those observed in the middle segment of *sql-1(tm2409)* animals, while OSM-3::GFP and XBX-1::GFP moved significantly slower than in *sql-1(tm2409)* animals (Table 1). Compared to *gpa-3QL* animals OSM-3::GFP and KAP-1::GFP

Table 1: *sql-1* affects anterograde IFT velocities in the middle segment of *C. elegans'* sensory cilia.

	Ciliary kinesins				IFT-A particle			
	KAP-1		OSM-3		CHE-11		DAF-10	
Genotype	**average ± sd**	**n**	**average ± sd**	**n**	**average ± sd**	**n**	**average ± sd**	**n**
wild type	0.70 ± 0.10	194	0.70 ± 0.17	212	0.69 ± 0.21	118	0.69 ± 0.16	213
kap-1	0.70 ± 0.16	90	1.17 ± 0.24[a]	130	ND		ND	
osm-3	0.49 ± 0.10[a]	91	0.70 ± 0.14	150	ND		ND	
sql-1	0.59 ± 0.09[a,2]	210	0.89 ± 0.19[a,1]	192	0.84 ± 0.19[a,1]	195	0.67 ± 0.17[2]	212
kap-1; sql-1	ND		1.19 ± 0.19[a]	219	ND		1.10 ± 0.19[a]	211
sql-1; osm-3	0.52 ± 0.08[a]	207	ND		NA		0.49 ± 0.07[a]	210
gpa-3	0.57 ± 0.14[a,*]	197	1.04 ± 0.24[a,1,*]	152	0.78 ± 0.16[1,2,*]	190	ND	
sql-1; gpa-3	0.59 ± 0.11[a,2]	211	0.86 ± 0.17[a,b,1]	240	ND		0.70 ± 0.11[1,2]	205
gpa-3QL	0.56 ± 0.12[a,2,*]	148	0.84 ± 0.22[a,1,*]	178	0.73 ± 0.23[1,2,*]	222	ND	
sql-1; gpa-3QL	0.60 ± 0.11[a,2]	190	0.78 ± 0.16[c,1]	214	ND		0.68 ± 0.16[2]	201
kap-1; gpa-3QL	ND		1.19 ± 0.32[a]	231	ND		ND	
kap-1; sql-1; gpa-3QL	ND		0.94 ± 0.23[a,e,f,g]	204	ND		0.86 ± 0.18[a,f]	198
sql-1; osm-3; gpa-3QL	0.50 ± 0.07 [a,c]	202	ND		ND		ND	

	IFT-B particle				Dynein (cargo)	
	OSM-1		CHE-13		XBX-1	
Genotype	**average ± sd**	**n**	**average ± sd**	**n**	**average ± sd**	**n**
wild type	0.70 ± 0.26	224	0.70 ± 0.16	132	0.72 ± 0.16	195
kap-1	ND		ND		1.03 ± 027[a,2]	213
osm-3	ND		ND		ND	
sql-1	0.82 ± 017[a,1]	227	0.67 ± 0.12[1,2]	207	0.82 ± 0.16[a,1]	188

kap-1; sql-1	ND		1.17 ± 0.25[a]	205	1.01 ± 0.20[a,2]	211
sql-1; osm-3	ND		0.50 ± 0.06[a]	219	0.52 ± 0.09[a]	204
gpa-3	0.80 ± 0.20[a,1,2,*]	196	ND		0.77 ± 0.23[1,2,*]	202
sql-1; gpa-3	ND		0.69 ± 0.12[1,2]	204	0.79 ± 0.16[1]	220
gpa-3QL	0.77 ± 0.27[1,*]	201	ND		0.73 ± 0.23[1,2,*]	201
sql-1; gpa-3QL	ND		0.69 ± 0.11[1,2]	226	0.62 ± 0.11[a,c,d,2]	208
kap-1; gpa-3QL	ND		ND		ND	
kap-1; sql-1; gpa-3QL	ND		0.79 ± 0.18[f,2]	211	ND	
sql-1; osm-3; gpa-3QL	ND		ND		ND	

Average anterograde IFT velocities (in µm/s) ± standard deviation (sd) of KAP-1::GFP, OSM-3::GFP, CHE-11::GFP, DAF-10::GFP, OSM-1::GFP, CHE-13::GFP and XBX-1::GFP in wild type and mutant backgrounds. Velocities annotated with * were previously described in (Burghoorn et al., 2010). Statistically significant differences ($P < 0.001$) compared to IFT velocities in wild type animals are indicated with [a], compared to *gpa-3* animals with [b], compared to *sql-1(tm2409)* animals with [c], compared to *gpa-3QL* animals with [d], compared to *kap-1; sql-1(tm2409)* animals with [e], compared to *kap-1; sql-1(tm2409)* animals with [f], and compared to *kap-1; gpa-3QL* with [g]. Statistically significant differences ($P < 0.001$) of IFT velocities of each of the GFP markers compared to the velocities of KAP-1::GFP and OSM-3::GFP in the same mutant background are indicated with [1] and [2], respectively. Statistical analysis was performed using an ANOVA, followed by a Bonferroni post hoc test. Abbreviations: n, number of IFT particles measured; ND, not determined.

moved at similar speeds in *sql-1(tm2409); gpa-3QL* animals, while XBX-1::GFP moved slower in the double mutant.

Interestingly, in distal segments of *sql-1(tm2409); gpa-3QL* animals all measured components of the IFT complex (OSM-3, DAF-10, CHE-13, and XBX-1) moved slower than the expected 1.15 μm/s, the velocity of the IFT complex in the distal segments of wild type, *sql-1(tm2409)*, and *gpa-3QL* animals (Table S1), although not all these speeds are significantly slower, probably due to the large variation in speeds. One possible explanation would be that in *sql-1(tm2409); gpa-3QL* animals kinesin-II would be able to enter the distal segment, as previously observed in *dyf-5* mutant animals (Burghoorn et al., 2007). However we could not detect any KAP-1::GFP in the distal segments of *sql-1(tm2409); gpa-3QL* animals (Figure S4). A second explanation would be that the intrinsic velocity of OSM-3 is affected in *sql-1(tm2409); gpa-3QL* animals. To test this we generated *sql-1(tm2409); kap-1; gpa-3QL* animals in which the IFT complex is transported by only OSM-3 in both segments. In these animals OSM-3::GFP, DAF-10::GFP, and CHE-13::GFP indeed moved at reduced velocities (0.79-0.94 μm/s) in the middle segments (Table 1). In the middle segments of the respective double mutants, *sql-1(tm2409); kap-1* and *kap-1; gpa-3QL*, all IFT::GFP fusions measured moved at 1.10-1.19 μm/s, the velocity of IFT mediated by OSM-3 alone (Table 1). Together these data suggest that in the absence of SQL-1 and presence of a dominant active GPA-3 motility of OSM-3 kinesin is affected.

Discussion

Summary

In this study we identified and characterized SQL-1 (suppressor of *gpa-3QL* – 1), the *C. elegans* orthologue of mammalian GMAP210. Loss of *sql-1* suppresses the ciliary length defect of *gpa-3QL* animals and probably as a result of that also the dye filling defect of these animals. Loss-of-function of *sql-1* by itself does not affect cilia length, however overexpression of *sql-1* results in an increase of cilia length. SQL-1 is ubiquitously expressed and localizes to the Golgi apparatus. Loss of *sql-1* has a mild effect on Golgi integrity. Importantly, mutation of *sql-1* affects the IFT machinery and partially uncouples kinesin-II and OSM-3. Genetic epistasis analyses suggest that *sql-1* and *gpa-3* function in the same genetic pathway.

SQL-1/GMAP210 functions

GMAP210 localizes to the Golgi apparatus. Two domains have been identified that mediate this localization, the N-terminal ALPS domain, and the C-terminal GRAB domain (Cardenas et al., 2009; Follit et al., 2008; Gillingham et al., 2004). SQL-1 also localizes to the Golgi apparatus, as determined using immunofluorescence and with GFP fusion constructs. In the sensory neurons, SQL-1 is mostly restricted to the cell bodies, with sometimes SQL-1 spots in the dendrite, but never in or close to the cilium. Interestingly, not only full length SQL-1 fused to GFP localizes to the Golgi apparatus, but also a fusion protein containing the 302 most N-terminal amino acids localizes there. Since SQL-1 does not seem to have an ALPS domain and the GRAB domain is not present in the shortened fragment, Golgi targeting of this fragment must be mediated by a different, still uncharacterized SQL-1 domain.

Several functions have been ascribed to GMAP210. One of these proposed functions is maintaining the structure of the Golgi apparatus. Fragmentation of the Golgi apparatus has been observed in cultured HeLa cells after RNAi against GMAP210, as well as in primary dermal fibroblasts isolated from GMAP210 -/- mice (Rios et al., 2004; Smits et al., 2010; Yadav et al., 2009). Interestingly, others did not observe any structural Golgi defects in similar experiments (Follit et al., 2008; Gillingham et al., 2004). We visualized the Golgi apparatus of *C. elegans* specifically in the ASI neurons with AMAN-2::GFP, and observed more dispersed or even diffuse AMAN-2::GFP fluorescence in *sql-1(tm2409)*. This suggests that in *C. elegans* SQL-1 is required for maintaining Golgi integrity.

Follit et al. have shown that GMAP210 interacts with complex B protein IFT20 and plays a role in sorting and/or transport to the ciliary membrane (Follit et al., 2008). They found that mouse embryonic kidney cells lacking GMAP210 could still form cilia, showing that GMAP210 is not required for cilia assembly, although these cilia were slightly shorter. Consistent with a role in vesicular transport to the cilium, it was shown that in the absence of GMAP210 polycystin-2 levels in the cilium were lower. The interaction between GMAP210 and IFT20 is not conserved in *C. elegans*, since SQL-1 did not co-immunoprecipitate with IFT-20, and IFT-20 did not co-immunoprecipitate with SQL-1. This is in line with low level of conservation of the IFT20-binding domain in *C. elegans*, as proposed previously (Follit et al., 2008). In the cell bodies of sensory neurons we did not observe any localization of IFT-20::GFP to the Golgi apparatus, where mammalian IFT20 resides in cultured cells (Follit et al., 2006). In addition, in *ift-20* mutant animals the ciliary membrane protein ODR-10 still localizes to the sensory cilia (Kaplan

et al., 2010). Thus, it is very well possible that the role of IFT20 as adaptor protein in trafficking ciliary membrane proteins is not conserved in *C. elegans*. Mutation of *sql-1* does not affect cilia length, where the absence of GMAP210 in cultured mammalian cells results in slightly shorter cilia. Interestingly, animals that overexpress SQL-1 do show a cilia length increase, indicating that also SQL-1 plays a role in the regulation of cilium length.

Mutation of *sql-1* affects IFT

In the absence of *sql-1* the velocities of different components of the IFT machinery are affected. In *sql-1(tm2409)* animals we observed a reduced velocity of KAP-1::GFP, 0.59 μm/s instead of ~0.7 μm/s in wild type animals, and an increased velocity of OSM-3::GFP, 0.89 μm/s. Since the intrinsic velocities of OSM-3 and kinesin-II are not affected in *sql-1* mutant animals, there is a partial separation of OSM-3 and kinesin-II, where IFT is mediated by kinesin-II alone, OSM-3 alone, and kinesin-II and OSM-3 together. Based on the observed speeds, we calculated that approximately 38 % of OSM-3 motor proteins moved independently from kinesin-II and that 61 % of kinesin-II motor proteins moved independently from OSM-3.

The complex A protein CHE-11, complex B protein OSM-1 and dynein motor subunit XBX-1 moved in *sql-1(tm2409)* animals at approximately the same velocity as OSM-3, suggesting that these proteins are in the same complexes as OSM-3. Surprisingly, the complex A protein DAF-10 and the complex B protein CHE-13 moved at approximately 0.7 μm/s in *sql-1(tm2409)* animals. This could mean that CHE-13 and DAF-10 are present in all three particles, i.e. those transported by kinesin-II only, those transported by OSM-3 only and those transported by both kinesins, or that CHE-13 and DAF-10 are only present in the kinesin-II/OSM-3 IFT particles. Distribution analysis of DAF-10 and CHE-13 velocities in wild type and *sql-1* mutant animals overlap, suggesting they are only present in the kinesin-II/OSM-3 complex.

Our data are consistent with a model in which the middle segments of the sensory cilia of *sql-1(tm2409)* animals contain three types of particles: complete IFT particles, empty kinesin-II and incomplete IFT particles consisting of OSM-3, but not kinesin-II, and at least CHE-11, OSM-1 and XBX-1, but not DAF-10 and CHE-13 (Figure 5). These latter particles likely contain more IFT components; we found that also the complex B protein IFT-20 moves at the same speed as OSM-3, CHE-11, OSM-1 and XBX-1 in *sql-1(tm2409)* animals (data not shown).

Our finding that different IFT complex proteins have different velocities in *sql-1(tm2409)* animals indicates a destabilization of the IFT complex. CHE-11/IFT140 is part of the "core" of complex A (Behal et al., 2012; Mukhopadhyay et al., 2010; Ou et al., 2007) and interacts with complex B protein OSM-1/IFT172 in a co-IP (Follit et al., 2009), suggesting that the destabilized IFT particles in *sql-1* mutants might reflect the "core" of the IFT machinery. Further analyses using dual colour imaging to visualize the motility of additional IFT components simultaneously is necessary to reveal the makeup of the IFT particles in *sql-1* mutant animals.

At present, it is unclear how mutation of *sql-1* affects the stability of the IFT complex. Our data and those presented by Follit et al. (2008) indicate that SQL-1/GMAP210 only resides in the Golgi apparatus and not in the cilium. Therefore, it is likely that the IFT defect is caused by a sorting defect of vesicles destined for the cilium. E.g. vesicles could exit the Golgi apparatus prematurely, or fail to transport some proteins required for IFT or maintenance of the stability of the IFT complex. Other proteins required for the stability of the IFT complex include BBS and NPHP proteins. However, mutation of these proteins causes uncoupling complex A and B

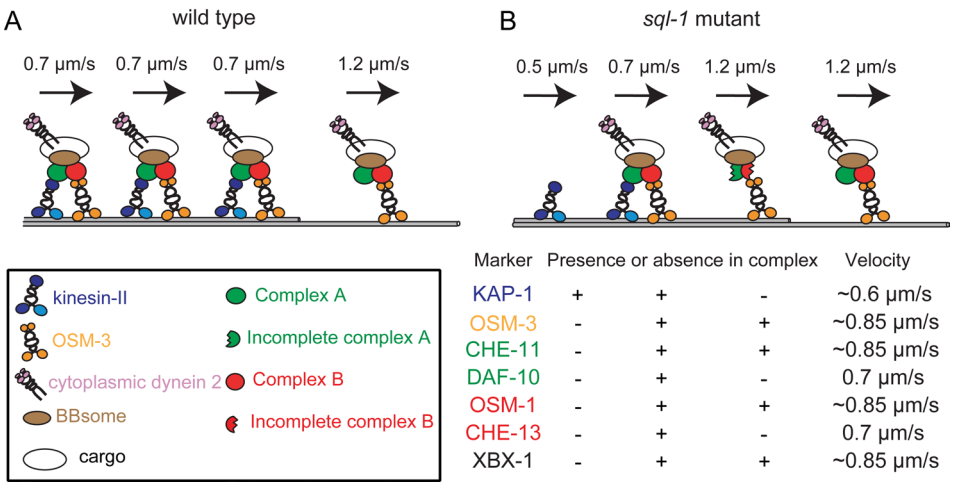

Marker	Presence or absence in complex			Velocity
KAP-1	+	+	-	~0.6 µm/s
OSM-3	-	+	+	~0.85 µm/s
CHE-11	-	+	+	~0.85 µm/s
DAF-10	-	+	-	0.7 µm/s
OSM-1	-	+	+	~0.85 µm/s
CHE-13	-	+	-	0.7 µm/s
XBX-1	-	+	+	~0.85 µm/s

Figure 5. Proposed model of IFT in the sensory cilia of *sql-1* mutant animals. (A) In wild type animals IFT particles in the middle segment of the sensory cilia are transported by both OSM-3 and kinesin-II. (B) In *sql-1* mutant animals IFT particles are destabilized, resulting in the existence of two additional types of IFT particles: A slow IFT particle composed of only kinesin-II, and a fast IFT particle composed of incomplete complex A (with at least CHE-11), incomplete complex B (with at least OSM-1 and IFT-20), and dynein, and transported by OSM-3. Bellow the schematic model of IFT in *sql-1* mutant animals the presence (+) or absence (-) of the GFP markers in the proposed IFT particles in *sql-1* mutant animals are shown, as well as the velocities of the tested GFP markers.

(BBS proteins) (Ou et al., 2005; Ou et al., 2007) or mainly affect the complex B protein OSM-6/IFT52 (Jauregui et al., 2008). Finally, the presence of other kinesins such as KLP-6 (Morsci and Barr, 2011) or another still unidentified ciliary kinesin, could also explain the differences in the velocities observed in *sql-1* mutant animals.

Interactions of *sql-1* and *gpa-3*

We identified *sql-1* as a suppressor of the dye filling defect of *gpa-3QL* animals. In agreement with the effect on dye filing mutation, of *sql-1* also suppressed the effect of *gpa-3QL* on cilium length. *gpa-3* and *sql-1* also interact at the level of the regulation of IFT. Mutation of *gpa-3* causes a separation of kinesin II and OSM-3, where complex A and B particle proteins move at an intermediate speed (Burghoorn et al., 2010). *sql-1(tm2409); gpa-3* animals showed very similar speeds as *sql-1(tm2409)* or *gpa-3* animals indicating that *sql-1* acts in the same genetic pathway as *gpa-3*.

Also in *gpa-3QL* animals we observed a partial separation of kinesin II and OSM-3, while complex A and B particle proteins moved at an intermediate velocity (Burghoorn et al., 2010). These data are consistent with two models in which the middle segments of the cilia of *gpa-3QL* animals contain three types of particles: in the first model the cilia contain complete IFT particles, empty kinesin-II and empty OSM-3, while in the second model the cilia contain complete IFT particles, IFT particles only lacking kinesin-II and IFT particle only lacking OSM-3. If the former is true, less fully loaded particles would reach the distal segment of the

cilium, explaining the length defect in *gpa-3QL* animals. Since, in *sql-1* mutant animals IFT particles are predominantly transported by OSM-3. Inactivation of *sql-1* in *gpa-3QL* animals would cause cargo to be transported predominantly by OSM-3, which would result in more loaded particles in the distal tip, and a suppression of the cilium length defect.

Interestingly, we found that simultaneous inactivation of *sql-1* and dominant activation of *gpa-3* affects the intrinsic velocity of OSM-3. In the distal segment of *sql-1(tm2409); gpa-3QL* animals, and both middle and distal segments of *sql-1(tm2409); kap-1; gpa-3QL* animals OSM-3 moved at 0.82-1.06 μm/s, significantly slower than the expected 1.15 μm/s. Consistently, all other IFT proteins moved slower in the distal segments of *sql-1(tm2409); gpa-3QL* animals. The reduced speed of OSM-3 in *sql-1; gpa-3QL* double mutant animals likely affects the speed of the whole IFT machinery. In wild type animals KAP-1 by itself moves at 0.5 μm/s, OSM-3 by itself moves at 1.15 μm/s and the complex with both kinesins moves at 0.7 μm/s. This implies that the drag of OSM-3, moving 0.7 μm/s faster than kinesin-II, increases kinesin-II speed by 0.2 μm/s. In *sql-1; gpa-3QL* animals OSM-3 moves approximately 0.44 μm/s faster than kinesin-II. If we assume similar kinetics this would increase kinesin-II speed by 0.13 μm/s and the whole complex would move at 0.63 μm/s. In the middle segments of *sql-1; gpa-3QL* animals KAP-1::GFP moved at 0.6 μm/s which is close to the presumed speed of the whole IFT complex calculated above, and removal of *osm-3* reduced KAP-1::GFP speed to 0.5 μm/s, suggesting that most kinesin-II moves together with OSM-3. OSM-3::GFP however, moved at 0.78 μm/s and this speed increased to 0.94 μm/s upon removal of *kap-1*, suggesting that almost 50 % of OSM-3 moves separately from kinesin-II. DAF-10, CHE-13 and XBX-1 moved at intermediate speeds of 0.62-0.69 μm/s, suggesting that they are transported by kinesin-II/OSM-3 particles and OSM-3 particles. Since OSM-3::GFP moves considerably faster, probably also a pool of unattached OSM-3::GFP exists. Based on our findings and these calculations, we propose that the cilia middle segments of *sql-1; gpa-3QL* animals contain three types of particles: complete IFT particles, transported by kinesin-II and OSM-3, IFT particles transported by OSM-3 alone and OSM-3 moving separately.

Concluding remarks

From our and previously reported data it is clear that SQL-1/GMAP210 functions at the Golgi apparatus in routing of proteins to the cilium. Absence of SQL-1 leads to alterations in the IFT machinery, uncoupling of the two kinesins and destabilization of complex A and B. How these effects come about is unclear, but it seems likely that absence of SQL-1 in the Golgi affects the routing of one or more proteins that are required in the cilium for proper IFT.

Material and Methods

Strains and Constructs

Worms were cultured using standard methods (Brenner, 1974). Wild-type animals were *C. elegans* Bristol N2. Alleles used in this study were *sql-1(gj202)III*, *sql-1(tm2440)III*, *sql-1(tm4995)III*, *sql-1(tm2409)III*, *gpa-3(pk35)V*, *gpa-3QL(syIs25)X*, *gpa-3QL(syIs24)IV*, *ift-20(gk548)I*, *osm-3(p802)IV*, *kap-1(ok676)II*. *sql-1* alleles *tm2409*, *tm2440* and *tm4955* were obtained from NBP-Japan. Published transgenes used were: *gpa-4::gfp*, *gpa-15::gfp*, *osm-3::gfp*, *kap-1::gfp*, *che-11::gfp*, *osm-1::gfp*, *che-13::gfp*, *xbx-1::yfp*, p_{glr-1}*::aman-2::yfp*, p_{arl13}*::gfp::rab-8* (Haycraft et al., 2003; Jansen et al., 1999; Kaplan et al., 2010; Qin et al., 2001; Rolls et al., 2002; Schafer et al., 2003; Signor et al., 1999; Snow et al., 2004). Also several new constructs were generated. *osm-3::gfp* was created by fusing a 1 kb *osm-3* promoter fragment to *osm-3::gfp* (gift from Piali Sengupta), *kap-1::gfp* was created by fusing a 0,8 kb *kap-1* promoter fragment to *kap-1::gfp* (gift from Piali Sengupta), P_{osm-3}*::daf-10::gfp* was generated by replacing the *osm-3* ORF in *osm-3::gfp* with the *daf-10* cDNA (gift from Piali Sengupta), *ift-20::gfp* was generated by fusion-PCR (Hobert, 2002). The translational *sql-1::gfp* and p_{gpa-4}*::sql-1::gfp* constructs were made by fusing the *sql-1* promoter fragment (2,2 kb) or the *gpa-4* promoter fragment (2,5 kb) with the *sql-1* cDNA in pPD95.77 (gift from Andrew Fire). The *sql-1* constructs were made by introducing a stop codon in the translational *sql-1::gfp* construct, at the 3' end of *sql-1*. A P_{gpa-4}*::aman-2::yfp* was made by fusing the *gpa-4* promoter to the translation start site of *aman-2* (gift from Tom Rapoport). A P_{gpa-4}*::aman-2::gfp* construct was made by subcloning a PCR product of *aman-2* into P_{gpa-4}*::gpa-4::gfp* in frame with *gfp*. Microinjections were performed as described (Mello and Fire, 1995). IFT constructs were injected at concentrations ranging from 20 ng to 50 ng/µl and analyzed for correct expression by imaging IFT particles in wild-type animals. The *sql-1* construct was injected in wild type animals at concentrations up to 150 ng/µl to generate transgenic lines that overexpress *sql-1* approximately 2 – 3 fold.

Identification and characterization of *sql-1*

gpa-3QL(syIs25)X animals were mutagenized with 50 mM ethyl methanesulfonate (EMS) to generate random mutations. 100 cultures were started with 12 EMS-treated animals each. The F2 and F3 progeny of the mutagenized animals were subjected to dye filling and 12 animals that took up fluorescent dye were individually picked onto new culture dishes. The progeny of these putative suppressor mutants was subjected to dye filling. This procedure identified nine independent suppressor mutants, including *sql-1(gj202)*. Using SNP mapping (Wicks et al., 2001) we mapped *sql-1(gj202)* to a region of approximately 120 kb on chromosome III. To identify the mutated genes, *gpa-3QL(syIs25)X; sql-1(gj202)* mutant animals were injected with long range PCR fragments spanning the 35 kbp region containing the predicted genes Y111B2A.4, Y111B2A.5 and Y111B2A.26. The dye filling defect was only restored in animals injected with PCR fragments spanning all three genes, not with each of the genes individually. Sequencing identified an A to T mutation in the predicted gene Y111B2A.5. We used RT-PCR to characterize the ORF of wild type and *sql-1* mutant animals. Rescue was confirmed by injecting 5 ng/µl *sql-1* or *sql-1::GFP* construct into *gpa-3QL(syIs25)X; sql-1(tm2409)* mutant animals.

Immunofluorescence and Microscopy

Animals were permeabilized, fixed and stained according to standard methods (Finney and Ruvkun, 1990). For SQL-1 rabbit polyclonal antibody production, the N-terminal cDNA of *sql-1* (exon 3-8) and the C-terminal cDNA of *sql-1* (exon 7-18) were cloned into pGST-Parallel (pGEX4T1 derivate, (Sheffield et al., 1999)). Polyclonal antibodies were generated by collecting serum from rabbits immunized with either the N-terminal or the C-terminal, *E. coli* produced, purified SQL-1 proteins fused to gluthatione S-transferase (immunization performed by Harlan Laboratories). Antibodies were affinity purified prior to immunofluorescence staining. Secondary antibodies were goat-anti-rabbit Alexa 594-conjugated (Molecular Probes, Eugen, OR). Specificity of the antibody was confirmed by the absence of immunoreactivity in *sql-1(tm2409)* mutant animals. SQV-8 antibody was a gift from Jon Audhya. GPA-3 antibody staining was performed as described (Lans et al., 2004). Dye filling was performed using DiO (Molecular probes) as described (Perkins et al., 1986). Antibody staining, localization of fluorescent proteins, cilia morphology and cilia lengths were measured using a Zeiss Imager Z1 microscope with a 100x (NA 1.4) objective.

Immunoblotting

Total lysates of 40 worms were solubilized with Laemmli loading buffer. After electrophoresis on an 8 % SDS-PAGE gel, proteins were transferred to membranes and probed with antibodies against SQL-1 (affinity purified), ECL-horseradish peroxidase-conjugated anti-rabbit (Dako), and detected with ECL Plus Western blot detection system (Amersham).

IP

Strains used were Bristol N2 and *gj2180[ift-20::gfp]*. Worms were collected from 9 full 10 cm plates and washed 3 times with M9, once with cold 100 mM NaCl, and resuspended in homogenization buffer (15 mM HEPES pH 7.6, 10 mM KCl, 1.5 mM MgCl2, 0.1 mM EDTA, 0.5 mM EGTA, 44 mM sucrose, 1 mM DTT, protease inhibitor). Worms were lysed by sonication, and after clearing of the lysates by centrifugation, they were loaded onto antibody coupled protein A sepharose CL-4B beads (GE Healthcare). Rabbit polyclonal anti-SQL-1 and rabbit polyclonal anti-GFP (Abcam) antibodies were bound according to the manufacturer's instructions. Lysates were incubated overnight at 4°C, washed 5 times with IP buffer (20 mM Tris-HCl pH 7.5, 150 mM NaCl, 5 mM MgCl2, 5 % glycerol, 0.1 % NP40, protease inhibitor), separated on a 11 % SDS-PAGE gel and blotted. Western blots were incubated with rabbit polyclonal anti-SQL-1 and mouse monoclonal anti-GFP (NeuroMab). Secondary antibodies used were ECL-horseradish peroxidase-conjugated anti-rabbit (Dako) and anti-mouse (GE Healthcare), respectively, which were detected with ECL Plus Western blot detection system (Amersham).

Live imaging of IFT particles

Live imaging of the GFP-tagged IFT particles was carried out as described (Snow et al., 2004). Images were acquired on a Zeiss confocal microscope CLSM510 with a 63x (NA1.4) objective. Worms were mounted on an agarose pad and anaesthetized with 10 mM levamisole. Kymographs were generated in ImageJ with the Kymograph plugin, written by J. Rietdorf

Calculations

The observed OSM-3::GFP and KAP-1::GFP speeds are each composed of the speed of the fraction that moves together with the other kinesin (at 0.70 μm/seconds, OSM-3::GFP speed in *osm-3* animals, and KAP-1::GFP speed in *kap-1* animals) and the fraction that moves separately (at 1.17 μm/seconds, OSM-3::GFP speed in *kap-1* animals, or 0.49 μm/seconds, KAP-1::GFP speed in *osm-3* animals). The formula used to calculate the fraction of OSM-3 that moves separately *(x)* in *sql-1* mutants is: $x_{osm-3} = (v_{sql-1}–v_{together})/(v_{max}–v_{together})$, where v_{sql-1} is the OSM-3::GFP speed measured in a *sql-1* mutant, $v_{together}$ is the OSM-3::GFP speed measured in *osm-3* animals and v_{max} is the OSM-3::GFP speed measured in *kap-1* animals. The formula used to calculate the fraction of KAP-1 that moves separately *(x)* is: $x_{kap-1} = (v_{sql-1}–v_{together})/(v_{max}–v_{together})$, where v_{sql-1} is the KAP-1::GFP speed measured in a *sql-1* mutant, $v_{together}$ is the KAP-1::GFP speed measured in *kap-1* animals and v_{max} is the KAP-1::GFP speed measured in *osm-3* animals.

References

Abd-El-Barr, M.M., K. Sykoudis, S. Andrabi, E.R. Eichers, M.E. Pennesi, P.L. Tan, J.H. Wilson, N. Katsanis, J.R. Lupski, and S.M. Wu. 2007. Impaired photoreceptor protein transport and synaptic transmission in a mouse model of Bardet-Biedl syndrome. *Vision Res*. 47:3394-407.

Abdul-Majeed, S., B.C. Moloney, and S.M. Nauli. 2012. Mechanisms regulating cilia growth and cilia function in endothelial cells. *Cell Mol Life Sci*. 69:165-73.

Behal, R.H., M.S. Miller, H. Qin, B.F. Lucker, A. Jones, and D.G. Cole. 2012. Subunit Interactions and Organization of the Chlamydomonas reinhardtii Intraflagellar Transport Complex A Proteins. *J Biol Chem*. 287:11689-703.

Berbari, N.F., J.S. Lewis, G.A. Bishop, C.C. Askwith, and K. Mykytyn. 2008. Bardet-Biedl syndrome proteins are required for the localization of G protein-coupled receptors to primary cilia. *Proc Natl Acad Sci U S A*. 105:4242-6.

Berman, S.A., N.F. Wilson, N.A. Haas, and P.A. Lefebvre. 2003. A novel MAP kinase regulates flagellar length in Chlamydomonas. *Curr Biol*. 13:1145-9.

Besschetnova, T.Y., E. Kolpakova-Hart, Y. Guan, J. Zhou, B.R. Olsen, and J.V. Shah. 2010. Identification of signaling pathways regulating primary cilium length and flow-mediated adaptation. *Curr Biol*. 20:182-7.

Blacque, O.E., M.J. Reardon, C. Li, J. McCarthy, M.R. Mahjoub, S.J. Ansley, J.L. Badano, A.K. Mah, P.L. Beales, W.S. Davidson, R.C. Johnsen, M. Audeh, R.H. Plasterk, D.L. Baillie, N. Katsanis, L.M. Quarmby, S.R. Wicks, and M.R. Leroux. 2004. Loss of C. elegans BBS-7 and BBS-8 protein function results in cilia defects and compromised intraflagellar transport. *Genes Dev*. 18:1630-42.

Brenner, S. 1974. The genetics of Caenorhabditis elegans. *Genetics*. 77:71-94.

Burghoorn, J., M.P. Dekkers, S. Rademakers, T. de Jong, R. Willemsen, and G. Jansen. 2007. Mutation of the MAP kinase DYF-5 affects docking and undocking of kinesin-2 motors and reduces their speed in the cilia of Caenorhabditis elegans. *Proc Natl Acad Sci U S A*. 104:7157-62.

Burghoorn, J., M.P. Dekkers, S. Rademakers, T. de Jong, R. Willemsen, P. Swoboda, and G. Jansen. 2010. Dauer pheromone and G-protein signaling modulate the coordination of intraflagellar transport kinesin motor proteins in C. elegans. *J Cell Sci*. 123:2077-84.

Cardenas-Rodriguez, M., and J.L. Badano. 2009. Ciliary biology: understanding the cellular and genetic basis of human ciliopathies. *Am J Med Genet C Semin Med Genet*. 151C:263-80.

Cardenas, J., S. Rivero, B. Goud, M. Bornens, and R.M. Rios. 2009. Golgi localisation of GMAP210 requires two distinct cis-membrane binding mechanisms. *BMC Biol*. 7:56.

Cole, D.G., and W.J. Snell. 2009. SnapShot: Intraflagellar transport. *Cell*. 137:784-784 e1.

Drin, G., J.F. Casella, R. Gautier, T. Boehmer, T.U. Schwartz, and B. Antonny. 2007. A general amphipathic alpha-helical motif for sensing membrane curvature. *Nat Struct Mol Biol*. 14:138-46.

Emmer, B.T., D. Maric, and D.M. Engman. 2010. Molecular mechanisms of protein and lipid targeting to ciliary membranes. *J Cell Sci*. 123:529-36.

Finney, M., and G. Ruvkun. 1990. The unc-86 gene product couples cell lineage and cell identity in C. elegans. *Cell*. 63:895-905.

Follit, J.A., J.T. San Agustin, F. Xu, J.A. Jonassen, R. Samtani, C.W. Lo, and G.J. Pazour. 2008. The Golgin GMAP210/TRIP11 anchors IFT20 to the Golgi complex. *PLoS Genet*. 4:e1000315.

Follit, J.A., R.A. Tuft, K.E. Fogarty, and G.J. Pazour. 2006. The intraflagellar transport protein IFT20 is associated with the Golgi complex and is required for cilia assembly. *Mol Biol Cell*. 17:3781-92.

Follit, J.A., F. Xu, B.T. Keady, and G.J. Pazour. 2009. Characterization of mouse IFT complex B. *Cell Motil Cytoskeleton*. 66:457-68.

Gillingham, A.K., A.H. Tong, C. Boone, and S. Munro. 2004. The GTPase Arf1p and the ER to Golgi cargo receptor Erv14p cooperate to recruit the golgin Rud3p to the cis-Golgi. *J Cell Biol*. 167:281-92.

Golden, J.W., and D.L. Riddle. 1982. A pheromone influences larval development in the nematode Caenorhabditis elegans. *Science*. 218:578-80.

Hadwiger, G., S. Dour, S. Arur, P. Fox, and M.L. Nonet. 2010. A monoclonal antibody toolkit for C. elegans. *PLoS One*. 5:e10161.

Haycraft, C.J., J.C. Schafer, Q. Zhang, P.D. Taulman, and B.K. Yoder. 2003. Identification of CHE-13, a novel intraflagellar transport protein required for cilia formation. *Exp Cell Res*. 284:251-63.

Hedgecock, E.M., J.G. Culotti, J.N. Thomson, and L.A. Perkins. 1985. Axonal guidance mutants of Caenorhabditis elegans identified by filling sensory neurons with fluorescein dyes. *Dev Biol*. 111:158-70.

Hildebrandt, F., T. Benzing, and N. Katsanis. 2011. Ciliopathies. *N Engl J Med*. 364:1533-43.

Hobert, O. 2002. PCR fusion-based approach to create reporter gene constructs for expression analysis in transgenic C. elegans. *Biotechniques*. 32:728-30.

Infante, C., F. Ramos-Morales, C. Fedriani, M. Bornens, and R.M. Rios. 1999. GMAP-210, A cis-Golgi network-associated protein, is a minus end microtubule-binding protein. *J Cell Biol*. 145:83-98.

Jansen, G., K.L. Thijssen, P. Werner, M. van der Horst, E. Hazendonk, and R.H. Plasterk. 1999. The complete family of genes encoding G proteins of Caenorhabditis elegans. *Nat Genet*. 21:414-9.

Jauregui, A.R., K.C. Nguyen, D.H. Hall, and M.M. Barr. 2008. The Caenorhabditis elegans nephrocystins act as global modifiers of cilium structure. *J Cell Biol*. 180:973-88.

Jin, H., S.R. White, T. Shida, S. Schulz, M. Aguiar, S.P. Gygi, J.F. Bazan, and M.V. Nachury. 2010. The conserved Bardet-Biedl syndrome proteins assemble a coat that traffics membrane proteins to cilia. *Cell*. 141:1208-19.

Kaplan, O.I., A. Molla-Herman, S. Cevik, R. Ghossoub, K. Kida, Y. Kimura, P. Jenkins, J.R. Martens, M. Setou, A. Benmerah, and O.E. Blacque. 2010. The AP-1 clathrin adaptor facilitates cilium formation and functions with RAB-8 in C. elegans ciliary membrane transport. *J Cell Sci*. 123:3966-77.

Lans, H., S. Rademakers, and G. Jansen. 2004. A network of stimulatory and inhibitory Galpha-subunits regulates olfaction in Caenorhabditis elegans. *Genetics*. 167:1677-87.

Mazelova, J., L. Astuto-Gribble, H. Inoue, B.M. Tam, E. Schonteich, R. Prekeris, O.L. Moritz, P.A. Randazzo, and D. Deretic. 2009. Ciliary targeting motif VxPx directs assembly of a trafficking module through Arf4. *EMBO J*. 28:183-92.

Mello, C., and A. Fire. 1995. DNA transformation. *Methods Cell Biol*. 48:451-82.

Miyoshi, K., K. Kasahara, I. Miyazaki, and M. Asanuma. 2009. Lithium treatment elongates primary cilia in the mouse brain and in cultured cells. *Biochem Biophys Res Commun*. 388:757-62.

Morsci, N.S., and M.M. Barr. 2011. Kinesin-3 KLP-6 Regulates Intraflagellar Transport in Male-Specific Cilia of Caenorhabditis elegans. *Curr Biol*. 21:1239-44.

Mukhopadhyay, S., Y. Lu, S. Shaham, and P. Sengupta. 2008. Sensory signaling-dependent remodeling of olfactory cilia architecture in C. elegans. *Dev Cell*. 14:762-74.

Mukhopadhyay, S., X. Wen, B. Chih, C.D. Nelson, W.S. Lane, S.J. Scales, and P.K. Jackson. 2010. TULP3 bridges the IFT-A complex and membrane phosphoinositides to promote trafficking of G protein-coupled receptors into primary cilia. *Genes Dev*. 24:2180-93.

Nachury, M.V., A.V. Loktev, Q. Zhang, C.J. Westlake, J. Peranen, A. Merdes, D.C. Slusarski, R.H. Scheller, J.F. Bazan, V.C. Sheffield, and P.K. Jackson. 2007. A core complex of BBS proteins cooperates with the GTPase Rab8 to promote ciliary membrane biogenesis. *Cell*. 129:1201-13.

Nishimura, D.Y., M. Fath, R.F. Mullins, C. Searby, M. Andrews, R. Davis, J.L. Andorf, K. Mykytyn, R.E. Swiderski, B. Yang, R. Carmi, E.M. Stone, and V.C. Sheffield. 2004. Bbs2-null mice have neurosensory deficits, a defect in social dominance, and retinopathy associated with mislocalization of rhodopsin. *Proc Natl Acad Sci U S A*. 101:16588-93.

Omori, Y., T. Chaya, K. Katoh, N. Kajimura, S. Sato, K. Muraoka, S. Ueno, T. Koyasu, M. Kondo, and T. Furukawa. 2010. Negative regulation of ciliary length by ciliary male germ cell-associated kinase (Mak) is required for retinal photoreceptor survival. *Proc Natl Acad Sci U S A*. 107:22671-6.

Ou, G., O.E. Blacque, J.J. Snow, M.R. Leroux, and J.M. Scholey. 2005. Functional coordination of intraflagellar transport motors. *Nature*. 436:583-7.

Ou, G., M. Koga, O.E. Blacque, T. Murayama, Y. Ohshima, J.C. Schafer, C. Li, B.K. Yoder, M.R. Leroux, and J.M. Scholey. 2007. Sensory ciliogenesis in Caenorhabditis elegans: assignment of IFT components into distinct modules based on transport and phenotypic profiles. *Mol Biol Cell*. 18:1554-69.

Ou, Y., Y. Ruan, M. Cheng, J.J. Moser, J.B. Rattner, and F.A. van der Hoorn. 2009. Adenylate cyclase regulates elongation of mammalian primary cilia. *Exp Cell Res*. 315:2802-17.

Pazour, G.J., and R.A. Bloodgood. 2008. Targeting proteins to the ciliary membrane. *Curr Top Dev Biol*. 85:115-49.

Perkins, L.A., E.M. Hedgecock, J.N. Thomson, and J.G. Culotti. 1986. Mutant sensory cilia in the nematode Caenorhabditis elegans. *Dev Biol*. 117:456-87.

Qin, H., J.L. Rosenbaum, and M.M. Barr. 2001. An autosomal recessive polycystic kidney disease gene homolog is involved in intraflagellar transport in C. elegans ciliated sensory neurons. *Curr Biol*. 11:457-61.

Rios, R.M., A. Sanchis, A.M. Tassin, C. Fedriani, and M. Bornens. 2004. GMAP-210 recruits gamma-tubulin complexes to cis-Golgi membranes and is required for Golgi ribbon formation. *Cell*. 118:323-35.

Rios, R.M., A.M. Tassin, C. Celati, C. Antony, M.C. Boissier, J.C. Homberg, and M. Bornens. 1994. A peripheral protein associated with the cis-Golgi network redistributes in the intermediate compartment upon brefeldin A treatment. *J Cell Biol*. 125:997-1013.

Rolls, M.M., D.H. Hall, M. Victor, E.H. Stelzer, and T.A. Rapoport. 2002. Targeting of rough endoplasmic reticulum membrane proteins and ribosomes in invertebrate neurons. *Mol Biol Cell*. 13:1778-91.

Rosenbaum, J.L., and G.B. Witman. 2002. Intraflagellar transport. *Nat Rev Mol Cell Biol*. 3:813-25.

Schafer, J.C., C.J. Haycraft, J.H. Thomas, B.K. Yoder, and P. Swoboda. 2003. XBX-1 encodes a dynein light intermediate chain required for retrograde intraflagellar transport and cilia assembly in Caenorhabditis elegans. *Mol Biol*

Cell. 14:2057-70.

Sheffield, P., S. Garrard, and Z. Derewenda. 1999. Overcoming expression and purification problems of RhoGDI using a family of "parallel" expression vectors. *Protein Expr Purif*. 15:34-9.

Short, B., A. Haas, and F.A. Barr. 2005. Golgins and GTPases, giving identity and structure to the Golgi apparatus. *Biochim Biophys Acta*. 1744:383-95.

Signor, D., K.P. Wedaman, J.T. Orozco, N.D. Dwyer, C.I. Bargmann, L.S. Rose, and J.M. Scholey. 1999. Role of a class DHC1b dynein in retrograde transport of IFT motors and IFT raft particles along cilia, but not dendrites, in chemosensory neurons of living Caenorhabditis elegans. *J Cell Biol*. 147:519-30.

Silverman, M.A., and M.R. Leroux. 2009. Intraflagellar transport and the generation of dynamic, structurally and functionally diverse cilia. *Trends Cell Biol*. 19:306-16.

Smits, P., A.D. Bolton, V. Funari, M. Hong, E.D. Boyden, L. Lu, D.K. Manning, N.D. Dwyer, J.L. Moran, M. Prysak, B. Merriman, S.F. Nelson, L. Bonafe, A. Superti-Furga, S. Ikegawa, D. Krakow, D.H. Cohn, T. Kirchhausen, M.L. Warman, and D.R. Beier. 2010. Lethal skeletal dysplasia in mice and humans lacking the golgin GMAP-210. *N Engl J Med*. 362:206-16.

Snow, J.J., G. Ou, A.L. Gunnarson, M.R. Walker, H.M. Zhou, I. Brust-Mascher, and J.M. Scholey. 2004. Two anterograde intraflagellar transport motors cooperate to build sensory cilia on C. elegans neurons. *Nat Cell Biol*. 6:1109-13.

Tam, L.W., N.F. Wilson, and P.A. Lefebvre. 2007. A CDK-related kinase regulates the length and assembly of flagella in Chlamydomonas. *J Cell Biol*. 176:819-29.

Wang, Q., J. Pan, and W.J. Snell. 2006. Intraflagellar transport particles participate directly in cilium-generated signaling in Chlamydomonas. *Cell*. 125:549-62.

Ward, S., N. Thomson, J.G. White, and S. Brenner. 1975. Electron microscopical reconstruction of the anterior sensory anatomy of the nematode Caenorhabditis elegans.?2UU. *J Comp Neurol*. 160:313-37.

Wicks, S.R., R.T. Yeh, W.R. Gish, R.H. Waterston, and R.H. Plasterk. 2001. Rapid gene mapping in Caenorhabditis elegans using a high density polymorphism map. *Nat Genet*. 28:160-4.

Wiens, C.J., Y. Tong, M.A. Esmail, E. Oh, J.M. Gerdes, J. Wang, W. Tempel, J.B. Rattner, N. Katsanis, H.W. Park, and M.R. Leroux. 2010. Bardet-Biedl syndrome-associated small GTPase ARL6 (BBS3) functions at or near the ciliary gate and modulates Wnt signaling. *J Biol Chem*. 285:16218-30.

Yadav, S., S. Puri, and A.D. Linstedt. 2009. A primary role for Golgi positioning in directed secretion, cell polarity, and wound healing. *Mol Biol Cell*. 20:1728-36.

Zwaal, R.R., J.E. Mendel, P.W. Sternberg, and R.H. Plasterk. 1997. Two neuronal G proteins are involved in chemosensation of the Caenorhabditis elegans Dauer-inducing pheromone. *Genetics*. 145:715-27.

Supplementary Material

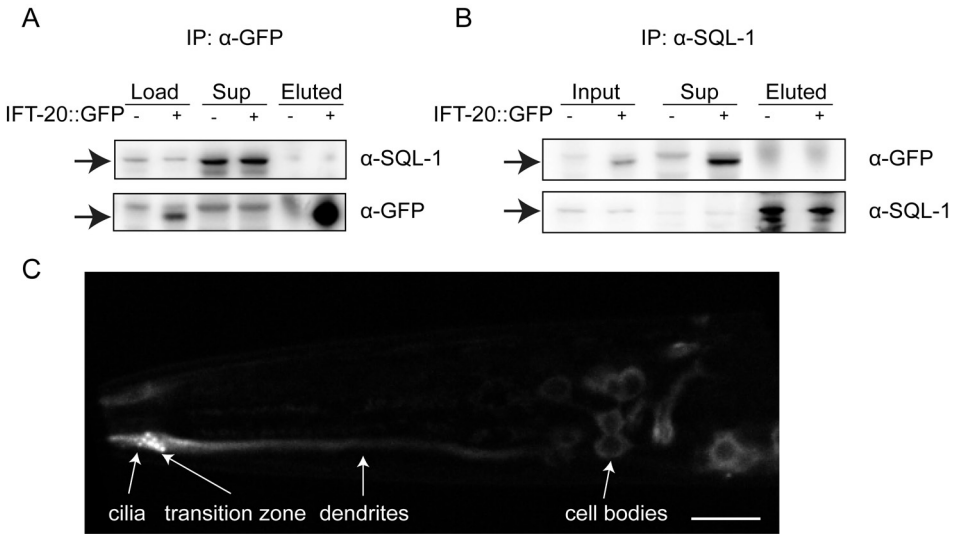

Figure S1. SQL-1 does not interact with IFT-20. Immunoblots showing co-immunoprecipitation assays with anti-GFP (A) and anti-SQL-1 (B) coupled to protein A sepharose. Whole worm lysates of wild type animals and animals expressing *ift-20::gfp* (Load) were incubated with anti-GFP and anti-SQL-1 antibody beads. The supernatant (Sup) was removed, the beads were washed, and immunoprecipitated protein was eluted (Eluted). In both cases, the bottom panel shows that the anti-GFP and anti-SQL-1 antibody beads successfully pulled down IFT-20::GFP and SQL-1, respectively. However, SQL-1 did not co-immunoprecipitate with anti-GFP beads, and IFT-20::GFP did not co-immunoprecipitate with anti-SQL-1 beads. (C) Fluorescence image (combination of two focal planes) of animals expressing *ift-20::gfp* in the sensory neurons, illustrating that IFT-20::GFP localizes predominantly in cilia and transition zones, and diffusely throughout the sensory neurons. Anterior is towards the left. Scale bar, 10 μm.

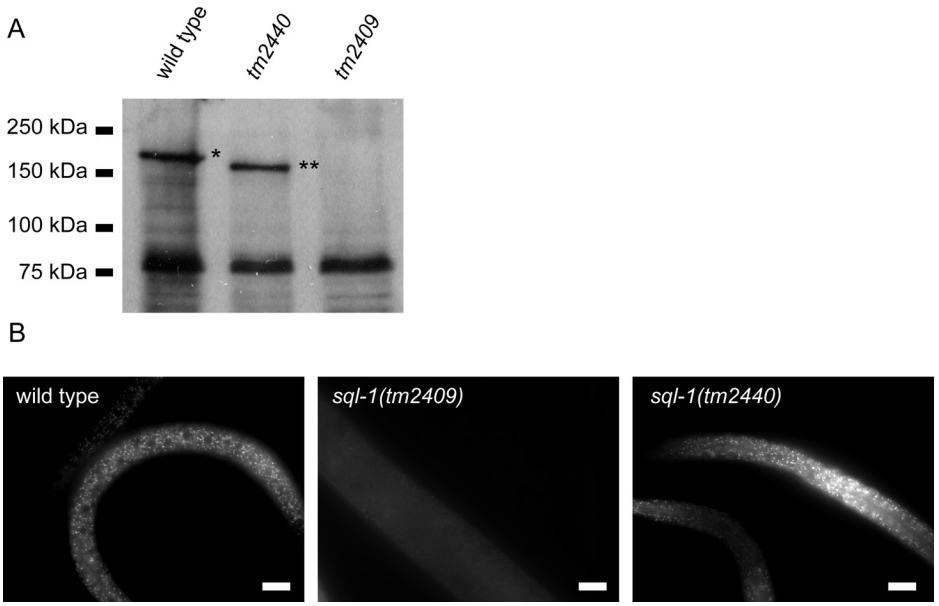

Figure S2. SQL-1 could not be detected in *sql-1(tm2409)* animals. (A) Immunoblotting of whole worm lysates collected from wild type, *tm2440*, and *tm2409* animals, with an antibody raised against the C-terminal end of SQL-1. * marks wild type SQL-1 , ** marks truncated SQL-1 in *tm2440* animals. (B) Immunofluorescence with the antibody raised against the N-terminal half of SQL-1 on wild type, *tm2440* and *tm2409* animals. Scale bar, 20 μm

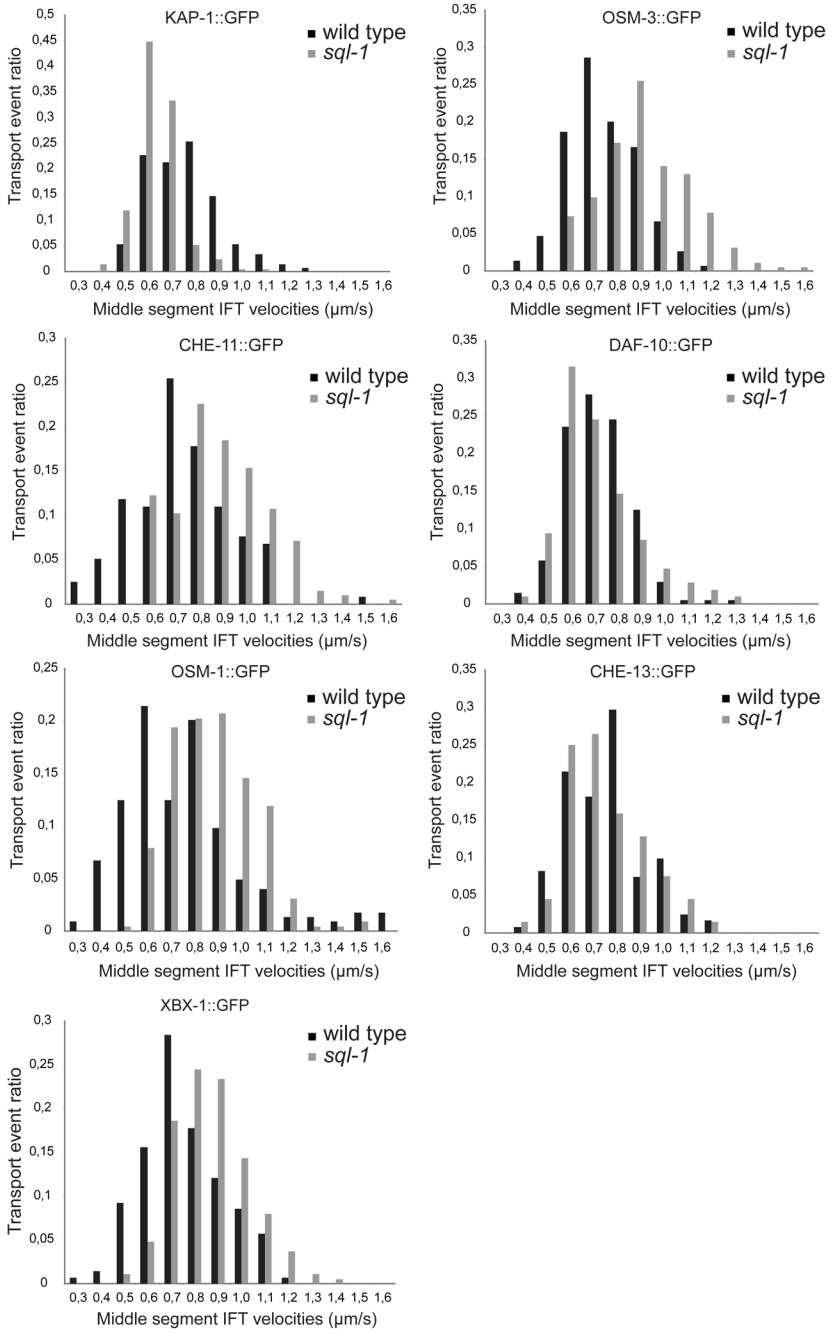

Figure S3. Kinesin-II and OSM-3 are partially uncoupled in the middle segment of the sensory cilia of *sql-1* animals. Distribution of transport events of OSM-3::GFP, KAP-1::GFP, CHE-11::GFP, DAF-10::GFP, OSM-1::GFP, CHE-13::GFP, and XBX-1::GFP in the middle segments of wild type and *sql-1(tm2409)* animals.

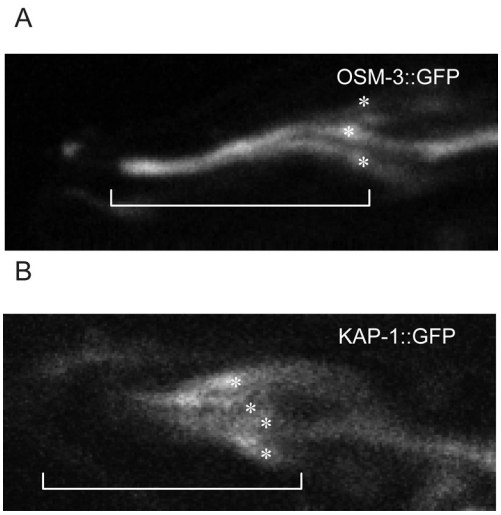

Figure S4. Kinesin-II is restricted to the middle segment of the sensory cilia of *sql-1(tm2409); gpa-3QL* animals. Localization of KAP-1::GFP and OSM-3::GFP in the sensory cilia of *sql-1(tm2409); gpa-3QL* animals, * marks the transition zone.

Table S1. *sql-1* affects anterograde IFT velocities in distal segment.

	Ciliary kinesins		IFT-A particle			
	OSM-3		CHE-11		DAF-10	
Genotype	**average ± sd**	**n**	**average ± sd**	**n**	**average ± sd**	**n**
wild type	1.17 ± 0.21	152	1.20 ± 0.27	49	1.19 ± 0.30	211
kap-1	1.23 ± 0.28	42	ND		ND	
sql-1	1.09 ± 0.25	127	1.19 ± 0.29	86	1.19 ± 0.23	208
kap-1;sql-1	1.23 ± 0.23	205	ND		1.26 ± 0.27	218
gpa-3	1.12 ± 0.45[*]	65	1.22 ± 0.33[*]	46	ND	
sql-1; gpa-3	1.11 ± 0.20	199	ND		1.24 ± 0.27	146
gpa-3QL	1.10 ± 0.31[*]	72	1.11 ± 0.21[*]	65	ND	
sql-1; gpa-3QL	0.82 ± 0.17[a,b,c]	168	ND		0.98 ± 0.24[a,b]	206
kap-1; gpa-3QL	1.17 ± 0.26[*]	66	ND		ND	
sql-1; kap-1; gpa-3QL	1.06 ± 0.25	200	ND		1.08 ± 0.21	213

	IFT-B particle				Dynein (cargo)	
	OSM-1		CHE-13		XBX-1	
Genotype	**average ± sd**	**n**	**average ± sd**	**n**	**average ± sd**	**n**
wild type	1.10 ± 0.30	76	1.16 ± 0.21	64	1.17 ± 0.23	86
kap-1	ND		ND		1.15 ± 0.28	214
sql-1	1.10 ± 0.20	210	1.29 ± 0.32	215	1.09 ± 0.25	129
kap-1;sql-1	ND		1.15 ± 0.28	203	1.16 ± 0.24	220
gpa-3	1.18 ± 0.26[*]	51	ND		1.14 ± 0.23[*]	86
sql-1; gpa-3	ND		1.14 ± 0.23	215	1.17 ± 0.21	201
gpa-3QL	1.09 ± 0.18[*]	65	ND		1.28 ± 0.27[*]	76
sql-1; gpa-3QL	ND		1.07 ± 0.26[b]	208	1.08 ± 0.23	204
kap-1; gpa-3QL	ND		ND		ND	
sql-1; kap-1; gpa-3QL	ND		0.89 ± 0.16[a,b,c]	201	ND	

Average IFT velocities (in μm/s) ± standard deviation (sd) of OSM-3::GFP, CHE-11::GFP, DAF-10::GFP, OSM-1::GFP, CHE-13::GFP and XBX-1::GFP in wild type and mutant backgrounds. Velocities annotated with [*] have previously been described in (Burghoorn et al., 2010). Statistically significant differences ($P < 0.001$) compared to IFT velocity in wild type animals are indicated with [a], compared to *sql-1(tm2409)* animals with [b], and compared to *gpa-3QL* animals with [c]. Statistical analysis was performed using an ANOVA, followed by a Bonferroni post hoc test. Abbreviations: n, number of IFT particles measured; ND, not determined.

Chapter 5
Discussion and prospects

Introduction

Primary cilia are microtubule-based organelles that can be found on the surface of most eukaryotic cells. They perform specialized sensory functions, including chemosensation, mechanosensation, and photosensation (Satir and Christensen, 2008). There is a large diversity in cilia length and in cilia morphology. In vertebrates the most common primary cilium is a slender antenna-like structure of approximately 5-10 μm. These primary cilia can for example be found on kidney epithelial cells. Conversely, olfactory cilia can be ~200 μm long (McEwen et al., 2008). Photoreceptor cells have a specialized and morphological distinct cilium, known as the outer segment (Ramamurthy and Cayouette, 2009). In addition to the ciliary axoneme this domain also contains disk membranes, which are essential for photosensation. The nematode *Caenorhabditis elegans* has a subset of ciliated neurons that are responsible for sensing their chemical and physical environments (Inglis et al., 2007). These sensory cilia include rod-like cilia (the channel cilia), but also morphologically distinct cilia, with wing- or finger-like membranous appendages (e.g. AWA/B/C and AFD neuron cilia).

Primary cilia are not static, but instead their length and morphology appear to be regulated by several signaling pathways (Miyoshi et al., 2011). Several examples suggest that alteration of cilia length and morphology is achieved by modulation of intraflagellar transport (IFT) (Besschetnova et al., 2010; Burghoorn et al., 2007; Burghoorn et al., 2010; Mukhopadhyay et al., 2007), a specialized motor protein-based transport system that delivers ciliary proteins to the tip of the cilium. Anterograde IFT is mediated by two ciliary kinesins, kinesin-II and KIF17/OSM-3. Retrograde IFT is mediated by cytoplasmic dynein 2. Axonemal proteins slowly turnover, thus a continual delivery of ciliary precursor proteins is required to balance the turnover of axonemal proteins. The lengthening of cilia requires the delivery of additional cilairy precursor proteins. This could be achieved by several changes in the IFT machinery, such as IFT particle size, IFT velocity, frequency of IFT events, and cargo selection.

Study of IFT dynamics

In chapter 2, we show that two *v-ros* cross-hybridizing kinases (RCKs), MRK (MAK-related kinase) and MOK (MAPK/MAK/MRK overlapping kinase), negatively regulate cilia length. By visualizing IFT using GFP-tagged components of the IFT machinery in cultured renal epithelial cells, we show that depletion of MRK results in an increase of the anterograde IFT velocity of all tested IFT components. Depletion of MRK did not affect retrograde transport. Increased anterograde velocity, together with unchanged retrograde velocity, would result in an increase in the delivery of ciliary precursors proteins required for elongation of the cilium. MOK also negatively regulated cilia length, but did not affect anterograde or retrograde IFT velocities. Possibly, other parameters such as IFT frequency or IFT particle size are altered in renal epithelial cells depleted of MOK. Unfortunately, our kymographs showed too much background fluorescence from the cell body to quantify these parameters.

A nice example of what would be possible is provided by studies in *Chlamydomas*. Both flagella of *Chlamydomas* can adhere to a cover glass (Bloodgood, 1995). This allows visualization of IFT particles with total internal reflection fluorescence (TIRF) microscopy, where the fluorescent cell bodies remain outside the field of illumination. Using TIRF it was shown that in *Chlamydomas* IFT particles form long and slow trains when a flagellum is elongating and that IFT particles

form short and fast trains when the flagellum has a steady length (Engel et al., 2009). These data show that there is more to IFT dynamics then only IFT velocities.

Thus, it would be interesting to determine IFT particle size and IFT frequency in cilia of cultured mammalian cells, and e.g. test whether these parameters change when MOK or MRK are inactivated. In our current approach cells were inverted on a coverslip, but still cilia were outside of the TIRF imaging zone (~100 nm of the coverslip). Perhaps this problem could be overcome by using other (flatter) cells. Alternatively, photoactivatable fluorescent proteins could be used to visualize only IFT proteins residing in the cilium. In addition to velocity measurements based on kymographs, the use of other microscopy techniques, such as single molecule and FRAP, could yield imporant information on the dynamics of IFT proteins and ciliary motor proteins on the microtubule axis (in cultured mammalian cells).

In addition to a microscopy approach to study IFT, it would be possible to study IFT using a biochemical approach. Cultured mammalian cells have been shown to shed their primary cilium in stressful circumstances (Overgaard et al., 2009). These free cilia can be isolated from the medium, and analyzed with subsequent proteomic analyses. Recently, it was shown that this is technically feasible (Ishikawa et al., 2012). As described previously, lengthening of cilia requires an influx of ciliary precursors. If this occurs by a shift in the cargo transported by the IFT machinery, from more functional proteins (such as membrane receptors) to more structural proteins (i.e. axonemal tubulin), this might be detectable in the protein composition of the isolated cilia. These changes are probably not very apparent when comparing the levels of structural proteins such as axonemal tubulin, since these proteins are quite abundant in cilia with a constant length as well as in growing cilia. It seems more likely, that such an approach would show differences in the levels of adaptor proteins that link specific cargo to the IFT complex, like for example the BBSome which acts as an adaptor complex to target GPCRs to the cilium. The adaptor protein NudC, which was co-purified with MRK and MOK (Chapter 3), could be such a cargo-specific adaptor protein.

Modulation of the velocity of motor proteins

Elongation of cilia length, both by the activation of adenyl cyclase (Besschetnova et al., 2010) and depletion of MRK (Chapter 2), is accompanied by in increase in the anterograde velocity of the IFT machinery. How this increase is achieved remains unknown. Thus far, three different mechanisms have been shown to regulate kinesin motility *in vivo*. Firstly, posttranslational modifications of specific kinesin subunits can affect their motility (Figure 1B). For example, phosphorylation of KIF5 motors by JNK weakens their affinity for microtubules (Morfini et al., 2006). Secondly, the motility of motor proteins can be affected by modifications of the microtubule track (e.g. polyglutamylation, tyrosination/detyrosination, and acetylation) (Figure 1C), or its nucleotide-binding state (i.e. GTP versus GDP). Several examples of regulation of motor protein motility by tubulin modifications have been described (Cai et al., 2009; Dunn et al., 2008; Konishi and Setou, 2009; Nakata et al., 2011; Reed et al., 2006), but the most notable examples of regulation of motor motility by tubulin modifications has been described in sensory cilia of *C. elegans´* male-specific CEM neurons. Mutation of CCPP-1, a tubulin deglutamylating enzyme, increases the velocity of OSM-3 in these cilia (O'Hagan et al., 2011). Interestingly, we identified tubulin tyrosine ligase-like family member 3 as a potential binding partner of MRK in our pull-down assays (Chapter 3). Thirdly, the motility of motor proteins can be influenced by

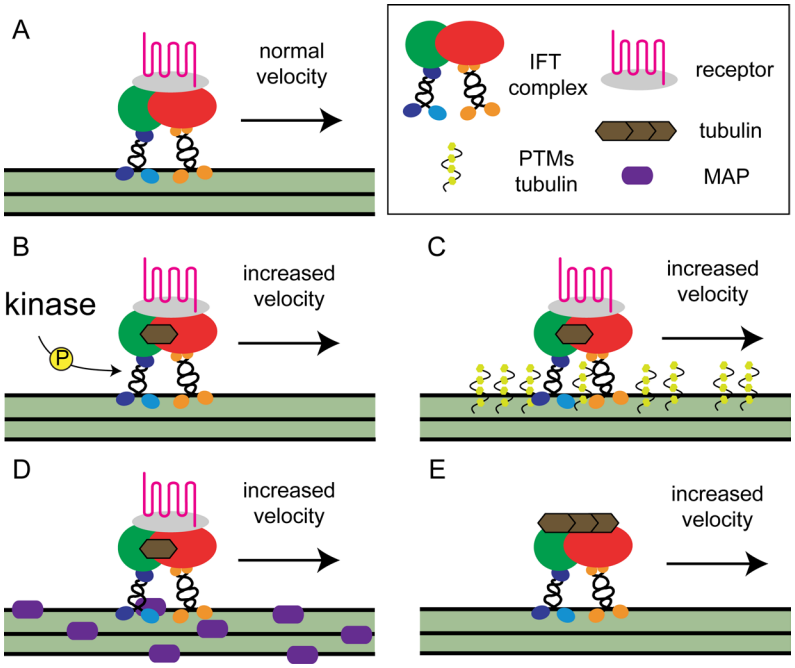

Figure 1. Overview of four possible models by which anterograde IFT velocities could be increased. (A) Ciliary precursor proteins are delivered at the distal tip by anterograde IFT, where they are required to balance the continuous turnover of axonemal proteins. The anterograde velocity and the delivery of ciliary precursor proteins could be increased by placing PTMs on the kinesin motor (B), modifying PTMs present on axonemal tubulin (C), introduction or removal of MAPs (D), and by changes is the transported cargo (E).

MT-associated proteins (MAPs) (Figure 1D). The MAPs tau, MAP1B and MAP4 all have been shown to negatively influence motor-based transport (Ebneth et al., 1998; Jimenez-Mateos et al., 2006; Tokuraku et al., 2007). Intriguingly, the third RCK, MAK, binds to and phosphorylates the photoreceptor-specific MAP retinitis pigmentosa 1 (RP1). RP1 overexpression results in an increase of cilia length (Omori et al., 2010), thus probably RP1 has a positive effect on IFT. A fourth explanation for an increase of anterograde IFT velocities could be a shift in cargo. A cilium that increases in length requires the delivery of tubulin. IFT particles loaded with (membrane) receptors are embedded in the ciliary membrane, while IFT particles loaded with only tubulin might not associate with the membrane and therefore experience less friction than IFT particles loaded with (membrane) receptors, resulting in increased velocity (Figure 1E).

A cilium length regulating signaling cascade

Several signaling proteins have been described to alter cilia length (Avasthi and Marshall, 2011; Miyoshi et al., 2011). Recently, the TOR pathway has been reported to positively regulate cilia length (Yuan et al., 2012). In chapter 2 we show that the effects of MRK- and MOK-depletion on cilia can be suppressed by the addition of the mTOR inhibitor rapamycin (Chapter 2), suggesting that MRK and MOK act through mTOR. mTOR is a serine/threonine protein

kinase that acts as a master regulator of cell growth, cell proliferation, cell motility, cell survival, protein synthesis, and transcription (Weber and Gutmann, 2012). Interestingly, MRK has been shown to phosphorylate Raptor (regulatory associated protein of mTOR) (Fu et al., 2009; Wu et al., 2012), which, together with mTOR, mLST8/GβL, PRAS40, and Deptor (Kim et al., 2002; Kim et al., 2003; Peterson et al., 2009; Vander Haar et al., 2007), forms the mTORC1 complex which directly regulates protein synthesis in mammals. Upstream, MRK activity can be regulated by (de)phosphorylation of Thr-157 by CCRK (cell cycle-related kinase) and PP5 (protein phosphatase 5) (Fu et al., 2006). In zebrafish, CCRK has been shown to regulate ciliary membrane and axonemal growth (Ko et al., 2010), and in *Chlamydomonas* a CCRK homologue, LF2p, negatively regulates cilia length (Tam et al., 2007). Thus, CCRK appears to have a function in regulating cilia a length. In a speculative model of a signaling pathway that regulates cilium length MRK activity is regulated the kinase CCRK and the phosphatase PP5. When activated, MRK phoshorylates Raptor, resulting in the inhibition of cilia lengthening by mTORC1 (Figure 2).

But how does mTOR promote cilia elongation? An increase in the level of soluble tubulin positively regulates cilia length (Sharma et al., 2011). The mTORC1 complex directly regulates protein synthesis in mammals, and an increase of ciliary precursor synthesis could explain the mTORC1-mediated lengthening of primary cilia. Possibly, MRK/MOK would act as negative regulator of cilia length by suppressing the synthesis of tubulin via inhibition of mTOR. If this is true, treatment of cells with an inhibitor of protein synthesis (for example cycloheximide) in cells depleted of MRK or MOK would not result in an increase of cilia length, and cells treated with both cycloheximide and rapamycin should result in the same cilia length as cycloheximide alone and rapamycin alone.

If the sole function of MRK/MOK is the modulation of mTORC1 it would be sufficient for MRK and MOK to reside in the cytosol, since Raptor, CCRK, and PP5 do not appear to localize in the cilium. However, we observed that MRK and MOK also localize to the cilium in cultured renal epithelial cells. Possibly, they have additional upstream or downstream partners in the cilium. In order to better understand the ciliary function of MRK and MOK it is vital to get a clear overview of their protein partners. In chapter 3, we performed pull-down experiments on lysates of HEK293T cells expressing tagged MRK/MOK, followed by mass spectrometry analysis of co-purified proteins. This analysis yielded a range of potential MRK and MOK binding partners. Unfortunately, they did not include any of the published binding partners of MRK (CCRK, PP5, Raptor, and Scythe). It could be that the reported MRK-binding partners could are not expressed in HEK293T cells, or maybe this interaction only occurs in ciliated cells. Pull-down experiments on lysates of ciliated IMCD-3 cells, that stably express tagged MRK or MOK, could teach us more about the ciliary function of these two kinases. In addition, pull-down experiments on lysates of *C. elegans* expressing tagged DYF-5 would also be informative. This does not mean that there are no interesting proteins in the pull-down assays in HEK293T cells. The list of proteins identified in the original pull-down assays in HEK293T cells features known ciliary proteins such as centrosomal protein 164kDa, pericentrin, centrosomal protein 170kDa, dynein light chain 1/LC8, tubulin tyrosine ligase-like family member 3, intraflagellar transport 74, and male germ cell-associated kinase. For these proteins it would be interesting to confirm their interaction with co-IP experiments, especially when these proteins would also be present in future mass spec data of pull-down experiments with lysates of ciliated IMCD-3 cells and lysates of *C. elegans* expressing tagged DYF-5. In addition, the interaction between MRK and

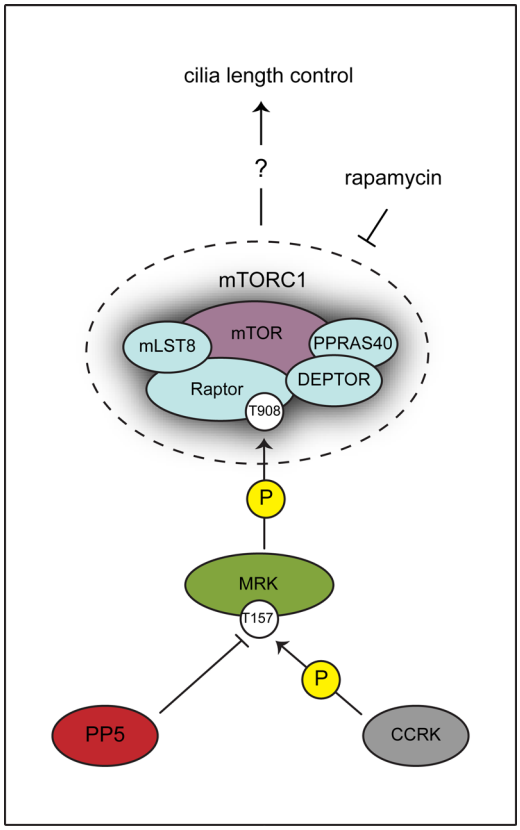

Figure 2. A speculative model of MRKs position in a cilia length regulating signaling cascade. MRK activity is regulated by the phosphorylation-state of Thr-157, which can be phosphorylated by CCRK and dephosphorylated by PP5. MRK phosphorylates Raptor at Thr-908, thereby inhibiting mTORC1-mediated elongation of cilia length. The mTOR inhibitor rapamycin can block mTORC1-mediated elongation of cilia length in the absence of MRK.

Raptor, CCRK, and PP5 should be studies in more detail using co-IP experiments. Finally, the role of these proteins in cilia length regulation and their relationship to MRK and MOK should be analyzed by testing the effects of their depletion or overexpression on cilia length, as well as subcellular localization pattern.

The role of membrane trafficking in regulation of cilia length and IFT

Not only the transport of ciliary proteins inside the cilium, but also transport of ciliary proteins to the ciliary base is important in modulating cilia length and function. For example, the small GTPase Rab8, which has been implicated in docking and fusion of vesicles at the ciliary base, increases cilia length when overexpressed (Nachury et al., 2007). Furthermore, a functional genomic screen for modulators cilium length also identified several proteins involved in vesicle trafficking (Kim et al., 2010). In chapter 4, we described the identification and characterization of the *C. elegans* gene *sql-1*. SQL-1 belongs to the Golgin family, which has been proposed

to function in maintaining the organization of the Golgi apparatus (Short et al., 2005). Overexpression of *sql-1* results in an increase of cilia length, indicating that *sql-1* can also regulate cilia length. Silencing of the mammalian homologue of *sql-1,* GMAP210, in primary mouse embryonic fibroblasts resulted in a decrease of cilia length (Follit et al., 2008). GMAP210 binds to complex B protein IFT20 (Follit et al., 2009). Mammalian IFT20 is unique among the IFT complex proteins because it not only localizes to the cilium, but also to the Golgi apparatus, where it functions as an adaptor protein for targeting vesicles to the cilium (Follit et al., 2006). SQL-1/GMAP210 could thus function in sorting of proteins/vesicle to the cilium. This function would also explain its role as cilia length regulator. Using live imaging of fluorescently tagged IFT proteins we showed that mutation of *sql-1* destabilizes the IFT complex. This can also be explained by a role of SQL-1 in sorting of proteins/vesicles to the cilium. In *sql-1(lf)* animals certain proteins would not, or to lesser extent, reach the cilium, including proteins required for maintaining a stable IFT complex.

Because of its localization pattern and its effect on cilia length and IFT, it is likely that SQL-1 is involved in sorting and/or transport of proteins destined for the cilium. The mechanisms behind these processes are far from understood, but recent studies have identified several key proteins involved. However, how these proteins cooperate to get ciliary proteins to the ciliary compartment is also unclear. In *C. elegans*, some of these proteins have been shown to have distinct localization patterns. For example, STAM-1, HGRS-1, and RAB-5, localize directly beneath the ciliary base (Hu et al., 2007), while RAB-8 localizes in motile spots in the cell bodies and dendrites of the ciliated neurons (Kaplan et al., 2010). UNC-101, a component of Clathrin adaptor (AP) complexes, is restricted to the cell body and does not co-localize with RAB-8 (Kaplan et al., 2010). Co-localization studies with these different markers, as well as of homologues of mammalian proteins described to function in protein transport to the cilium, could help to determine where SQL-1 exactly functions during protein transport to the cilium.

Although the interaction between SQL-1/GMAP210 and IFT-20 is not conserved in *C. elegans,* we clearly show that SQL-1 has a ciliary function. It would be interesting to identify the binding partners of SQL-1, to resolve through which proteins SQL-1 acts on cilia length and IFT. There are, however, some difficulties to overcome. SQL-1 is not only expressed in the ciliated neurons, but is ubiquitously expressed, and thus many of the identified binding partners might not directly have a ciliary function. This problem could be overcome by a pull-down experiment with the lysate of animals that express *sql-1* only in the ciliated neurons. This approach would strongly reduce the amount of SQL-1 protein, and would require very large *C. elegans* cultures to obtain enough starting material.

Final remarks

In conclusion, primary cilia are highly dynamic organelles, whose length and morphology are tightly regulated by various signaling pathways. This study, as well as other studies, show the importance of IFT in the modulation of cilia length. However, further research is necessary to gain more insight in the signal transduction pathways that regulate cilia length and the molecular mechanism behind the modulation of IFT velocities.

References

Avasthi, P., and W.F. Marshall. 2011. Stages of ciliogenesis and regulation of ciliary length. *Differentiation*.

Besschetnova, T.Y., E. Kolpakova-Hart, Y. Guan, J. Zhou, B.R. Olsen, and J.V. Shah. 2010. Identification of signaling pathways regulating primary cilium length and flow-mediated adaptation. *Curr Biol*. 20:182-7.

Bloodgood, R.A. 1995. Flagellar surface motility: gliding and microsphere movements. *Methods Cell Biol*. 47:273-9.

Burghoorn, J., M.P. Dekkers, S. Rademakers, T. de Jong, R. Willemsen, and G. Jansen. 2007. Mutation of the MAP kinase DYF-5 affects docking and undocking of kinesin-2 motors and reduces their speed in the cilia of Caenorhabditis elegans. *Proc Natl Acad Sci U S A*. 104:7157-62.

Burghoorn, J., M.P. Dekkers, S. Rademakers, T. de Jong, R. Willemsen, P. Swoboda, and G. Jansen. 2010. Dauer pheromone and G-protein signaling modulate the coordination of intraflagellar transport kinesin motor proteins in C. elegans. *J Cell Sci*. 123:2077-84.

Cai, D., D.P. McEwen, J.R. Martens, E. Meyhofer, and K.J. Verhey. 2009. Single molecule imaging reveals differences in microtubule track selection between Kinesin motors. *PLoS Biol*. 7:e1000216.

Dunn, S., E.E. Morrison, T.B. Liverpool, C. Molina-Paris, R.A. Cross, M.C. Alonso, and M. Peckham. 2008. Differential trafficking of Kif5c on tyrosinated and detyrosinated microtubules in live cells. *J Cell Sci*. 121:1085-95.

Ebneth, A., R. Godemann, K. Stamer, S. Illenberger, B. Trinczek, and E. Mandelkow. 1998. Overexpression of tau protein inhibits kinesin-dependent trafficking of vesicles, mitochondria, and endoplasmic reticulum: implications for Alzheimer's disease. *J Cell Biol*. 143:777-94.

Engel, B.D., W.B. Ludington, and W.F. Marshall. 2009. Intraflagellar transport particle size scales inversely with flagellar length: revisiting the balance-point length control model. *J Cell Biol*. 187:81-9.

Follit, J.A., J.T. San Agustin, F. Xu, J.A. Jonassen, R. Samtani, C.W. Lo, and G.J. Pazour. 2008. The Golgin GMAP210/TRIP11 anchors IFT20 to the Golgi complex. *PLoS Genet*. 4:e1000315.

Follit, J.A., R.A. Tuft, K.E. Fogarty, and G.J. Pazour. 2006. The intraflagellar transport protein IFT20 is associated with the Golgi complex and is required for cilia assembly. *Mol Biol Cell*. 17:3781-92.

Follit, J.A., F. Xu, B.T. Keady, and G.J. Pazour. 2009. Characterization of mouse IFT complex B. *Cell Motil Cytoskeleton*. 66:457-68.

Fu, Z., J. Kim, A. Vidrich, T.W. Sturgill, and S.M. Cohn. 2009. Intestinal cell kinase, a MAP kinase-related kinase, regulates proliferation and G1 cell cycle progression of intestinal epithelial cells. *Am J Physiol Gastrointest Liver Physiol*. 297:G632-40.

Fu, Z., K.A. Larson, R.K. Chitta, S.A. Parker, B.E. Turk, M.W. Lawrence, P. Kaldis, K. Galaktionov, S.M. Cohn, J. Shabanowitz, D.F. Hunt, and T.W. Sturgill. 2006. Identification of yin-yang regulators and a phosphorylation consensus for male germ cell-associated kinase (MAK)-related kinase. *Mol Cell Biol*. 26:8639-54.

Hu, J., S.G. Wittekind, and M.M. Barr. 2007. STAM and Hrs down-regulate ciliary TRP receptors. *Mol Biol Cell*. 18:3277-89.

Inglis, P.N., G. Ou, M.R. Leroux, and J.M. Scholey. 2007. The sensory cilia of Caenorhabditis elegans. *WormBook*:1-22.

Ishikawa, H., J. Thompson, J.R. Yates, 3rd, and W.F. Marshall. 2012. Proteomic analysis of mammalian primary cilia. *Curr Biol*. 22:414-9.

Jimenez-Mateos, E.M., C. Gonzalez-Billault, H.N. Dawson, M.P. Vitek, and J. Avila. 2006. Role of MAP1B in axonal retrograde transport of mitochondria. *Biochem J*. 397:53-9.

Kaplan, O.I., A. Molla-Herman, S. Cevik, R. Ghossoub, K. Kida, Y. Kimura, P. Jenkins, J.R. Martens, M. Setou, A. Benmerah, and O.E. Blacque. 2010. The AP-1 clathrin adaptor facilitates cilium formation and functions with RAB-8 in C. elegans ciliary membrane transport. *J Cell Sci*. 123:3966-77.

Kim, D.H., D.D. Sarbassov, S.M. Ali, J.E. King, R.R. Latek, H. Erdjument-Bromage, P. Tempst, and D.M. Sabatini. 2002. mTOR interacts with raptor to form a nutrient-sensitive complex that signals to the cell growth machinery. *Cell*. 110:163-75.

Kim, D.H., D.D. Sarbassov, S.M. Ali, R.R. Latek, K.V. Guntur, H. Erdjument-Bromage, P. Tempst, and D.M. Sabatini. 2003. GbetaL, a positive regulator of the rapamycin-sensitive pathway required for the nutrient-sensitive interaction between raptor and mTOR. *Mol Cell*. 11:895-904.

Kim, J., J.E. Lee, S. Heynen-Genel, E. Suyama, K. Ono, K. Lee, T. Ideker, P. Aza-Blanc, and J.G. Gleeson. 2010. Functional genomic screen for modulators of ciliogenesis and cilium length. *Nature*. 464:1048-51.

Ko, H.W., R.X. Norman, J. Tran, K.P. Fuller, M. Fukuda, and J.T. Eggenschwiler. 2010. Broad-minded links cell cycle-related kinase to cilia assembly and hedgehog signal transduction. *Dev Cell*. 18:237-47.

Konishi, Y., and M. Setou. 2009. Tubulin tyrosination navigates the kinesin-1 motor domain to axons. *Nat Neurosci*. 12:559-67.

McEwen, D.P., P.M. Jenkins, and J.R. Martens. 2008. Olfactory cilia: our direct neuronal connection to the external world. *Curr Top Dev Biol*. 85:333-70.

Miyoshi, K., K. Kasahara, I. Miyazaki, and M. Asanuma. 2011. Factors that influence primary cilium length. *Acta Med Okayama*. 65:279-85.

Morfini, G., G. Pigino, G. Szebenyi, Y. You, S. Pollema, and S.T. Brady. 2006. JNK mediates pathogenic effects of polyglutamine-expanded androgen receptor on fast axonal transport. *Nat Neurosci*. 9:907-16.

Mukhopadhyay, S., Y. Lu, H. Qin, A. Lanjuin, S. Shaham, and P. Sengupta. 2007. Distinct IFT mechanisms contribute to the generation of ciliary structural diversity in C. elegans. *EMBO J*. 26:2966-80.

Nachury, M.V., A.V. Loktev, Q. Zhang, C.J. Westlake, J. Peranen, A. Merdes, D.C. Slusarski, R.H. Scheller, J.F. Bazan, V.C. Sheffield, and P.K. Jackson. 2007. A core complex of BBS proteins cooperates with the GTPase Rab8 to promote ciliary membrane biogenesis. *Cell*. 129:1201-13.

Nakata, T., S. Niwa, Y. Okada, F. Perez, and N. Hirokawa. 2011. Preferential binding of a kinesin-1 motor to GTP-tubulin-rich microtubules underlies polarized vesicle transport. *J Cell Biol*. 194:245-55.

O'Hagan, R., B.P. Piasecki, M. Silva, P. Phirke, K.C. Nguyen, D.H. Hall, P. Swoboda, and M.M. Barr. 2011. The Tubulin Deglutamylase CCPP-1 Regulates the Function and Stability of Sensory Cilia in C. elegans. *Curr Biol*.

Omori, Y., T. Chaya, K. Katoh, N. Kajimura, S. Sato, K. Muraoka, S. Ueno, T. Koyasu, M. Kondo, and T. Furukawa. 2010. Negative regulation of ciliary length by ciliary male germ cell-associated kinase (Mak) is required for retinal photoreceptor survival. *Proc Natl Acad Sci U S A*. 107:22671-6.

Overgaard, C.E., K.M. Sanzone, K.S. Spiczka, D.R. Sheff, A. Sandra, and C. Yeaman. 2009. Deciliation is associated with dramatic remodeling of epithelial cell junctions and surface domains. *Mol Biol Cell*. 20:102-13.

Peterson, T.R., M. Laplante, C.C. Thoreen, Y. Sancak, S.A. Kang, W.M. Kuehl, N.S. Gray, and D.M. Sabatini. 2009. DEPTOR is an mTOR inhibitor frequently overexpressed in multiple myeloma cells and required for their survival. *Cell*. 137:873-86.

Ramamurthy, V., and M. Cayouette. 2009. Development and disease of the photoreceptor cilium. *Clin Genet*. 76:137-45.

Reed, N.A., D. Cai, T.L. Blasius, G.T. Jih, E. Meyhofer, J. Gaertig, and K.J. Verhey. 2006. Microtubule acetylation promotes kinesin-1 binding and transport. *Curr Biol*. 16:2166-72.

Satir, P., and S.T. Christensen. 2008. Structure and function of mammalian cilia. *Histochem Cell Biol*. 129:687-93.

Sharma, N., Z.A. Kosan, J.E. Stallworth, N.F. Berbari, and B.K. Yoder. 2011. Soluble levels of cytosolic tubulin regulate ciliary length control. *Mol Biol Cell*. 22:806-16.

Short, B., A. Haas, and F.A. Barr. 2005. Golgins and GTPases, giving identity and structure to the Golgi apparatus. *Biochim Biophys Acta*. 1744:383-95.

Tam, L.W., N.F. Wilson, and P.A. Lefebvre. 2007. A CDK-related kinase regulates the length and assembly of flagella in Chlamydomonas. *J Cell Biol*. 176:819-29.

Tokuraku, K., T.Q. Noguchi, M. Nishie, K. Matsushima, and S. Kotani. 2007. An isoform of microtubule-associated protein 4 inhibits kinesin-driven microtubule gliding. *J Biochem*. 141:585-91.

Vander Haar, E., S.I. Lee, S. Bandhakavi, T.J. Griffin, and D.H. Kim. 2007. Insulin signalling to mTOR mediated by the Akt/PKB substrate PRAS40. *Nat Cell Biol*. 9:316-23.

Weber, J.D., and D.H. Gutmann. 2012. Deconvoluting mTOR biology. *Cell Cycle*. 11:236-48.

Wu, D., J.R. Chapman, L. Wang, T.E. Harris, J. Shabanowitz, D.F. Hunt, and Z. Fu. 2012. Intestinal cell kinase (ICK) promotes activation of the mTOR complex 1 (mTORC1) through phosphorylation of raptor Thr-908. *J Biol Chem*.

Yuan, S., J. Li, D.R. Diener, M.A. Choma, J.L. Rosenbaum, and Z. Sun. 2012. Target-of-rapamycin complex 1 (Torc1) signaling modulates cilia size and function through protein synthesis regulation. *Proc Natl Acad Sci U S A*.

Addendum

Summary

Samenvatting

Curriculum Vitae

PhD portfolio

Dankwoord

Summary

Primary cilia are microtubule-based protrusions that can be found on the surface of almost all vertebrate cells, and have important sensory functions. There is wide variety in cilia length and morphology, probably reflecting their specific function in different types of tissue as well as organisms. Cilia are build and maintained by a motor protein based transport mechanism, known as intraflagellar transport (IFT). During IFT, motor protein transport multimeric proteins complexes along the microtubule axis of the cilium, delivering proteins to the distal tip and returning them to the cell body. Primary cilia are dynamic structures, and their length can be modulated by several signaling pathways. It is evident that IFT plays an important role in regulating cilia length.

In **chapter 1**, I give a general introduction to what is known about primary cilia and IFT. First, I discuss the general structure and sensory function of primary cilia. Next, I describe the four subcomplexes from which an IFT particle is composed, the ciliary kinesins, complex A, complex B, and the BBSome. Subsequently, I discuss the molecular mechanisms behind the cell's decision when to form and when to disassemble a primary cilium, and how the cell regulates cilia length. Finally, I discuss the implications of abnormal ciliogenesis and ciliary length control in human diseases.

In **chapter 2**, I describe the characterization of two members of the family of the *ros* cross-hybridizing kinases (RCKs), MRK and MOK. Both kinases localize to the primary cilia, where they negatively regulate cilia length. Using cultured kidney epithelial cells expressing GFP-tagged components of the IFT complex, I found that that silencing MRK resulted in an increase in the velocity of particles that move to tip of the cilium, but did affect the velocity of particles that move toward the cell body. This would result in delivery of more material at the distal tip, and elongation of the cilium. We propose that MRK regulates cilia length by, directly or indirectly, modulating the velocity of particles that move toward the tip. In addition, we show that the mTOR inhibitor rapamycin can block all the effects of MRK and MOK depletion, suggesting MRK and MOK act through the mTOR pathway.

In **chapter 3**, I used a proteomics approach to identify the binding partners of MRK and MOK. This analysis revealed a range of MRK and/or MOK binding proteins, including centrosomal proteins, proteins involved in microtubule-based motor transport, and in signal transduction. By comparing our mass spec results with known ciliary proteins and with proteins that contain the preferred phosphorylation consensus sequence of MRK I created a starting point for future experiments aiming to determine the ciliary function of MRK and MOK.

In **chapter 4**, I describe the identification and characterization of the gene *sql-1*. Because of the diverse array of in vivo tools available for studying intraflagellar transport, ciliary integrity, and cilia mutants, *C. elegans* is a popular model organism in cilia biology. In *C. elegans*, we performed a genetic screen to identify new genes that are involved cilia length regulation. One of the genes found in this screen, *sql-1,* localized to the Golgi apparatus, where it is required for maintaining Golgi organization. In addition, SQL-1 can regulate cilia length, and is required to preserve stability of the IFT complex.

In **chapter 5**, I discuss the results presented in chapters 2, 3 and 4 and suggest possible future experiments that can be done to further unravel the function of mammalian MRK and MOK, as well as *C. elegans*' SQL-1.

Samenvatting

Een primair cilium is een haarvormig organel dat uit de cel steekt. Cilia zijn aanwezig op bijna alle cellen van gewervelde dieren en hebben een belangrijke functie in het waarnemen van omgevingssignalen. Cilia worden opgebouwd en onderhouden door een specifiek transportsysteem; intraflagellair transport (IFT). Tijdens dit proces worden grote eiwitcomplexen door motoreiwitten getransporteerd langs de microtubuli die zich in het cilium bevinden. Er is een grote variëteit in lengte en morfologie van cilia. Dit is waarschijnlijk het gevolg van de specifieke functies die ze hebben in zowel verschillende weefsels als organismen. Verder zijn primaire cilia dynamische structuren. Hun lengte wordt gemoduleerd door meerdere signaaltransductiepaden. Waarschijnlijk speelt IFT een belangrijke rol in het reguleren van cilia lengte.

In **hoofdstuk 1** geef ik een algemene introductie over wat er bekend is over primaire cilia en IFT. Ik begin met het beschrijven van de algemene structuur en de functie van cilia. Vervolgens bespreek ik de vier subcomplexen waar IFT deeltjes uit bestaan. Dit zijn de motoreiwitten, complex A, complex B, en het BBSome. Daarna beschrijf ik de moleculaire mechanismen die verantwoordelijk zijn voor de beslissing van de cel om een cilium te bouwen, voor de regulatie van cilia lengte en voor de beslissing om het cilium af te breken. Tot slot bespreek ik de gevolgen van het niet correct functioneren van het cilium in ziekten bij de mens.

In **hoofdstuk 2** beschrijf ik de karakterisatie van twee eiwitten die behoren tot de familie van *ros* cross-hybridizing kinases (RCKs), zijnde MRK en MOK. Beide kinases bevinden zich in de cilia van gekweekte nierepitheelcellen waar ze de lengte van cilia reguleren. Uitschakelen van zowel het MRK gen als het MOK gen resulteert in een verlenging van het cilium. Het tot overexpressie brengen van MRK resulteert in een verkorting van het cilium. Om het effect van MRK en MOK op IFT te bestuderen brachten wij met GFP gelabelde IFT eiwitten tot expressie in gekweekte niercellen. Uitschakeling van MRK in deze cellen resulteerde in een versnelling van IFT deeltjes die naar de punt van het cilium gebracht worden, terwijl het transport terug naar de cel niet beïnvloed werd. Wij vermoeden dat MRK de lengte van cilia reguleert door, direct of indirect, de snelheid van IFT deeltjes te moduleren. Daarnaast laten we zien dat rapamycine (een remmer van het eiwit mTOR) de effecten die het uitschakelen van MRK en MOK op cilia lengte en IFT hebben, blokkeert. Dit suggereert dat MRK en MOK samenwerken via het mTOR signaaltransductiepad in de regulatie van cilia lengte en IFT.

In **hoofdstuk 3** heb ik een proteomics benadering gebruikt om de bindingspartners van MRK en MOK te identificeren. Bij deze benadering heb ik een scala aan MRK en/of MOK bindende eiwitten gedetecteerd, waaronder centrosomale eiwitten. Deze eiwitten zijn betrokken bij motortransport langs microtubuli en eiwitten die functioneren in signaaltransductie. Door de door ons gevonden resultaten te vergelijken met eiwitten waarvan we weten dat ze zich in het cilium bevinden en met eiwitten die de aminozuur sequentie bevatten die MRK fosforyleert, hebben wij een aantal belangrijke kandidaat eiwitten gevonden die kunnen helpen om in de toekomst de functie van MRK en MOK verder te bepalen.

In **hoofdstuk 4** beschrijf ik de identificatie en karakterisatie van het gen *sql-1*. De nematode *C. elegans* is een populair modelorganisme om cilia te bestuderen, onder andere omdat het redelijk eenvoudig is om IFT te visualiseren. Om nieuwe genen te identificeren die functioneren in de regulatie van cilia lengte hebben wij in *C. elegans* een genetische screen uitgevoerd. Eén van de genen gevonden in deze screen was *sql-1*. Wij laten zien dat *sql-1* tot expressie komt in alle

cellen van *C. elegans*. Tevens laten wij zien dat SQL-1 zich in het Golgi-apparaat bevindt. Daar is het nodig om de organisatie van het Golgi-apparaat te handhaven. Verder kan SQL-1 de lengte van het cilium reguleren en is het belangrijk voor de stabiliteit van het IFT complex.

In **hoofdstuk 5** bespreek ik de resultaten zoals beschreven in de hoofdstukken 2, 3 en 4 en beschrijf ik de mogelijke toekomstige experimenten die gedaan kunnen worden om de precieze functies van de zoogdiereiwitten MRK en MOK, evenals het *C. elegans* eiwit SQL-1, verder te ontrafelen.

Curriculum Vitae

Personalia:

Naam: Joost René Broekhuis

Geboren: 5 februari 1984 te Rotterdam

Opleiding:

1996 - 2001:	HAVO, Gemini College, Ridderkerk
2001 - 2005:	Bachelor Biologie en medisch laboratorium onderzoek, Hogeschool Rotterdam
2005 - 2007:	Master Moleculaire en cellulaire biologie, Universiteit Leiden

Publicaties:

Broekhuis, J.R., Verhey, K.J., and Jansen, G. 2012. MRK and MOK regulate cilia length and intraflagellar transport in renal epithelial cells. (Submitted)

Broekhuis, J.R., Rademakers, S., Burghoorn, J., and Jansen, G. 2012. SQL-1, homologue of GMAP210, modulates Intraflagellar Transport in *C. elegans*. (Submitted)

Broekhuis, J.R., Leong, W.Y., and Jansen, G. 2012. Regulation of cilium length and Intraflagellar Transport. *International Review of Cell & Molecular Biology*. (In press)

PhD portfolio

Name: Joost René Broekhuis
Department: Cell Biology and Genetics
Research School: Medical Genetic Centre (MGC)
PhD period: Sep 2007-Dec 2012
Promotor: Prof.dr. F.G. Grosveld
Co-promotor: Dr. G. Jansen

PhD Training	Year
General academic skills	
Reading and Discussing Literature	2007
Safe Laboratory techniques	2007
Molecular and Cell Biology	2008
Research skills	
In Vivo cellular imaging: From Molecule to Animal	2007
In the footsteps of Antoni van Leeuwenhoek - Advanced course in microscopy	2008
Workshop on Photoshop and Illustrator CS5	2011
International conferences	
17th International *C. elegans* Meeting, Los Angeles	2009
European *C. elegans* Neurobiology Meeting, Cambridge	2009
American Society for Cell Biology annual meeting, Philadelphia	2010
18th International *C. elegans* Meeting, Los Angeles	2011
American Society for Cell Biology annual meeting, Denver	2011
Retreats and Workshops	
PhD workshop Heidelberg	2008
PhD workshop Brugge	2009
PhD workshop Maastricht	2011
Teaching activities	
Supervising Master student	2008
Supervising Bachelor student	2010
Supervising Master student	2011

Dankwoord

Na vijf jaar zwoegen is hij bijna af, mijn proefschrift. Het enige wat nu nog rest is juist dat deel dat door de meeste mensen gelezen gaat worden, het dankwoord. De afgelopen vijf jaar hebben veel mensen bijgedragen aan de totstandkoming van dit proefschrift.

Gert, bedankt voor de kans die je mij hebt gegeven om in je lab te werken en voor de dagelijkse begeleiding. Vijf jaar geleden zijn we begonnen met het plan om IFT te gaan visualiseren. Dit bleek toch lastiger dan dat wij aanvankelijk dachten. Maar terwijl we probeerden dat draaiend te krijgen gaf je mij de kans om ook aan andere projecten te werken (zelf aan een *C. elegans* project), waardoor ik toch de positieve resultaten genereerde die nodig waren om de moed erin te houden en om een boekje te vullen.

Niels, Sjaak en Joost, bedankt dat jullie plaats wilden nemen in de kleine commissie en tijd wilden vrijmaken om mijn proefschrift te bestuderen. Jullie adviezen hebben zeker meegeholpen met het zetten van de laatste puntjes op de i.

Aniek, we waren de laatste tijd steeds vaker de enige twee mensen in ons nieuwe kantoor. Ik hoop dat er nu snel weer nieuwe collega's komen om je gezelschap te houden. Ik ga je gezelschap zeker missen. Ik vind het erg leuk dat je mijn paranimf wil zijn. Dave, ik zat toch een beetje in een vrouwenlab en het was daarom extra leuk om af en toe ook eens een mannenverhaal te horen. Vooral van je klusverhalen heb ik erg genoten. Bedankt dat je mijn paranimf wil zijn.

Suzanne, met je goede ideeën en proeven heb je een grote bijdrage geleverd aan dit proefschrift. Ik heb met veel plezier met je gewerkt aan het SQL-1 project. In het lab ben je in je element en hoe je het allemaal deed weet ik niet maar na een microscopiesessie kwam je toch altijd terug met minstens twee keer zoveel filmpjes als ik.

Toroti, you are truly unique, I cannot imagine that there is another Toroti out there. That time that we got lost in Heidelberg late at night together on the tandembike, or that time that we tried (but failed horribly) to go sightseeing in LA using LA's public transportation system, are moments I will never forget. I wish you all the best in the future.

Weng Yee, together we worked on the same protein. I'm positive you will also defend your findings on this protein in the near future. I wish you all the best with your future plans.

Hannes en Karen, hoewel het er op leek dat jullie steeds meer ruimte in gebruik gingen nemen, deelde ik met veel plezier een bench in het lab met jullie.

Rikke, Joost and Linh, I've had the pleasure to supervise the three of you during your internships in the lab and I hope you enjoyed this time as much as I did.

Uiteraard wil ik ook iedereen van de afdeling bedanken, zonder iedereen afzonderlijk te noemen, voor het goede gezelschap dat jullie waren tijdens het dagelijkse leven op het lab, maar ook tijdens de vele retreats. Specifiek wil ik wel Siska bedanken. Wanneer ik weer eens op zoek was naar iets of als ik tegen een probleem aanliep, heb je me regelmatig uit de brand geholpen. Ook heel belangrijk waren Bep, Marieke, Melle en Leo. Bedankt voor alles wat jullie voor mij geregeld hebben. Ook bedankt, de mensen van OIC, voor de altijd goed

functionerende microscopen. Reinier, zonder jouw hulp met de FACS sorter had ik nooit die stabiele cellijnen gehad die ik nodig had voor de belangrijkste proeven in hoofdstuk 2. Kerstin, thank you for your efforts to keep the cell culture room tidy and clean. Dick en Jeroen, bedankt voor alle mass spec analyses die jullie uitgevoerd hebben.

Pap, mam, Maarten en tante Nel, bedankt voor de interesse die jullie altijd toonden in mijn leven op het lab en jullie aanmoedigingen en steun. Lieve Karima, regelmatig kwam ik mopperend thuis over mislukte proeven en dat soort zaken. Maar jij hebt me altijd voorgehouden dat het allemaal goed zou komen en daar heb je gelijk in gekregen. Bedankt dat je me altijd gesteund hebt en voor alle leuke dingen die we samen gedaan hebben de afgelopen vijf jaar. En jouw idee voor de voorkant van dit proefschrift is erg goed uit de verf gekomen.

Joost